doi : 10.17596/0003150

R/V *Mirai* Cruise Report

MR11-08

WOCE-revisit cruise in the western Pacific

4th December, 2011 – 9th February, 2012

Japan Agency for Marine-Earth Science and Technology

(JAMSTEC)

Cruise Report ERRATA of the Nutrients part

page	Error	Correction
97	potassium nitrate CAS No. 7757-91-1	potassium nitrate CAS No. 7757-79-1

Content

I. Introduction

II. Observation

1. Cruise Narrative
2. Underway Observation
   2.1 Navigation
   2.2 Swath Bathymetry
   2.3 Surface meteorological observation
   2.4 Thermo-salinograph
   2.5 pCO_2
   2.6 ADCP
   2.7 Ceilometer observation
   2.8 Air-sea surface eddy flux measurement
   2.9 Lidar
   2.10 Isotopes in rainfall and water vapor
   2.11 Ship-borne Sky radiometer
   2.12 Tropospheric aerosol and gas observations by MAX-DOAS and auxiliary techniques
   2.13 Millimeter-wave radar
   2.14 Sea surface gravity
   2.15 On-board geomagnetic measurement
   2.16 Radiosonde
   2.17 Doppler radar

3. Station Observation
   3.1 $CTDO_2$ Measurements
   3.2 Bottle Salinity
   3.3 Density
   3.4 Oxygen
   3.5 Nutrients
   3.6 Chlorofluorocarbons and Sulfur hexafluoride
   3.7 Carbon items
   3.8 Chlorophyll-a
   3.9 Carbon isotopes

3.10 Radioactive cesium and tritium
3.11 LADCP
3.12 Expendable Microstructure Profiler
3.13 XCTD
3.14 Ocean-origin gases
3.15 PFCs
3.16 Iodine-129
3.17 Plankton net sampling

4. Floats, Drifters and Moorings
4.1 Argo floats

III. Notice on Using

I. Introduction

It is well known that climate changes of a timescale more than a decade are influenced by changes of oceanic conditions. Among various oceanic changes, we conducted shipboard observations focusing on storage and transport of anthropogenic CO_2, heat and freshwater in the ocean, which are important for global warming and relevant climate changes. Our observation line (Figs. 1.1.1 and 1.1.2) is a meridional line, which is set in the western Pacific, and traverses the main subtropical gyre in the ocean. By occupying the observation line, we intended to clarify: (1) storage of anthropogenic CO_2, dissolved oxygen, etc. in the subtropical gyre and the temporal changes, (2) temperature rise and transport of dissolved substances along the route of Circumpolar Deep Water, and (3) current degree of ocean acidification in the western Pacific. This study was conducted under the Global Ocean Ship-based Hydrographic Investigations Program (abbreviated as GO-SHIP, http://www.go-ship.org/).

In addition to the objectives listed above, we were also aimed at elucidating dispersion of radioactive substances, released into the sea unfortunately from the Fukushima Dai-ichi nuclear power plant.

During the 2nd leg, we could conduct hydrographic observations steadily. But during the 3rd leg, we had to give up some hydrographic casts due to big waves.

II. Observation

1. Cruise Narrative

Akihiko Murata (RIGC/JAMSTEC)

Yuichiro Kumamoto (RIGC/JAMSTEC)

1.1. Basic Information

Cruise track:	Figs. 1.1.1 and 1.1.2
Cruise code:	MR11-08
Expocode	Leg 1: 49NZ20111204 Leg 2: 49NZ20111220 Leg 3: 49NZ20120113
GHPO section designation:	P10
Ship name:	R/V Mirai
Ports of call:	Leg 1, Colombo, Sri Lanka – Koror, Palau Leg 2, Koror, Palau – Guam, USA Leg 3, Guam, USA – Sekinehama, Japan
Cruise date:	Leg 1, December 4, 2011 – December 20, 2011 Leg 2, December 20, 2011 – January 12, 2012 Leg 3, January 12, 2012 – February 9, 2012
Chief scientists:	Leg 1, Yuichiro Kumamoto (kumamoto@jamstec.go.jp) Leg 2, Akihiko Murata (murataa@jamstec.go.jp) Leg 3, Yuichiro Kumamoto (kumamoto@jamstec.go.jp) Ocean Climate Change Research Program Research Institute for Global Change (RIGC) Japan Agency for Marine-Earth Science and Technology (JAMSTEC) 2-15 Natsushima, Yokosuka, Kanagawa, Japan 237-0061 Fax: +81-46-867-9455
Number of Stations:	Leg 2, 59 stations Leg 3, 116 stations including 14 XCTD observations

Geographic Boundaries (for hydrographic stations):

10°S –43°N

140°E–151°E

Floats and drifters deployed: 2 floats

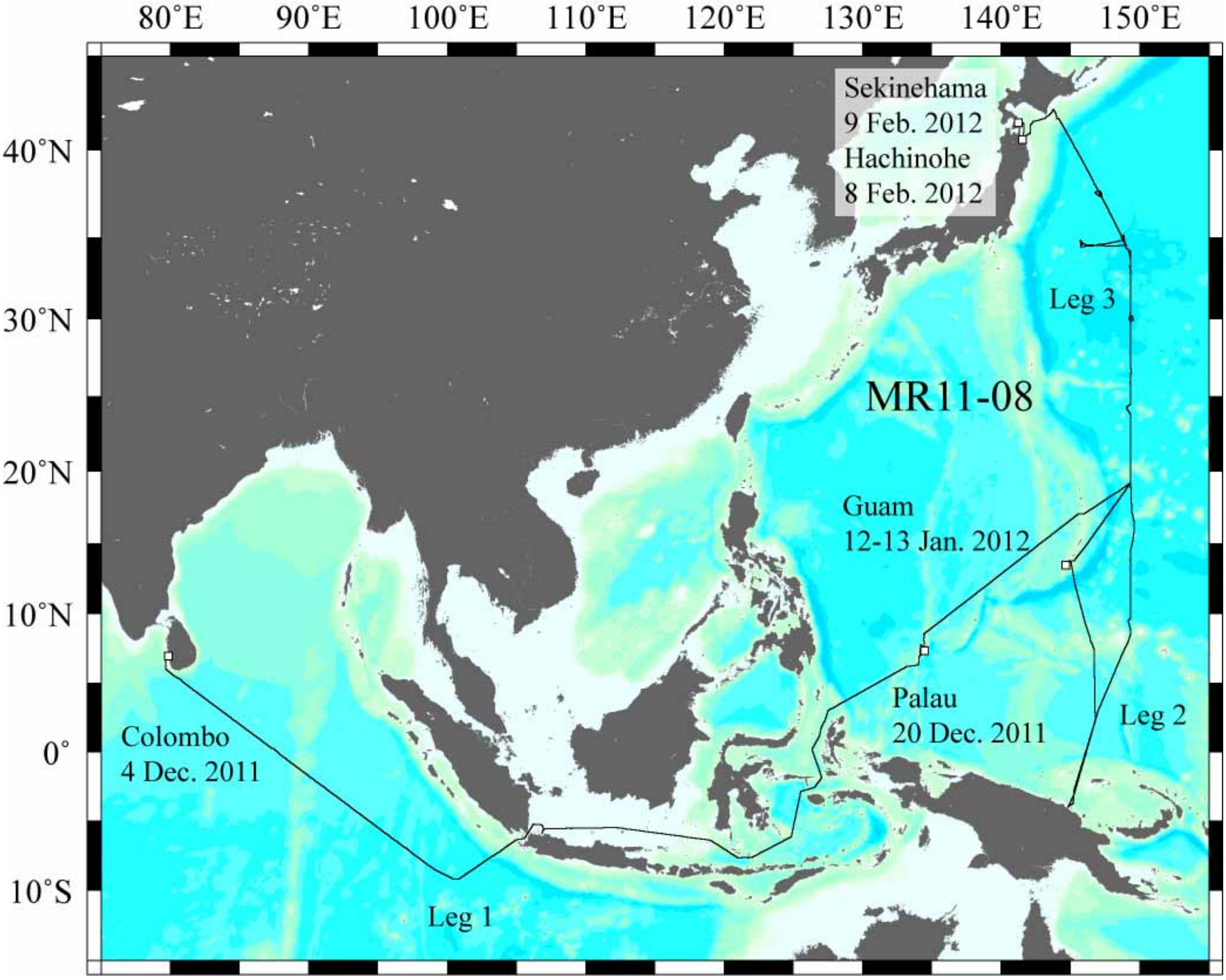

Fig. 1.1.1 Cruise map during the entire period.

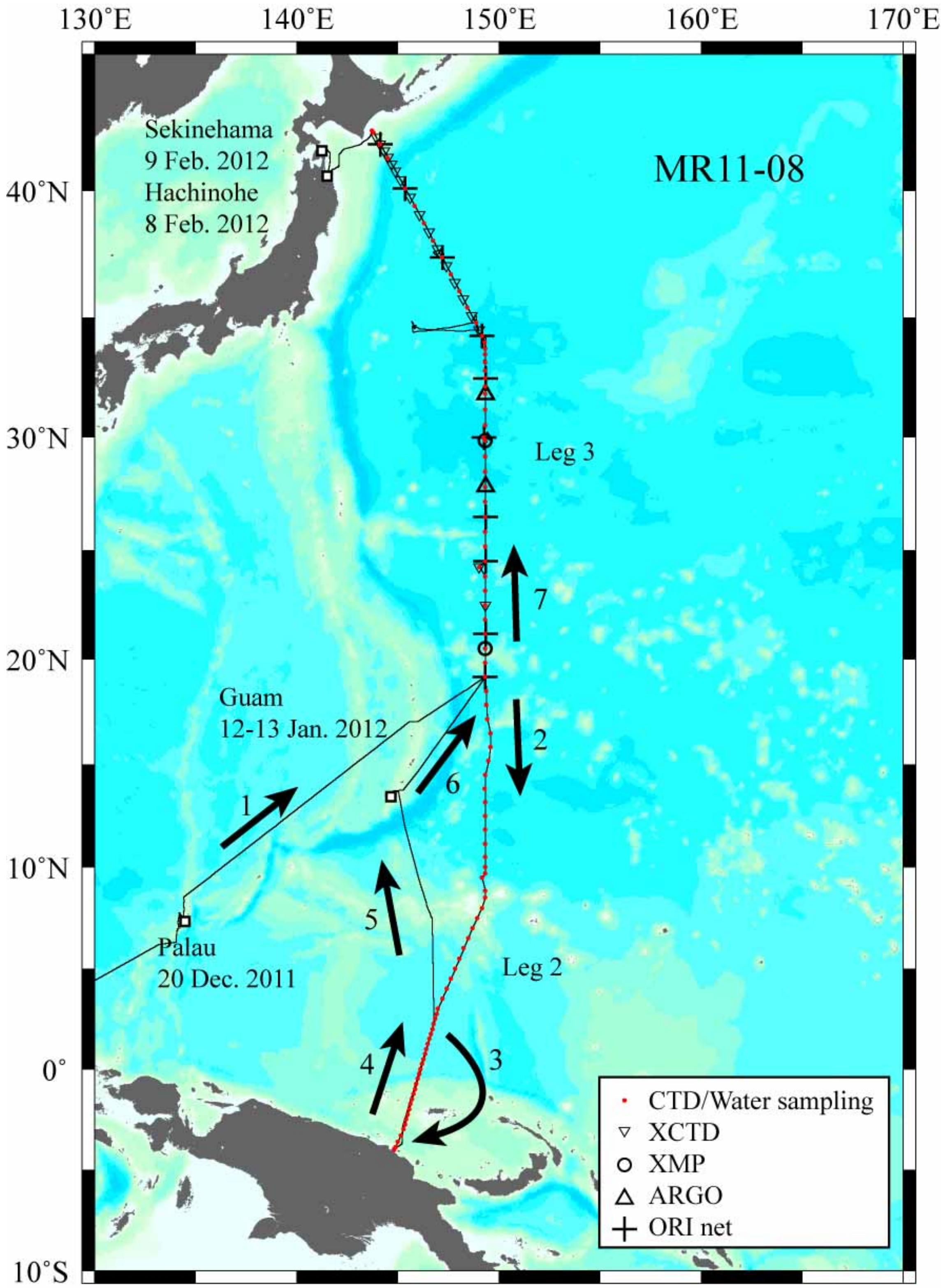

Fig. 1.1.2 Detailed cruise map for legs 2 and 3.

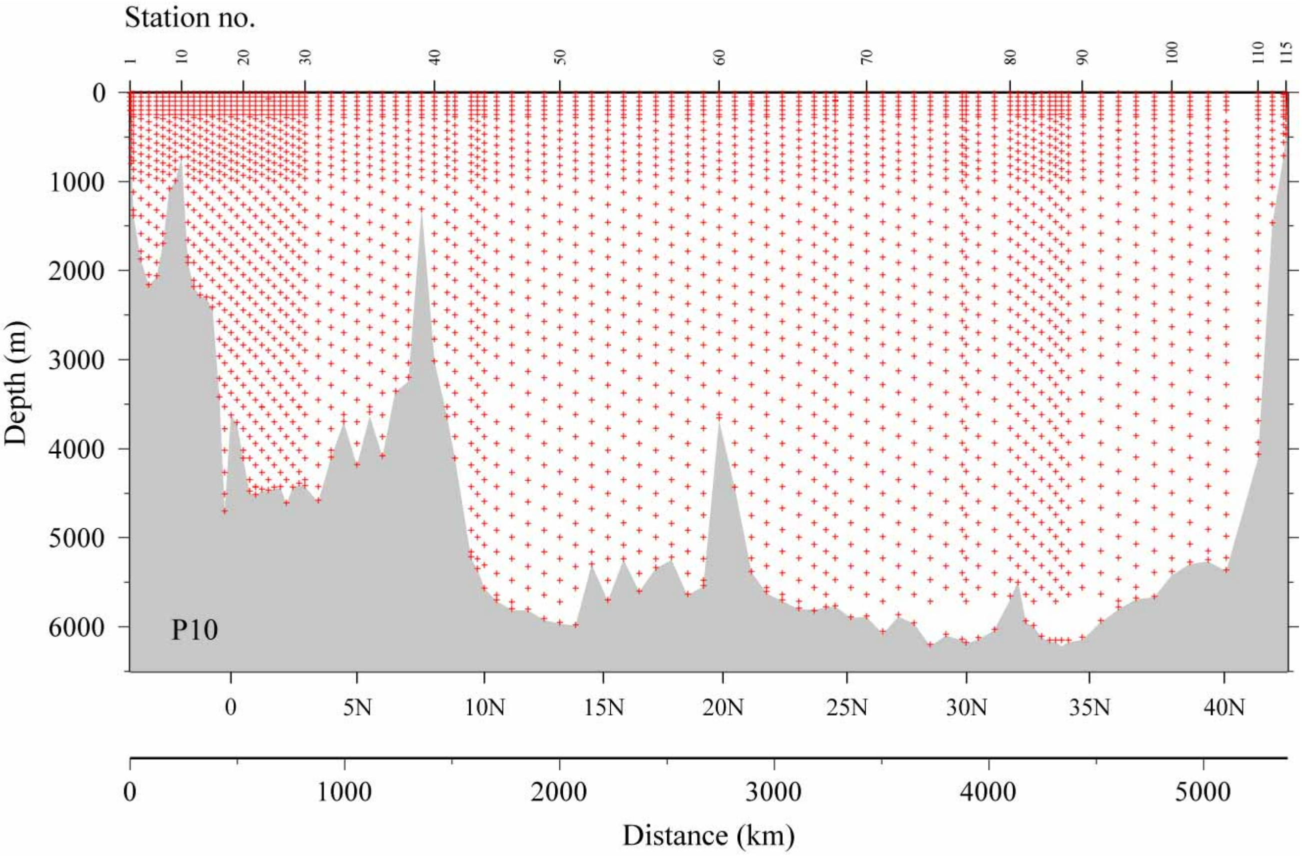

Fig. 1.1.3 Water sampling positions.

1.2. List of Cruise Participants

List of Participants for leg 1

Yuichiro Kumamoto	Chief scientist/carbon/water sampling	RIGC/JAMSTEC
Kenichi Sasaki	CFCs	MIO/JAMSTEC
Katsunori Sagishima	Chief technologist/nutrients/CFCs	MWJ
Shoko Tatamisashi	CFCs	MWJ
Tomonori Watai	pH/total alkalinity	MWJ
Ayaka Hatsuyama	pH/total alkalinity	MWJ
Hatsumi Aoyama	DIC	MWJ
Kazuho Yoshida	Chief technologist/meteorology/ geophysics/ADCP/XCTD	GODI
Ryo Kimura	Meteorology/geophysics/ADCP/XCTD	GODI

List of Participants for leg 2

Akihiko Murata	Chief Scientist/CTD/water sampling	RIGC/JAMSTEC
Yuichiro Kumamoto	DO/thermosalinograph /$\Delta^{14}C$	RIGC/JAMSTEC
Hiroshi Uchida	CTD/density/water sampling	RIGC/JAMSTEC
Shinya Kouketsu	LADCP/ADCP/water sampling	RIGC/JAMSTEC
Kazuhiko Hayashi	Water sampling	RIGC/JAMSTEC
Kenichi Sasaki	CFCs	MIO/JAMSTEC
Moyap Kilepak	Observer	University of Papua New Guinea
Benjamin Malai	Observer	National Weather Service/PNG
Osamu Yoshida	CH_4 and N_2O/water sampling	Rakuno Gakuen University
Yuki Okazaki	CH_4 and N_2O/water sampling	Rakuno Gakuen University
Shinichi Oikawa	CH_4 and N_2O/water sampling	Rakuno Gakuen University
Hikari Shimizu	CH_4 and N_2O/water sampling	Rakuno Gakuen University
Satoshi Ozawa	Chief technologist/CTD/water sampling	MWJ
Hirokatsu Uno	CTD/water sampling	MWJ
Fujio Kobayashi	Salinity	MWJ
Kenichi Kato	CTD/water sampling	MWJ
Shinsuke Toyoda	CTD/water sampling	MWJ
Hiroki Ushiromura	Salinity	MWJ
Shungo Oshitani	CTD/water sampling	MWJ
Kenichiro Sato	Nutrients	MWJ
Minoru Kamata	Nutrients	MWJ
Masanori Enoki	Nutrients	MWJ
Tomonori Watai	pH/total alkalinity	MWJ
Yoshiko Ishikawa	DIC/pCO_2	MWJ
Miyo Ikeda	DO	MWJ
Ayaka Hatsuyama	pH/total alkalinity	MWJ
Hatsumi Aoyama	DIC/pCO_2	MWJ
Masahiro Orui	CFCs	MWJ
Makoto Takada	Water sampling/radionuclides	MWJ
Katsunori Sagishima	CFCs	MWJ
Shoko Tatamisashi	CFCs	MWJ

Kanako Yoshida	DO	MWJ
Kanako Hatsuyama	pH/total alkalinity	MWJ
Yuki Miyajima	DO	MWJ
Elena Hayashi	Water sampling	MWJ
Tatsuya Ando	Water sampling	MWJ
Hitomi Takahashi	Water sampling	MWJ
Mizuho Yasui	Water sampling	MWJ
Daiki Hayashi	Water sampling	MWJ
Yusuke Ogiwara	Water sampling	MWJ
Satoshi Okumura	Chief technologist /meteorology/ geophysics/ADCP/XCTD	GODI
Kazuho Yoshida	Meteorology/geophysics/ADCP/XCTD	GODI
Ryo Kimura	Meteorology/geophysics/ADCP/XCTD	GODI

List of Participants for leg 3

Yuichiro Kumamoto	Chief scientist/DO/$\Delta^{14}C$	RIGC/JAMSTEC
Hiroshi Uchida	CTD/density/water sampling	RIGC/JAMSTEC
Katsuro Katsumata	XMP/LADCP/water sampling	RIGC/JAMSTEC
Toshimasa Doi	LADCP/water sampling	RIGC/JAMSTEC
Kazuhiko Hayashi	Water sampling	RIGC/JAMSTEC
Kenichi Sasaki	CFCs	MIO / JAMSTEC
Minoru Kitamura	Plankton	Biogeos/JAMSTEC
Eric Cruz	Plankton net dragging/water sampling	NMFS/NOAA
Nobuyoshi Yamashita	PFCs	AIST
Yuki Okazaki	CH_4 and N_2O/water sampling	Rakuno Gakuen University
Shinichi Oikawa	CH_4 and N_2O/water sampling	Rakuno Gakuen University
Hikari Shimizu	CH_4 and N_2O/water sampling	Rakuno Gakuen University
Yoshiko Ishikawa	Chief technologist /DIC/pCO_2	MWJ
Hideki Yamamoto	Water sampling/radionuclides	MWJ
Toru Idai	CTD/water sampling	MWJ
Kenichi Katayama	CTD/water sampling	MWJ
Naoko Miyamoto	CTD/water sampling	MWJ

Tatsuya Tanaka	Salinity	MWJ
Tamami Ueno	Salinity	MWJ
Kenichiro Sato	Nutrients	MWJ
Minoru Kamata	Nutrients	MWJ
Tomonori Watai	pH/total alkalinity	MWJ
Yasuhiro Arii	Nutrients	MWJ
Misato Kuwahara	DO	MWJ
Hatsumi Aoyama	DIC/pCO_2	MWJ
Makoto Takada	DIC/pCO_2	MWJ
Shinichiro Yokokawa	DO	MWJ
Katsunori Sagishima	CFCs	MWJ
Shoko Tatamisashi	CFCs	MWJ
Hironori Sato	DO	MWJ
Kanako Yoshida	DO	MWJ
Takami Mori	CTD/water sampling	MWJ
Yasumi Yamada	pH/total alkalinity	MWJ
Elena Hayashi	Water sampling	MWJ
Tatsuya Ando	Water sampling	MWJ
Rie Muranaka	Water sampling	MWJ
Shihomi Saito	Water sampling	MWJ
Emi Deguchi	Water sampling	MWJ
Erina Matsumoto	Water sampling	MWJ
Katsuhisa Maeno	Chief technologist /meteorology/ geophysics/ADCP/XCTD	GODI
Asuka Doi	Meteorology/geophysics/ADCP/XCTD	GODI
Kazuho Yoshida	Meteorology/geophysics/ADCP/XCTD	GODI
Toshimitsu Goto	Meteorology/geophysics/ADCP/XCTD	GODI

2. Underway Observation

2.1 Navigation

(1) Personnel

Kazuho Yoshida	*(Global Ocean Development Inc., GODI)*	*-leg1, leg2-*
Ryo Kimura	*(GODI)*	*-leg1, leg2-*
Satoshi Okumura	*(GODI)*	*-leg2-*
Katsuhisa Maeno	*(GODI)*	*-leg3-*
Asuka Doi	*(GODI)*	*-leg3-*
Toshimitsu Goto	*(GODI)*	*-leg3-*
Ryo Ohyama	*(MIRAI Crew)*	*-leg1, leg2, leg3-*

(2) System description

Ship's position and velocity were provided by Radio Navigation System on R/V Mirai. This system integrates GPS position, log speed, gyro compass heading and other basic data for navigation, and calculated speed/course over ground on workstation. Radio navigation System also distributed ship's standard time synchronized to GPS time server via Network Time Protocol. These data were logged on the network server as "SOJ" data every 5 seconds.

Sensors for navigation data are listed below;

i) GPS system: MultiFix6 (software version 1.01), Differential GPS system.
Receiver: Trimble SPS751, with two GPS antennas located on navigation deck, starboard side and port side, manually switched as to GPS receiving state and offset to radar-mast position, datum point.
Decoder: Fugro STARFIX 4100LR

ii) Doppler log: Furuno DS-30, which use three acoustic beam for current measurement under the hull.

iii) Gyrocompass: Tokimec TG-6000, sperry type mechanical gyrocompass.

iv) GPS time server: SEIKO TS-2540 Time Server, synchronizing to GPS satellite every 1 second.

(3) Data period (Times in UTC)

Leg1: 04:50 4th Dec. 2011 to 00:00 20th Dec. 2011
Leg2: 06:00 20th Dec. 2011 to 02:00 12th Jan. 2012
Leg3: 23:00 12th Jan. 2012 to 00:00 9th Feb. 2012

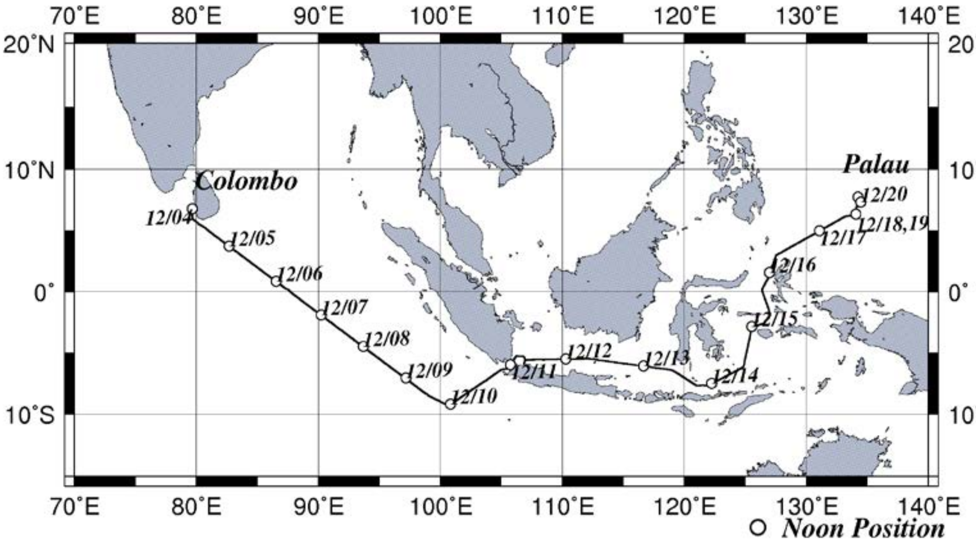

Fig.2.1-1 Cruise Track of MR11-08 Leg1

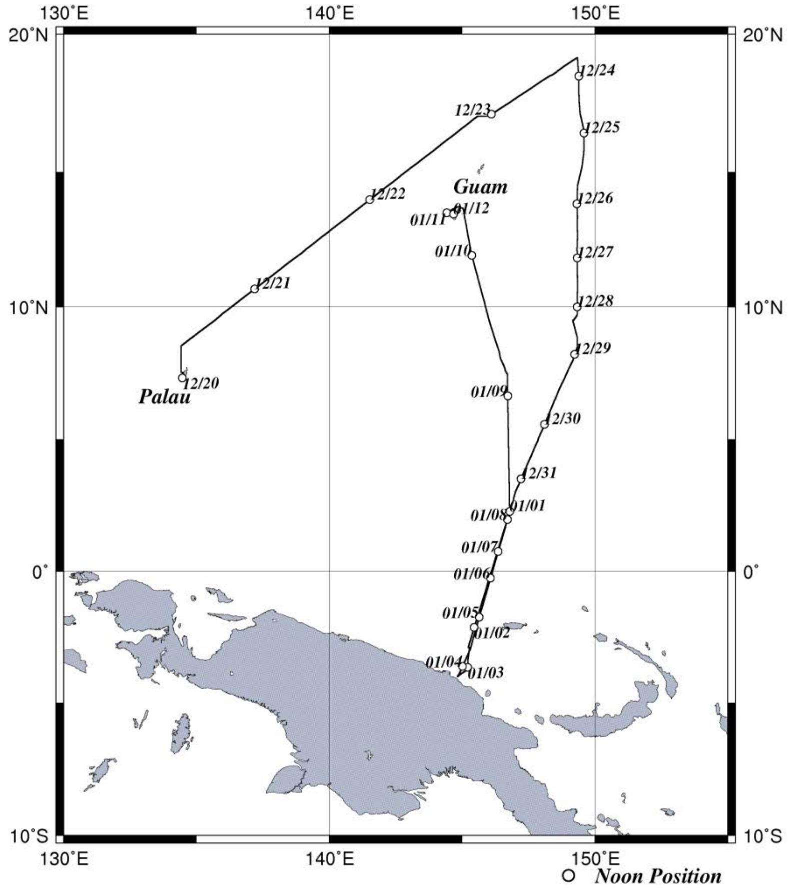

Fig.2.1-2 Cruise Track of MR11-08 Leg2

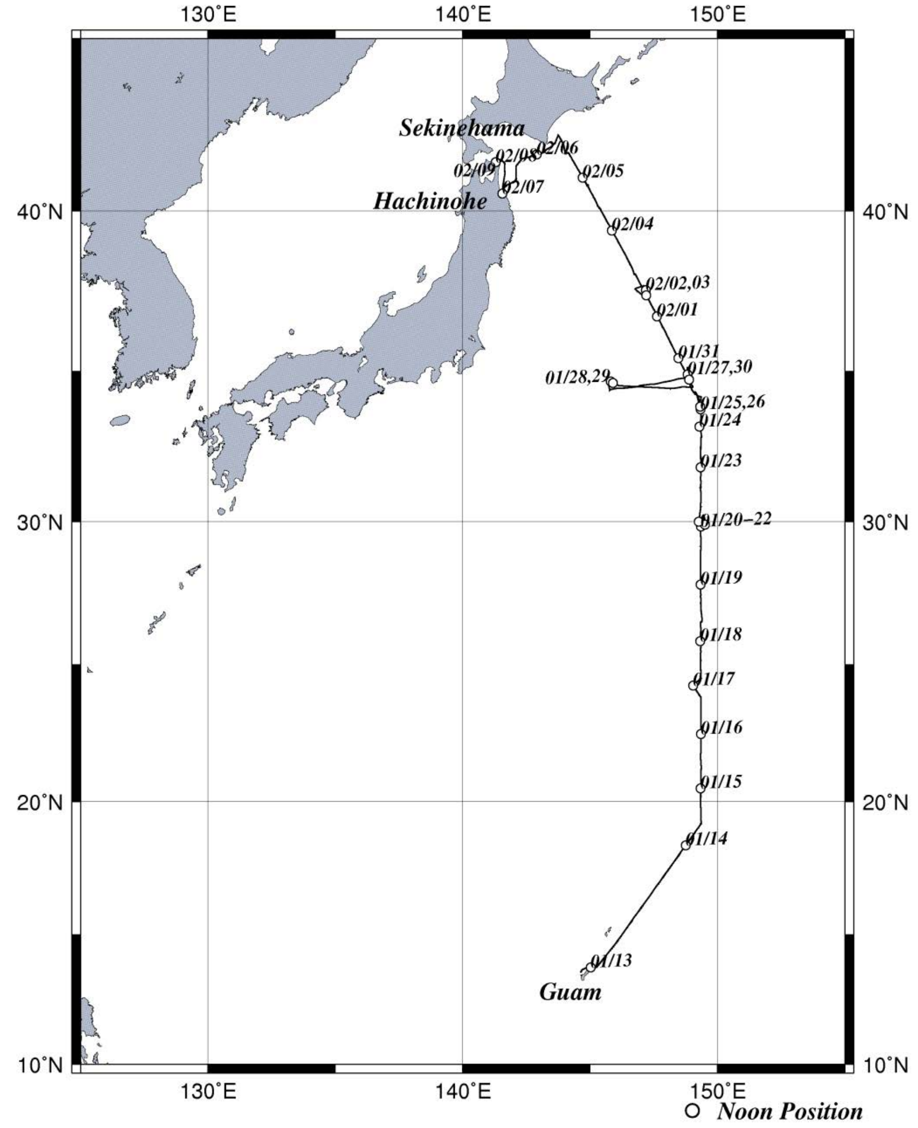

Fig.2.1-3 Cruise Track of MR11-08 Leg3

2.2 Swath Bathymetry

(1) Personnel

Takeshi Matsumoto	***(University of the Ryukyus)***	***: Principal Investigator (Not on-board)***
Naoto Hirano	***(Tohoku University)***	***: Principal Investigator (Not on-board)***
Kazuho Yoshida	***(GODI)***	***-leg1, leg2-***
Ryo Kimura	***(GODI)***	***-leg1, leg2-***
Satoshi Okumura	***(GODI)***	***-leg2-***
Katsuhisa Maeno	***(GODI)***	***-leg3-***
Asuka Doi	***(GODI)***	***-leg3-***
Toshimitsu Goto	***(GODI)***	***-leg3-***
Ryo Ohyama	***(MIRAI Crew)***	***-leg1, leg2, leg3-***

(2) Introduction

R/V MIRAI is equipped with a Multi narrow Beam Echo Sounding system (MBES), SEABEAM 2112 (SeaBeam Instruments Inc.). The objective of MBES is collecting continuous bathymetric data along ship's track to make a contribution to geological and geophysical investigations and global datasets.

(3) Data Acquisition

The "SEABEAM 2112" on R/V MIRAI was used for bathymetry mapping during the MR11-08 cruise from 4th December 2011 to 9th February 2012.

To get accurate sound velocity of water column for ray-path correction of acoustic multibeam, we used Surface Sound Velocimeter (SSV) data to get the sea surface (6.2m) sound velocity, and the deeper depth sound velocity profiles were calculated by temperature and salinity profiles from CTD or XCTD or ARGO data by the equation in Del Grosso (1974) during the cruise.

Table 2.2-1 shows system configuration and performance of SEABEAM 2112.004 system.

Table 2.2-1 System configuration and performance

SEABEAM 2112 (12 kHz system)	
Frequency:	12 kHz
Transmit beam width:	2 degree
Transmit power:	20 kW
Transmit pulse length:	3 to 20 msec.
Depth range:	100 to 11,000 m
Beam spacing:	1 degree athwart ship
Swath width:	150 degree (max)
	120 degree to 4,500 m

	100 degree to 6,000 m
	90 degree to 11,000 m
Depth accuracy:	Within < 0.5% of depth or +/-1m, whichever is greater, over the entire swath. (Nadir beam has greater accuracy; typically within < 0.2% of depth or +/-1m, whichever is greater)

(4) Data processing

i. Sound velocity correction

The continuous bathymetry data were split into small areas around each CTD station. For each small area, the bathymetry data were corrected with a sound velocity profile calculated from the CTD data or XCTD data in the area. The equation of Del Grosso (1974) was used for calculating sound velocity. The data processing is carried out using “mbprocess” command of MBsystem.

ii. Editing and Gridding

Gridding for the bathymetry data were carried out using the HIPS software version 7.1 (CARIS, Canada). Firstly, the bathymetry data during Ship’s turning was basically removed before “BASE surface” was made. A spike noise of each swath data was also removed using “swath editor” and “subset editor”. Then the bathymetry data was gridded by “Interpolate” function of the software with the parameters shown as table 2.2-2

Table 2.2-2 Parameters for interpolate of bathymetry data

BASE surface resolution:	50m
Interpolate matrix size:	5 x 5
Minimum number of neighbors for interpolate:	10

Finally, raw data and interpolated data are exported as ASCII data, and converted to 150m grid data using “xyz2grd” utility of GMT (Generic Mapping Tool) software.

(5) Data Archives

Bathymetric data obtained during this cruise will be submitted to the Data Management Group (DMG) of JAMSTEC, and will be archived there.

(6) Remarks (Times in UTC)

1) The observation was carried out within following periods,

Leg1: 10:00 5th Dec. 2011 to 08:30 10th Dec.2011

Leg2: 22:10 21th Dec. 2011 to 00:00 22th Dec. 2011
19:30 23th Dec. 2011 to 04:30 1st Jan. 2012
14:00 3rd Jan 2012 to 15:03 10th Jan. 2012

Leg3: 02:48 13th Jan. 2012 to 05:13 06th Feb 2012.

2) The following period, data acquisition was suspended due to system trouble and network trouble.

15:27 to 18:22 8th Dec. 2011
21:00 to 21:37 20th Dec. 2011
08:10 to 08:34 10th Jan. 2012
21:35 to 22:03 22th Jan. 2012
15:48 to 16:15 31th Jan. 2012

3) The following period, GPS data acquisition was suspended due to GPS trouble.

03:39 to 03:52 3rd Feb. 2012

2.3 Surface Meteorological Observations

(1) Personnel

Kazuho Yoshida (Global Ocean Development Inc., GODI) -leg1, leg2-
Ryo Kimura (GODI) -leg1, leg2-
Satoshi Okumura (GODI) -leg2-
Katsuhisa Maeno (GODI) -leg3-
Asuka Doi (GODI) -leg3-
Toshimitsu Goto (GODI) -leg3-
Ryo Ohyama (Mirai Crew) -leg1, leg2, leg3-

(2) Objectives

Surface meteorological parameters are observed as a basic dataset of the meteorology. These parameters provide the temporal variation of the meteorological condition surrounding the ship.

(3) Methods

Surface meteorological parameters were observed during the MR11-08 cruise from 4th December 2011 to 9th February 2012. In this cruise, we used two systems for the observation.

i. MIRAI Surface Meteorological observation (SMet) system

Instruments of SMet system are listed in Table 2.3-1 and measured parameters are listed in Table 2.3-2. Data were collected and processed by KOAC-7800 weather data processor made by Koshin-Denki, Japan. The data set consists of 6-second averaged data.

ii. Shipboard Oceanographic and Atmospheric Radiation (SOAR) measurement system

SOAR system designed by BNL (Brookhaven National Laboratory, USA) consists of major three parts.

a) Portable Radiation Package (PRP) designed by BNL – short and long wave downward radiation.
b) Zeno Meteorological (Zeno/Met) system designed by BNL – wind, air temperature, relative humidity, pressure, and rainfall measurement.
c) Scientific Computer System (SCS) developed by NOAA (National Oceanic and Atmospheric Administration, USA) – centralized data acquisition and logging of all data sets.

SCS recorded PRP data every 6 seconds, Zeno/Met data every 10 seconds. Instruments and their locations are listed in Table 2.3-3 and measured parameters are listed in Table 2.3-4.;

For the quality control as post processing, we checked the following sensors, before and after the cruise.

i. Young Rain gauge (SMet and SOAR)

Inspect of the linearity of output value from the rain gauge sensor to change Input value by adding fixed quantity of test water.

ii. Barometer (SMet and SOAR)

Comparison with the portable barometer value, PTB220, VAISALA

iii. Thermometer (air temperature and relative humidity) (SMet and SOAR)

Comparison with the portable thermometer value, HMP41/45, VAISALA

(4) Preliminary results

Fig. 2.3-1 shows the time series of the following parameters;

Wind (SMet)
Air temperature (SMet)
Relative humidity (SOAR)
Precipitation (SOAR, rain gauge)
Short/long wave radiation (SOAR)
Pressure (SMet)
Sea surface temperature (SMet)
Significant wave height (SMet)

(5) Data archives

These meteorological data will be submitted to the Data Management Group (DMG) of JAMSTEC just after the cruise.

(6) Remarks (Times in UTC)

1) The observation was carried out within the following periods

Leg1: 10:00 5th Dec. 2011 to 08:30 10th Dec. 2011
Leg2: 21:00 20th Dec. 2011 to 00:00 22th Dec. 2011
19:30 23th Dec.2011 to 04:30 1st Jan. 2012
14:00 3rd Jan. 2012 to 14:00 10th Jan. 2012
Leg3: 02:45 13th Jan. 2012 to 00:00 9th Feb 2012

2) The following periods, Sea surface temperature of SMet data was available.

Leg1: 10:00 5th Dec. 2011 to 08:30 11th Dec. 2011
Leg2: 08:00 20th Dec. 2011 to 05:29 10th Jan. 2012
Leg3: 02:45 13th Jan. 2012 to 23:00 5th Feb. 2012

3) The following period, SMer data was not available in due to system trouble.

17:25 to 22:04 7th Feb. 2012

Table 2.3-1 Instruments and installation locations of MIRAI Surface Meteorological observation system

Sensors	Type	Manufacturer	Location (altitude from surface)
Anemometer	KE-500	Koshin Denki, Japan	foremast (24 m)
Tair/RH	HMP45A	Vaisala, Finland	
with 43480 Gill aspirated radiation shield		R.M. Young, USA	compass deck (21 m) starboard side and port side
Thermometer: SST	RFN1-0	Koshin Denki, Japan	4th deck (-1m, inlet -5m)
Barometer	Model-370	Setra System, USA	captain deck (13 m)

			weather observation room
Rain gauge	50202	R. M. Young, USA	compass deck (19 m)
Optical rain gauge	ORG-815DR	Osi, USA	compass deck (19 m)
Radiometer (short wave)	MS-802	Eiko Seiki, Japan	radar mast (28 m)
Radiometer (long wave)	MS-202	Eiko Seiki, Japan	radar mast (28 m)
Wave height meter	MW-2	Tsurumi-seiki, Japan	bow (10 m)

Table 2.3-2 Parameters of MIRAI Surface Meteorological observation system

Parameter		Units	Remarks
1	Latitude	degree	
2	Longitude	degree	
3	Ship's speed	knot	Mirai log, DS-30 Furuno
4	Ship's heading	degree	Mirai gyro, TG-6000, Tokimec
5	Relative wind speed	m/s	6sec./10min. averaged
6	Relative wind direction	degree	6sec./10min. averaged
7	True wind speed	m/s	6sec./10min. averaged
8	True wind direction	degree	6sec./10min. averaged
9	Barometric pressure	hPa	adjusted to sea surface level 6sec. averaged
10	Air temperature (starboard side)	degC	6sec. averaged
11	Air temperature (port side)	degC	6sec. averaged
12	Dewpoint temperature (starboard side)	degC	6sec. averaged
13	Dewpoint temperature (port side)	degC	6sec. averaged
14	Relative humidity (starboard side)	%	6sec. averaged
15	Relative humidity (port side)	%	6sec. averaged
16	Sea surface temperature	degC	6sec. averaged
17	Rain rate (optical rain gauge)	mm/hr	hourly accumulation
18	Rain rate (capacitive rain gauge)	mm/hr	hourly accumulation
19	Down welling shortwave radiation	W/m2	6sec. averaged
20	Down welling infra-red radiation	W/m2	6sec. averaged
21	Significant wave height (bow)	m	hourly
22	Significant wave height (aft)	m	hourly
23	Significant wave period (bow)	second	hourly
24	Significant wave period (aft)	second	hourly

Table 2.3-3 Instruments and installation locations of SOAR system

Sensors (Zeno/Met)	Type	Manufacturer	Location (altitude from surface)
Anemometer	05106	R.M. Young, USA	foremast (25 m)
Tair/RH	HMP45A	Vaisala, Finland	
with 43408 Gill aspirated radiation shield		R.M. Young, USA	foremast (23 m)
Barometer	61202V	R.M. Young, USA	
with 61002 Gill pressure port		R.M. Young, USA	foremast (23 m)
Rain gauge	50202	R.M. Young, USA	foremast (24 m)
Optical rain gauge	ORG-815DA	Osi, USA	foremast (24 m)

Sensors (PRP)	Type	Manufacturer	Location (altitude from surface)
Radiometer (short wave)	PSP	Epply Labs, USA	foremast (25 m)
Radiometer (long wave)	PIR	Epply Labs, USA	foremast (25 m)
Fast rotating shadowband radiometer		Yankee, USA	foremast (25 m)

Table 2.3-4 Parameters of SOAR system

Parameter		Units	Remarks
1	Latitude	degree	
2	Longitude	degree	
3	SOG	knot	
4	COG	degree	
5	Relative wind speed	m/s	
6	Relative wind direction	degree	
7	Barometric pressure	hPa	
8	Air temperature	degC	
9	Relative humidity	%	
10	Rain rate (optical rain gauge)	mm/hr	
11	Precipitation (capacitive rain gauge)	mm	reset at 50 mm
12	Down welling shortwave radiation	W/m2	
13	Down welling infra-red radiation	W/m2	
14	Defuse irradiance	W/m2	

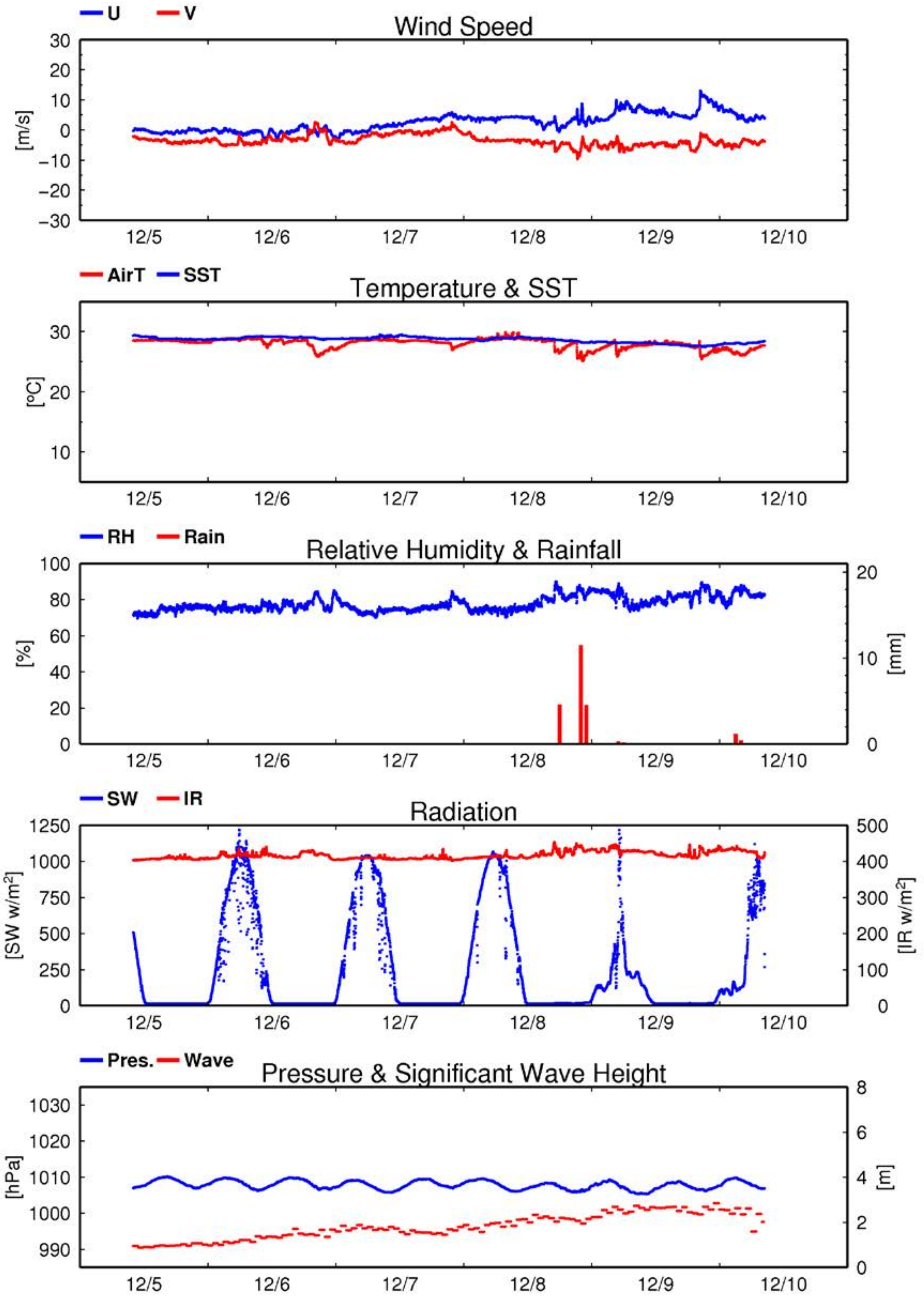

Fig. 2.3-1 Time series of surface meteorological parameters during the MR11-08 cruise

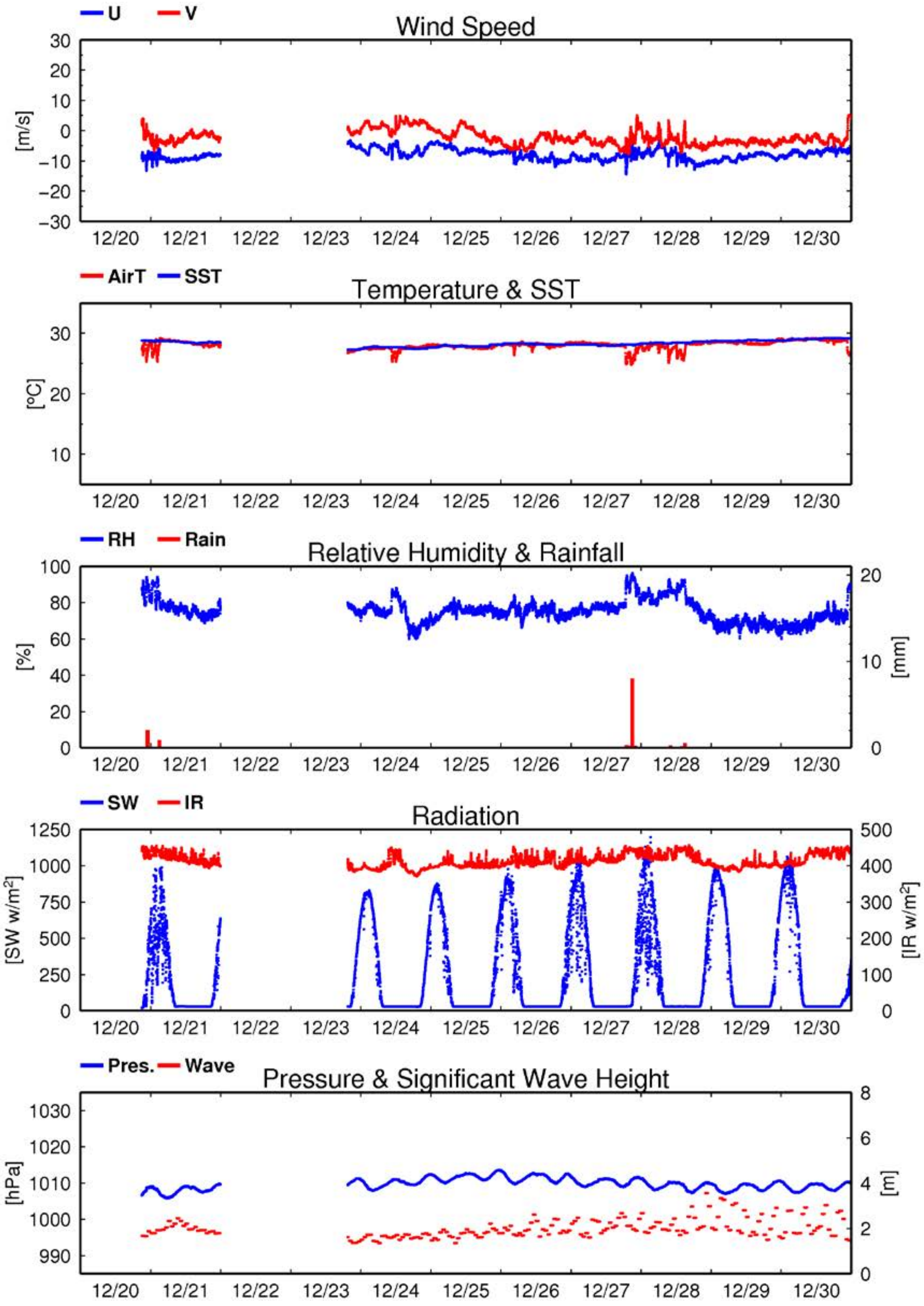

Fig. 2.3-1 (Continued)

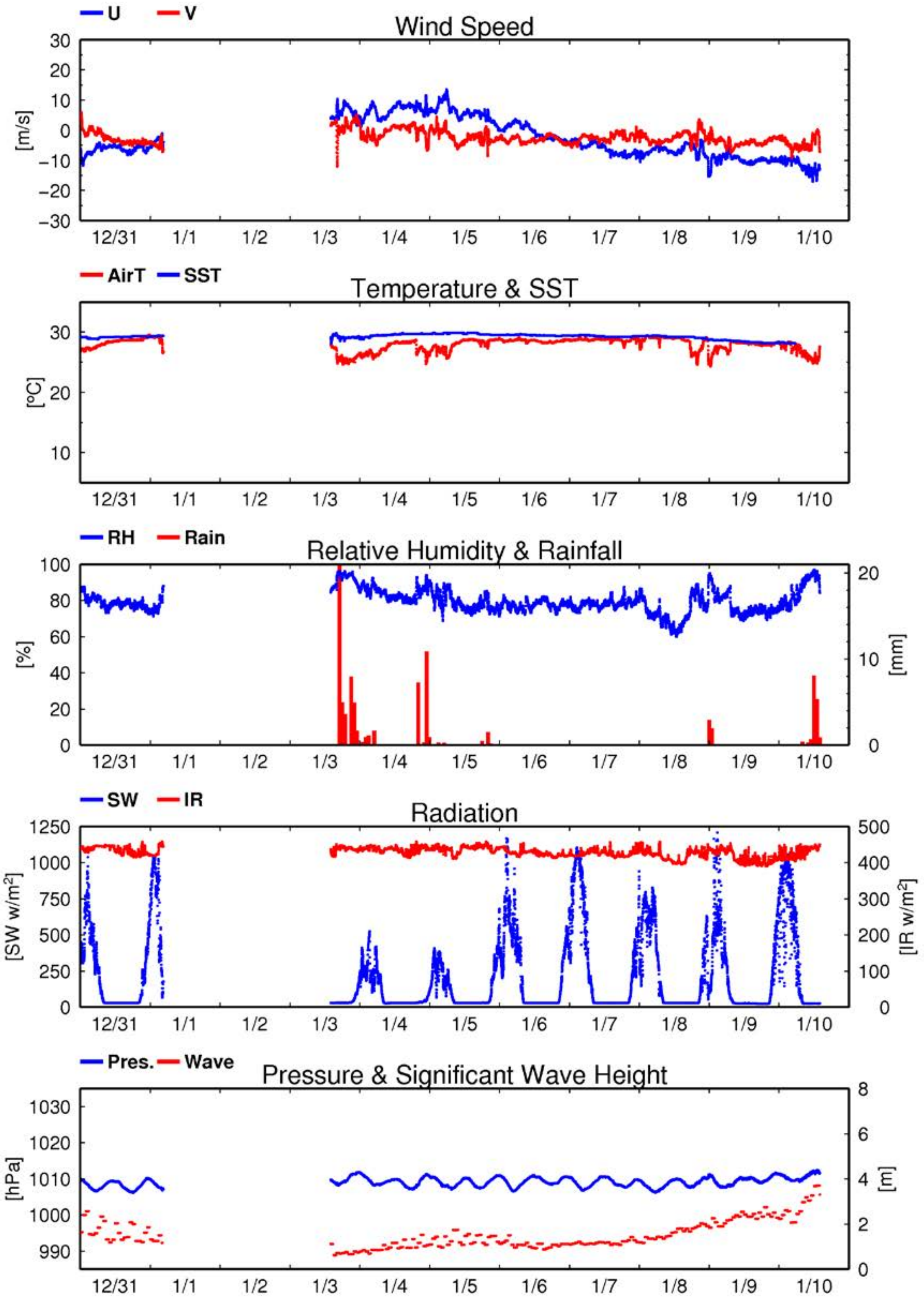

Fig. 2.3-1 (Continued)

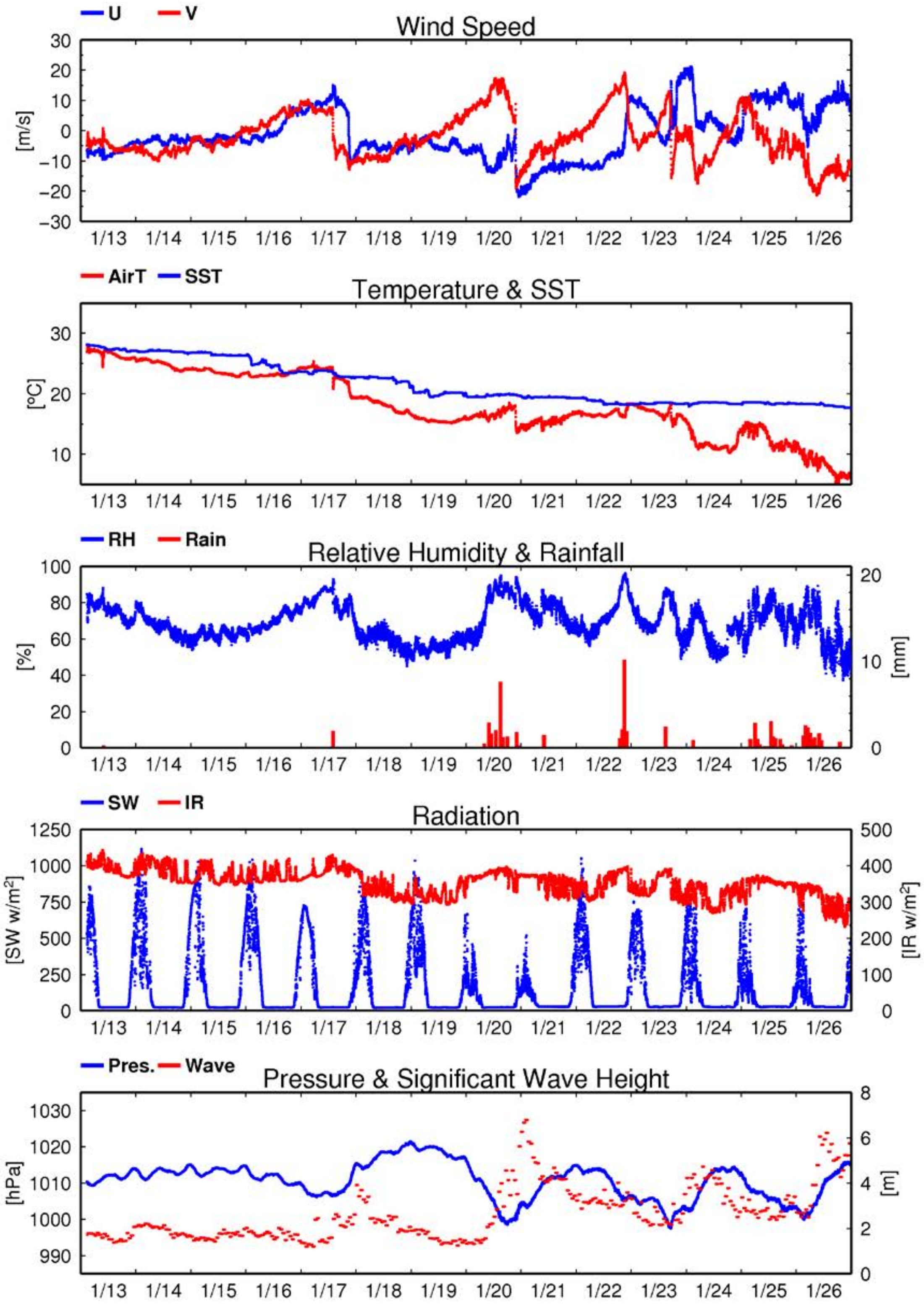

Fig. 2.3-1 (Continued)

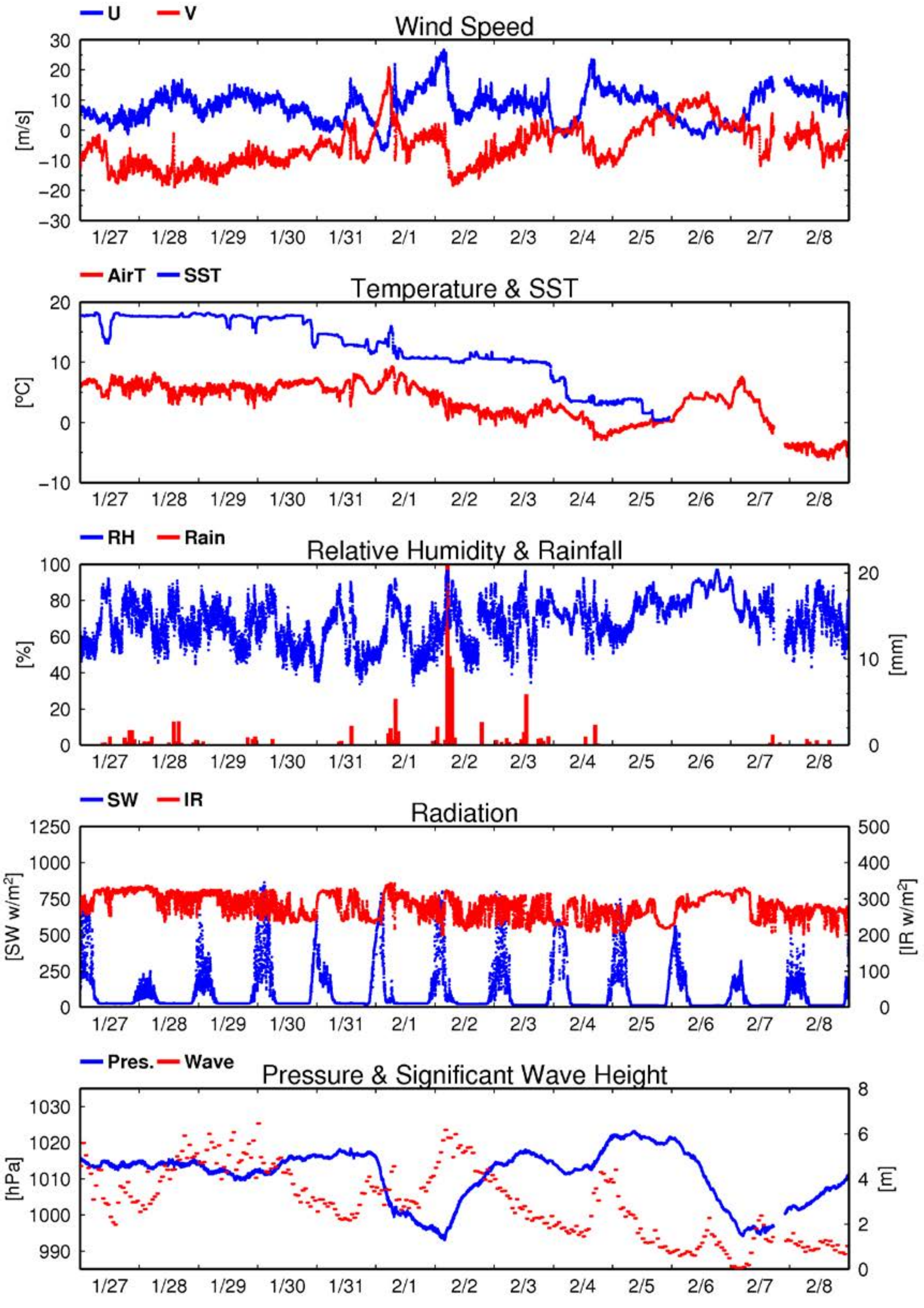

Fig. 2.3-1 (Continued)

2.4 Thermo-salinograph

May 11, 2012

(1) Personnel

Hiroshi Uchida (JAMSTEC)
Yuichiro Kumamoto (JAMSTEC) (Leg 1)
Katsunori Sagishima (MWJ) (Leg 1)
Miyo Ikeda (MWJ) (Leg 2)
Kanako Yoshida (MWJ) (Leg 2, 3)
Yuki Miyajima (MWJ) (Leg 2)
Misato Kuwahara (MWJ) (Leg 3)
Shinichiro Yokogawa (MWJ) (Leg 3)

(2) Objectives

The objective is to collect sea surface salinity, temperature, dissolved oxygen, and fluorescence data continuously along the cruise track.

(3) Materials and methods

The Continuous Sea Surface Water Monitoring System (Marine Works Japan Co, Ltd.) has six sensors and automatically measures salinity, temperature, dissolved oxygen, and fluorescence in near-sea surface water every one minute. This system is located in the sea surface monitoring laboratory and connected to shipboard LAN system. Measured data, time, and location of the ship were displayed on a monitor and stored in a data management PC. The near-surface water was continuously pumped up to the laboratory from about 4.5 m water depth and flowed into the system through a vinyl-chloride pipe. The flow rate of the surface seawater was controlled to be 5 dm^3/min. Manufacturer's specifications of the each sensor in this system are listed below.

i. Software

Seamoni-kun Ver.1.20

ii. Sensors

Temperature and conductivity sensor

Model:	SBE-45, SEA-BIRD ELECTRONICS, INC.
Serial number:	4563325-0362 (leg 1)
	4557820-0319 (legs 2, 3)
Measurement range:	Temperature –5 to 35ºC
	Conductivity 0 to 7 S m^{-1}
Initial accuracy:	Temperature 0.002ºC
	Conductivity 0.0003 S m^{-1}
Typical stability (per month):	Temperature 0.0002ºC

	Conductivity 0.0003 S m^{-1}
Resolution:	Temperatures 0.0001ºC
	Conductivity 0.00001 S m^{-1}

Bottom of ship thermometer

Model:	SBE 38, SEA-BIRD ELECTRONICS, INC.
Serial number:	3857820-0540
Measurement range:	–5 to +35ºC
Initial accuracy:	±0.001ºC
Typical stability (per 6 month):	0.001ºC
Resolution:	0.00025ºC

Dissolved oxygen sensor

Model:	OPTODE 3835, AANDERAA Instruments.
Serial number:	1519
Measuring range:	0 - 500 µmol L^{-1}
Resolution:	<1 µmol L^{-1}
Accuracy:	<8 µmol L^{-1} or 5% whichever is greater
Settling time (63%):	<25 s

Fluorometer

Model:	C3, TURNER DESIGNS
Serial number:	2300123

(4) Preliminary results

Data from the Continuous Sea Surface Water Monitoring System will be corrected by using the water sampled data for salinity, dissolved oxygen and chlorophyll-a. Details of the measurement methods is described in sections 3.2, 3.4, and 3.8 for salinity, dissolved oxygen and chlorophyll-a, respectively. Results of the comparisons are shown in Figs. 2.4.1, 2.4.2, and 2.4.3.

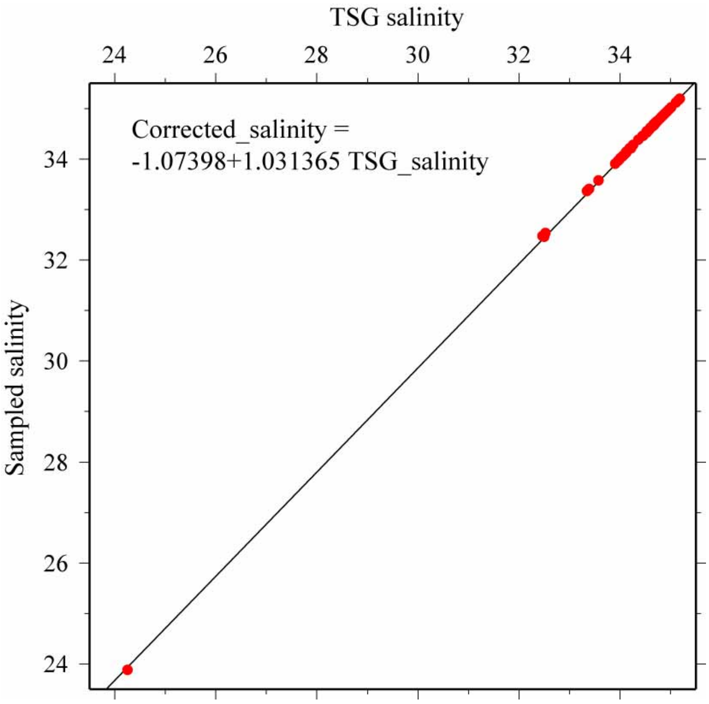

Figure 2.4.1. **Differences between TSG salinity and water sampled salinity.**

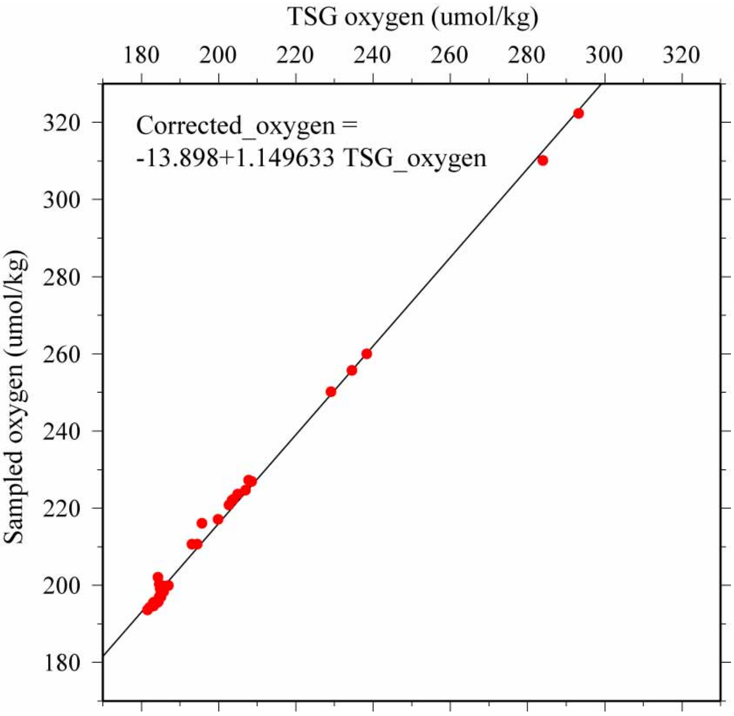

Figure 2.4.2. **Differences between TSG dissolved oxygen and water sampled dissolved oxygen.**

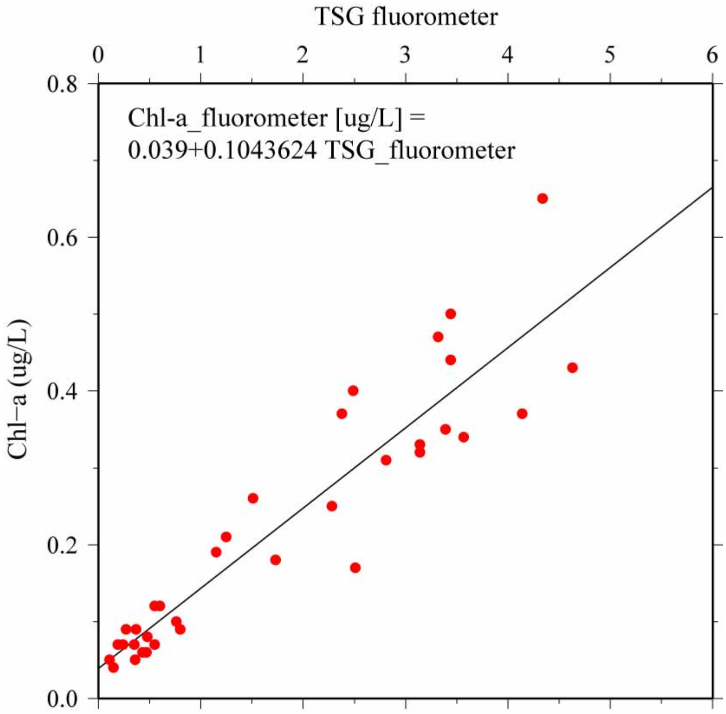

Figure 2.4.3. **Differences between TSG fluorometer output and water sampled chlorophyll-a.**

2.5. pCO_2

(1) Personnel

Akihiko Murata (JAMSTEC)

Yoshiko Ishikawa (MWJ)

Hatsumi Aoyama (MWJ)

Makoto Takada (MWJ)

(2) Objective

Concentrations of CO_2 in the atmosphere are now increasing at a rate of about 2.0 ppmv y^{-1} owing to human activities such as burning of fossil fuels, deforestation, and cement production. It is an urgent task to estimate as accurately as possible the absorption capacity of the oceans against the increased atmospheric CO_2, and to clarify the mechanism of the CO_2 absorption, because the magnitude of the anticipated global warming depends on the levels of CO_2 in the atmosphere, and because the ocean currently absorbs 1/3 of the 6 Gt of carbon emitted into the atmosphere each year by human activities.

In this cruise, we were aimed at quantifying how much anthropogenic CO_2 were absorbed in the surface ocean in the western Pacific. For the purpose, we measured pCO_2 (partial pressure of CO_2) in the atmosphere and surface seawater along the WHP P10 line at 149°E.

(3) Apparatus

Concentrations of CO_2 in the atmosphere and the sea surface were measured continuously during the cruise using an automated system with a non-dispersive infrared (NDIR) analyzer (Li-COR LI-7000). The automated system (Nippon ANS) was operated by about one and a half hour cycle. In one cycle, standard gasses, marine air and an air in a headspace of an equilibrator were analyzed subsequently. The nominal concentrations of the standard gas were 271, 331, 362 and 421 ppmv. The standard gases will be calibrated after the cruise.

The marine air taken from the bow was introduced into the NDIR by passing through a mass flow controller, which controlled the air flow rate at about 0.5 L/min, a cooling unit, a perma-pure dryer (GL Sciences Inc.) and a desiccant holder containing $Mg(ClO_4)_2$.

A fixed volume of the marine air taken from the bow was equilibrated with a stream of seawater that flowed at a rate of 4.7 L/min in the equilibrator. The air in the equilibrator was circulated with a pump at 0.7-0.8L/min in a closed loop passing through two cooling units, a perma-pure dryer (GL Science Inc.) and a desiccant holder containing $Mg(ClO_4)_2$.

(4) Results

Concentrations of CO_2 (xCO_2) of marine air and surface seawater are shown in Fig. 2.5.1, together with SST.

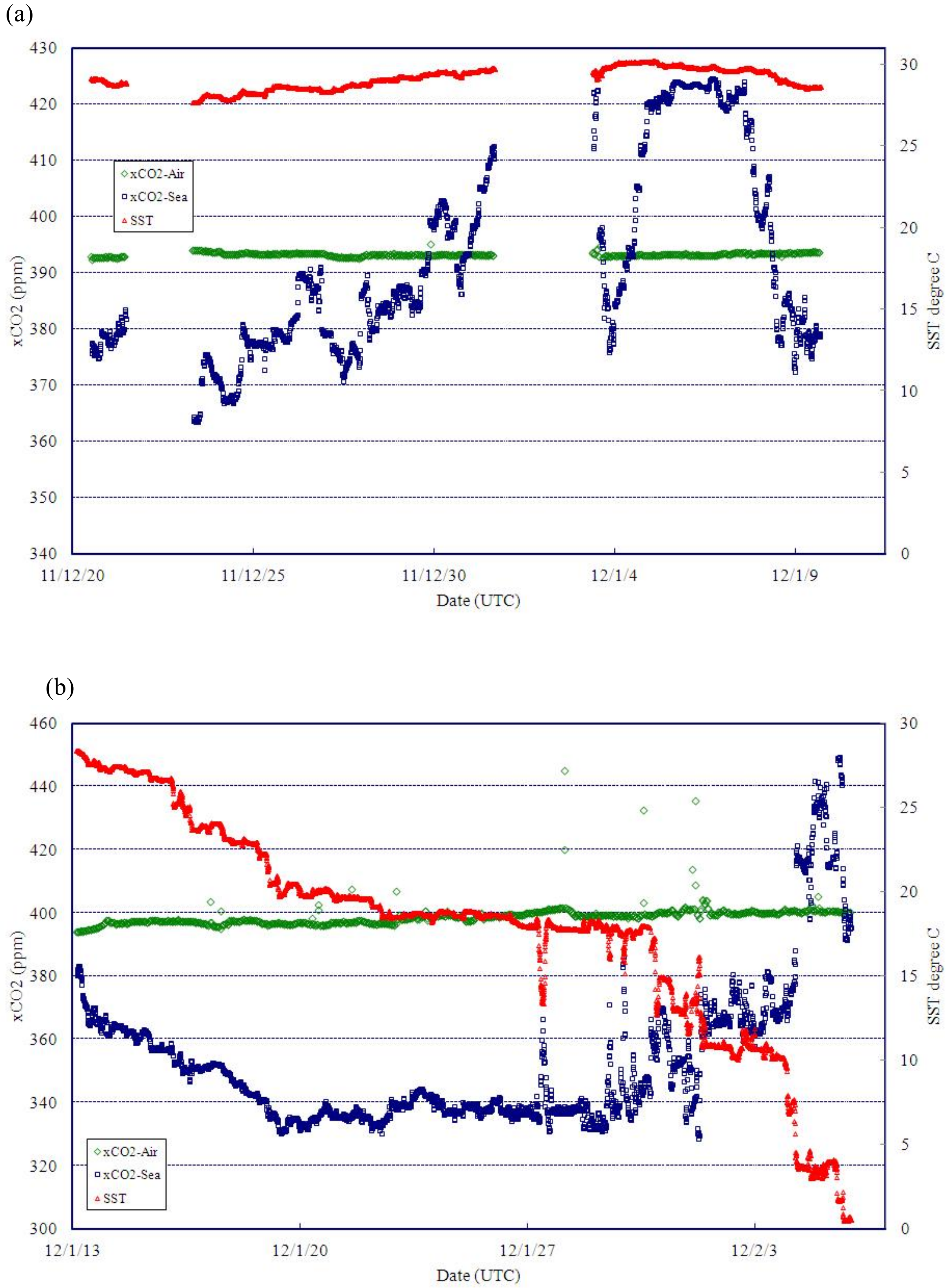

Fig. 2.5.1. Preliminary results of concentrations of CO_2 (xCO_2) in atmosphere (green) and surface seawater (blue), and SST (red) observed during (a) leg 2 and (b) leg 3 of MR11-08.

2.6 Shipboard ADCP

(1) Personnel

Shinya Kouketsu	***(JAMSTEC)***	***: Principal Investigator***
Kazuho Yoshida	***(Global Ocean Development Inc., GODI)***	***-leg1, leg2-***
Ryo Kimura	***(GODI)***	***-leg1, leg2-***
Satoshi Okumura	***(GODI)***	***-leg2-***
Katsuhisa Maeno	***(GODI)***	***-leg3-***
Asuka Doi	***(GODI)***	***-leg3-***
Toshimitsu Goto	***(GODI)***	***-leg3-***
Ryo Ohyama	***(MIRAI Crew)***	***-leg1, leg2, leg3-***

(2) Objective

To obtain continuous measurement of the current profile along the ship's track.

(3) Methods

Upper ocean current measurements were made in MR11-08 cruise, using the hull-mounted Acoustic Doppler Current Profiler (ADCP) system. For most of its operation the instrument was configured for water-tracking mode. Bottom-tracking mode, interleaved bottom-ping with water-ping, was made to get the calibration data for evaluating transducer misalignment angle in the shallow water. The system consists of following components;

1) R/V MIRAI has installed vessel-mount ADCP (75 kHz "Ocean Surveyor", Teledyne RD Instruments). It has a phased-array transducer with single assembly and creates 4 acoustic beams electronically.
2) For heading source, we use ship's gyro compass (Tokimec, Japan), continuously providing heading to the ADCP system directory. Also we have Inertial Navigation System (PHINS, iXSEA) which provide high-precision heading and attitude information are stored in ".N2R" data files.
3) DGPS system (Trimble SPS751 & StarFixXP) providing position fixes.
4) We used VmDas version 1.4.6 (TRDI) for data acquisition.
5) To synchronize time stamp of pinging with GPS time, the clock of the logging computer is adjusted to GPS time every 1 minute.
6) The sound speed at the transducer does affect the vertical bin mapping and vertical velocity measurement, is calculated from temperature, salinity (constant value; 35.0 psu) and depth (6.5 m; transducer depth) by equation in Medwin (1975).

Data was configured for 8-m intervals starting 19-m below the surface. Every ping was recorded as raw ensemble data (.ENR). Also, 60 seconds and 300 seconds averaged data were recorded as short term average

(.STA) and long term average (.LTA) data, respectively. Major parameters for the measurement (Direct Command) are shown in Table 2.6-1.

(4) Preliminary results

Fig.2.6-1, 2.6-2 and 2.6-3 shows surface current profile along the ship's track, averaged four depth cells from the top, 23 m to 55 m with 30 minutes average.

(5) Data archive

These data obtained in this cruise will be submitted to the Data Management Group (DMG) of JAMSTEC, and will be opened to the public via JAMSTEC home page.

(6) Remarks (Times in UTC)

The observation was carried out within following periods

Leg1:	10:00 5th Dec. 2011 to 08:30 10th Dec. 2011
Leg2:	22:10 21th Dec. 2011 to 00:00 22th Dec. 2011
	19:30 23th Dec. 2011 to 04:30 1st Jan. 2012
	14:00 3rd Jan. 2012 to 14:00 10th Jan. 2012
Leg3:	02:45 13th Jan. 2012 to 00:00 9th Feb. 2012

Table 2.6-1 Major parameters

Environmental Sensor Commands	
EA = +04500	Heading Alignment (1/100 deg)
EB = +00000	Heading Bias (1/100 deg)
ED = 00065	Transducer Depth (0 - 65535 dm)
EF = +001	Pitch/Roll Divisor/Multiplier (pos/neg) [1/99 - 99]
EH = 00000	Heading (1/100 deg)
ES = 35	Salinity (0-40 pp thousand)
EX = 00000	Coord Transform (Xform:Type; Tilts; 3Bm; Map)
EZ = 10200010	Sensor Source (C; D; H; P; R; S; T; U)
	C (1): Sound velocity calculates using ED, ES, ET (temp.)
	D (0): Manual ED
	H (2): External synchro
	P (0), R (0): Manual EP, ER (0 degree)
	S (0): Manual ES
	T (1): Internal transducer sensor
	U (0): Manual EU
Timing Commands	
TE = 00:00:02.00	Time per Ensemble (hrs:min:sec.sec/100)
TP = 00:02.00	Time per Ping (min:sec.sec/100)
Water-Track Commands	
WA = 255	False Target Threshold (Max) (0-255 count)
WB = 1	Mode 1 Bandwidth Control (0=Wid, 1=Med, 2=Nar)
WC = 120	Low Correlation Threshold (0-255)
WD = 111 100 000	Data Out (V; C; A; PG; St; Vsum; Vsum^2;#G;P0)
WE = 1000	Error Velocity Threshold (0-5000 mm/s)
WF = 0800	Blank After Transmit (cm)
WG = 001	Percent Good Minimum (0-100%)
WI = 0	Clip Data Past Bottom (0 = OFF, 1 = ON)
WJ = 1	Rcvr Gain Select (0 = Low, 1 = High)
WM = 1	Profiling Mode (1-8)
WN = 100	Number of depth cells (1-128)
WP = 00001	Pings per Ensemble (0-16384)
WS= 0800	Depth Cell Size (cm)
WT = 000	Transmit Length (cm) [0 = Bin Length]
WV = 0390	Mode 1 Ambiguity Velocity (cm/s radial)

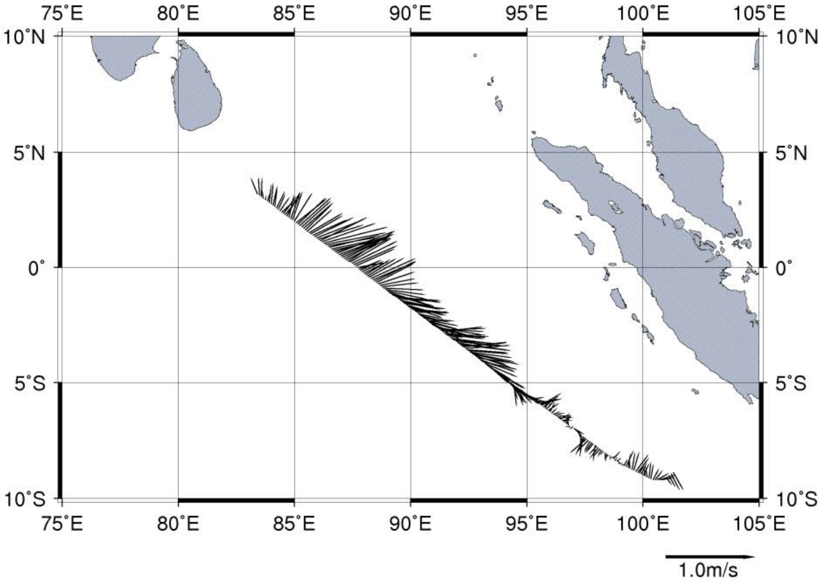

Fig 2.6-1 Current profile along the ship's track, from 23m to 55m, averaged every 30 minutes (Leg1).

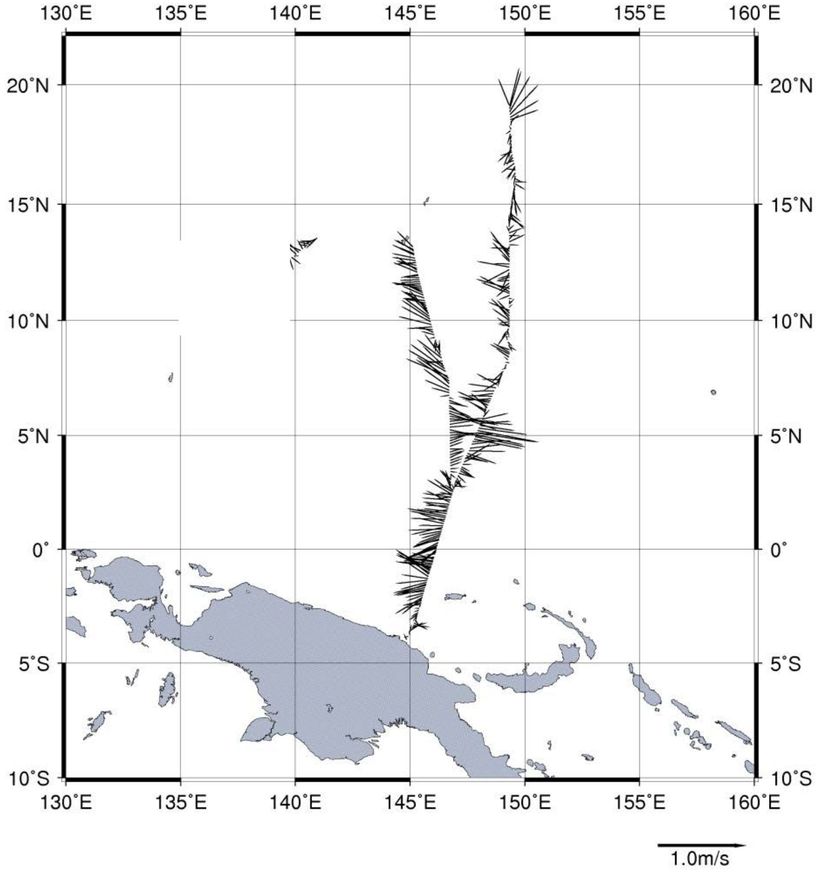

Fig 2.6-2 Current profile along the ship's track, from 23m to 55m, averaged every 30 minutes (Leg2).

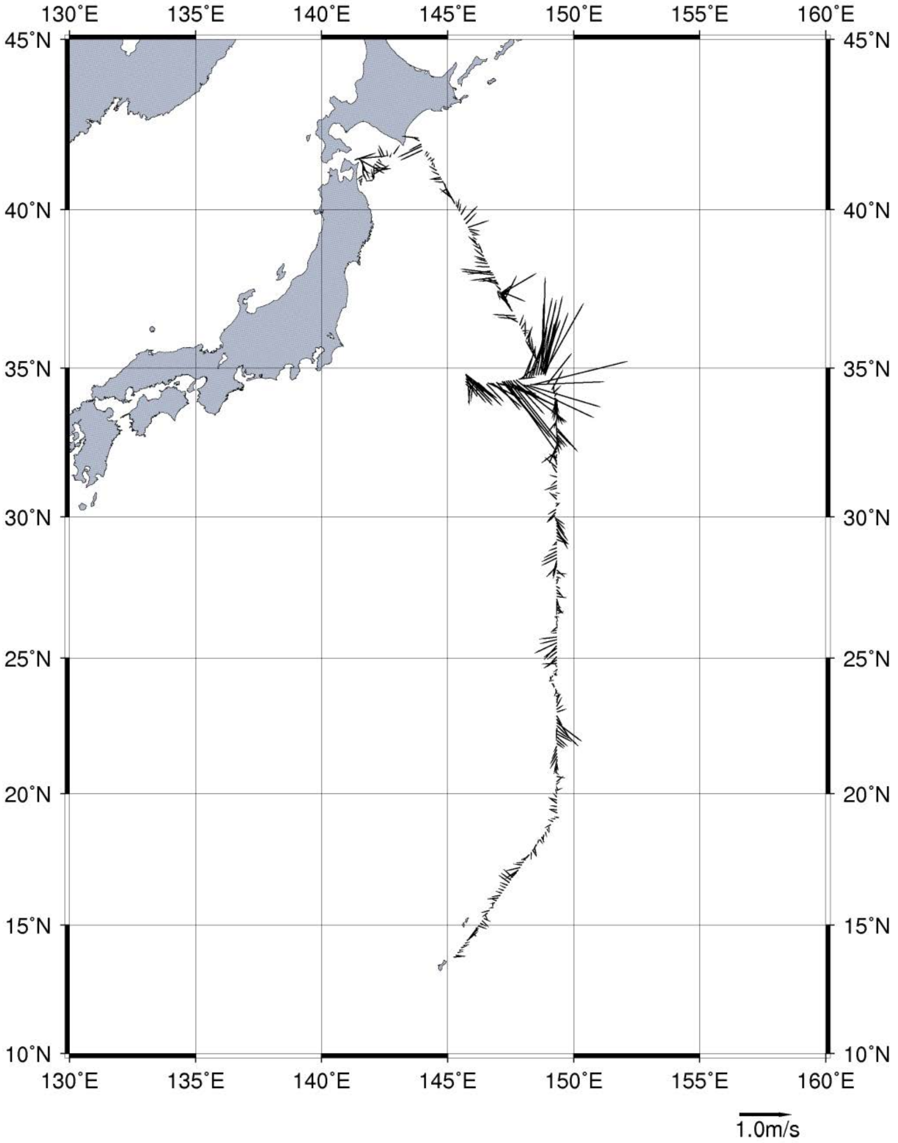

Fig 2.6-3 Current profile along the ship's track, from 23m to 55m, averaged every 30 minutes (Leg3).

2.7 Ceilometer observation

(1) Personnel

Kazuho Yoshida	***(Global Ocean Development Inc., GODI)***	***-leg1, leg2-***
Ryo Kimura	***(GODI)***	***-leg1, leg2-***
Satoshi Okumura	***(GODI)***	***-leg2-***
Katsuhisa Maeno	***(GODI)***	***-leg3-***
Asuka Doi	***(GODI)***	***-leg3-***
Toshimitsu Goto	***(GODI)***	***-leg3-***
Ryo Ohyama	***(MIRAI Crew)***	***-leg1, leg2, leg3-***

(2) Objectives

The information of cloud base height and the liquid water amount around cloud base is important to understand the process on formation of the cloud. As one of the methods to measure them, the ceilometer observation was carried out.

(3) Parameters

1. Cloud base height [m].
2. Backscatter profile, sensitivity and range normalized at 30 m resolution.
3. Estimated cloud amount [oktas] and height [m]; Sky Condition Algorithm.

(4) Methods

We measured cloud base height and backscatter profile using ceilometer (CT-25K, VAISALA, Finland). Major parameters for the measurement configuration are shown in Table 2.7-1;

Table 2.7-1 Major parameters

Laser source:	Indium Gallium Arsenide (InGaAs) Diode
Transmitting center wavelength:	905±5 nm at 25 degC
Transmitting average power:	8.9 mW
Repetition rate:	5.57 kHz
Detector:	Silicon avalanche photodiode (APD) Responsibility at 905 nm: 65 A/W
Measurement range:	0 ~ 7.5 km
Resolution:	50 ft in full range
Sampling rate:	60 sec
Sky Condition:	0, 1, 3, 5, 7, 8 oktas (9: Vertical Visibility) (0:Sky Clear, 1:Few, 3:Scattered, 5,7:Broken, 8:Overcast)

On the archive dataset, cloud base height and backscatter profile are recorded with the resolution of 30 m (100 ft).

(5) Preliminary results

Fig.2.7-1, Fig.2.7-2 and Fig.2.7-3 show the time series of 1st, 2nd and 3rd lowest cloud base height during the cruise.

(6) Data archives

The raw data obtained during this cruise will be submitted to the Data Management Group (DMG) of JAMSTEC.

(7) Remarks (Times in UTC)

1) The observation was carried out within the following periods.

Leg1: 10:00 5th Dec. 2011 to 08:30 10th Dec. 2011
Leg2: 21:00 20th Dec. 2011 to 00:00 22th Dec. 2011
19:30 23th Dec. 2011 to 04:30 1st Jan. 2012
14:00 3rd Jan. 2012 to 14:00 10th Jan. 2012
Leg3: 02:45 13th Jan. 2012 to 00:00 9th Feb. 2012

2) Window was cleaned at the following time.

02:40 20th Dec. 2011
05:51 25th Dec. 2011
03:55 3rd Jan. 2012
03:11 12th Jan. 2012
04:33 29th Jan. 2012

3) The following period, data acquisition was suspended due to the logging PC trouble.

14:12 to 20:01 9th Jan. 2012

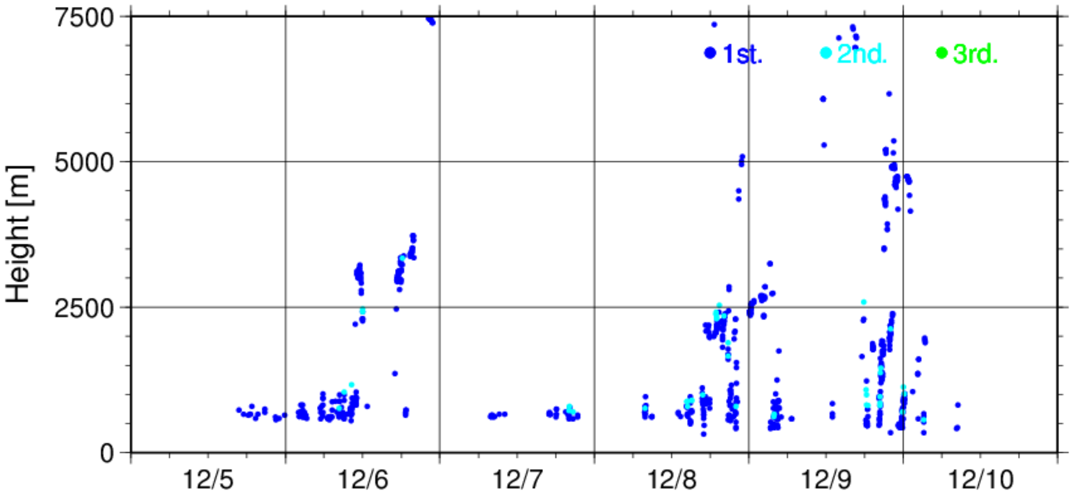

Fig. 2.7-1 1st, 2nd and 3rd lowest cloud base height during the MR11-08 leg1 cruise.

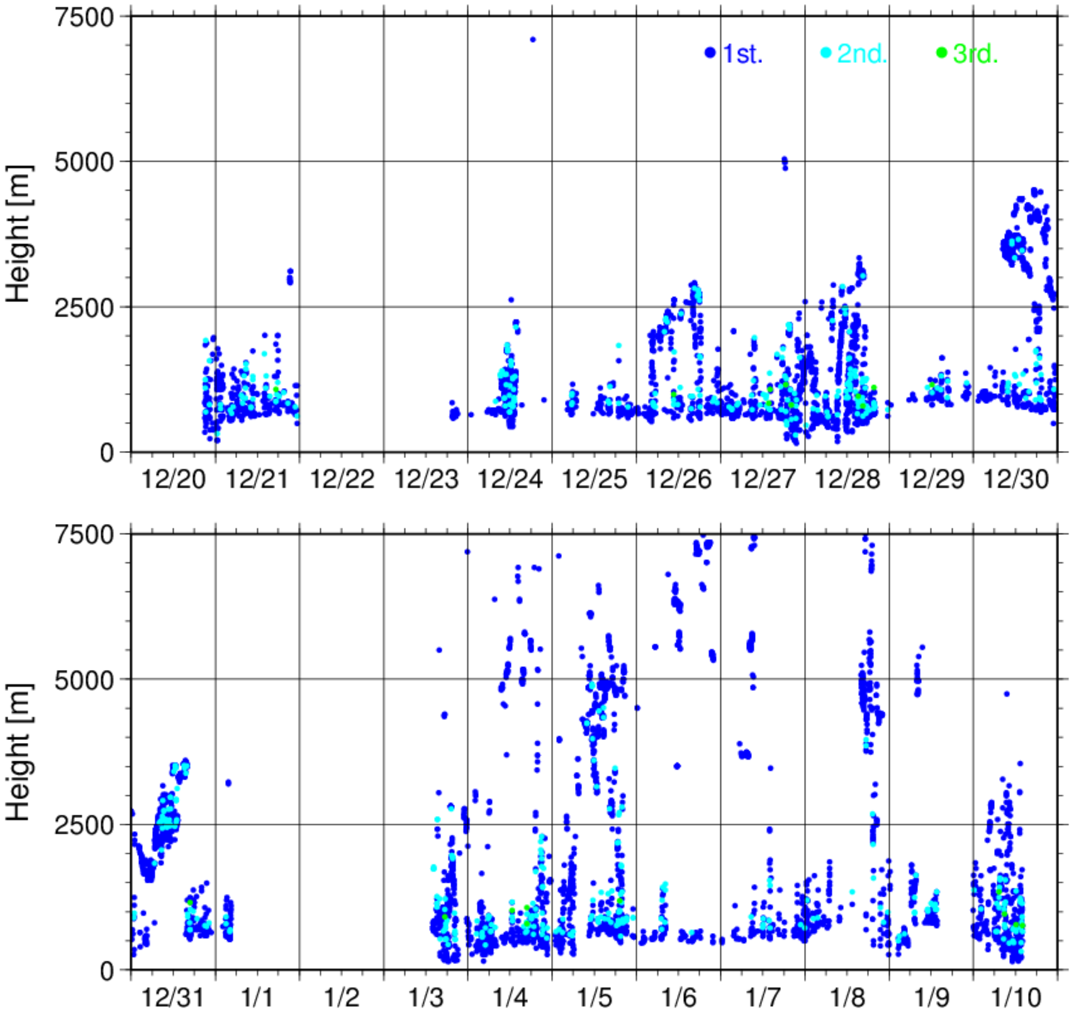

Fig. 2.7-2 1st, 2nd and 3rd lowest cloud base height during the MR11-08 leg2 cruise.

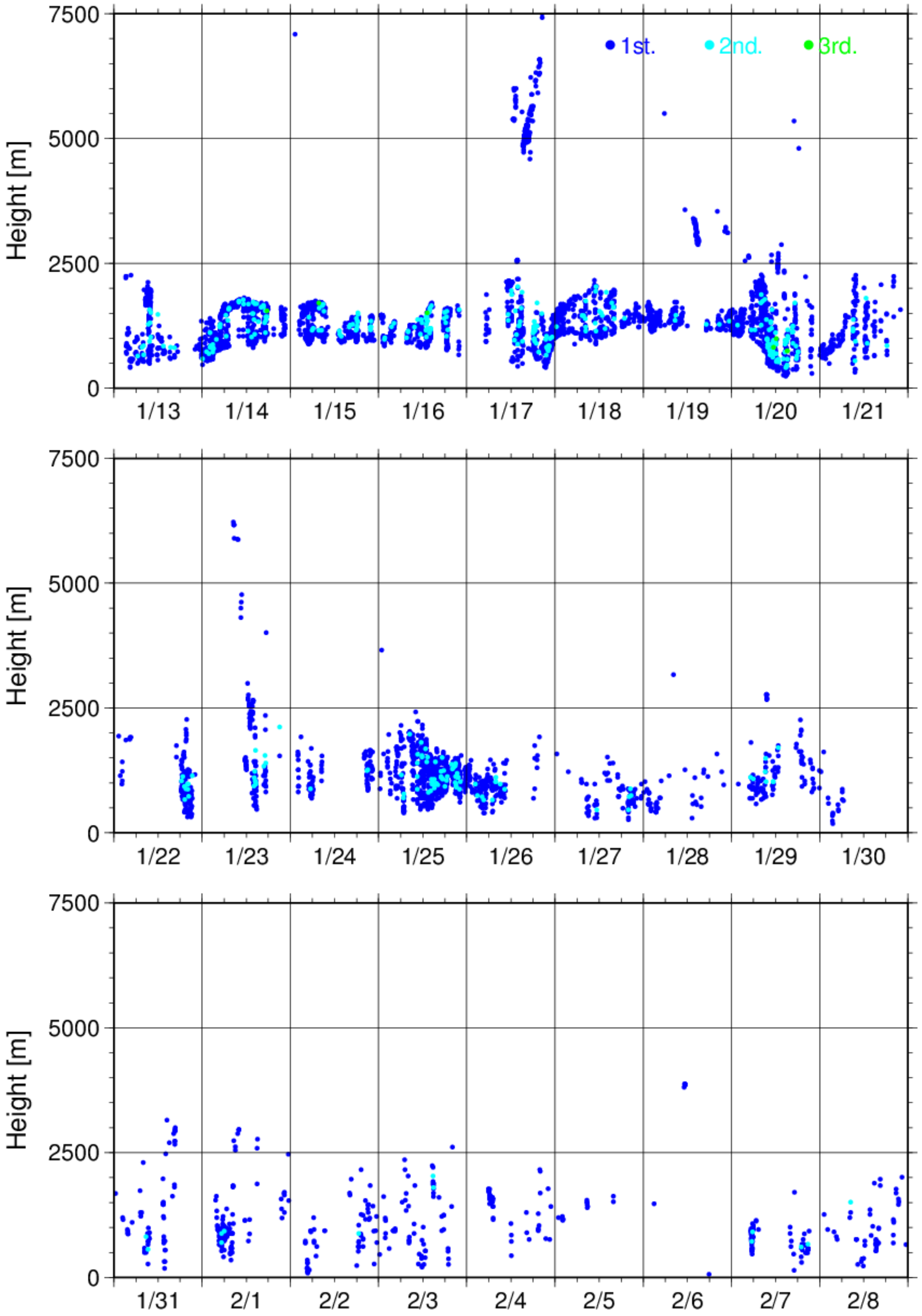

Fig. 2.7-3 1st, 2nd and 3rd lowest cloud base height during the MR11-08 leg3 cruise.

2.8 Air-sea surface eddy flux measurement

(1) Personnel

Osamu Tsukamoto	(Okayama University)	Principal Investigator	* not on board
Fumiyoshi Kondo	(University of Tokyo) * not on board		
Hiroshi Ishida	(Kobe University) * not on board		
Satoshi Okumura	(Global Ocean Development Inc. (GODI))		

(2) Objective

To better understand the air-sea interaction, accurate measurements of surface heat and fresh water budgets are necessary as well as momentum exchange through the sea surface. In addition, the evaluation of surface flux of carbon dioxide is also indispensable for the study of global warming. Sea surface turbulent fluxes of momentum, sensible heat, latent heat, and carbon dioxide were measured by using the eddy correlation method that is thought to be most accurate and free from assumptions. These surface heat flux data are combined with radiation fluxes and water temperature profiles to derive the surface energy budget.

(3) Instruments and Methods

The surface turbulent flux measurement system (Fig. 1) consists of turbulence instruments (Kaijo Co., Ltd.) and ship motion sensors (Kanto Aircraft Instrument Co., Ltd.). The turbulence sensors include a three-dimensional sonic anemometer-thermometer (Kaijo, DA-600) and an infrared hygrometer (LICOR, LI-7500). The sonic anemometer measures three-dimensional wind components relative to the ship. The ship motion sensors include a two-axis inclinometer (Applied Geomechanics, MD-900-T), a three-axis accelerometer (Applied Signal Inc., QA-700-020), and a three-axis rate gyro (Systron Donner, QRS-0050-100). LI7500 is a CO_2/H_2O turbulence sensor that measures turbulent signals of carbon dioxide and water vapor simultaneously. These signals are sampled at 10 Hz by a PC-based data logging system (Labview, National Instruments Co., Ltd.). By obtaining the ship speed and heading information through the Mirai network system it yields the absolute wind components relative to the ground. Combining wind data with the turbulence data, turbulent fluxes and statistics are calculated in a real-time basis. These data are also saved in digital files every 0.1 second for raw data and every 1 minute for statistic data.

(4) Observation log

The observation was carried out throughout this cruise.

(5) Data Policy and citation

All data are archived at Okayama University, and will be open to public after quality checks and corrections. Corrected data will be submitted to JAMSTEC Marine-Earth Data and Information Department.

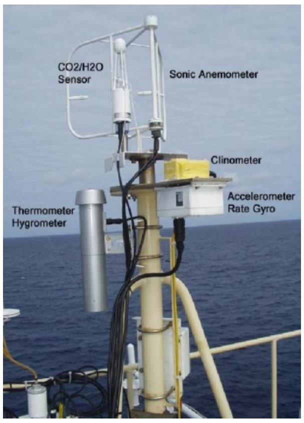

Fig. 1 Turbulent flux measurement system on the top deck of the foremast

2.9 Lidar

(1) Personnel

Nobuo Sugimoto (NIES)

Ichiro Matsui (NIES)

Atsushi Shimizu(NIES)

Tomoaki Nishizawa (NIES)

(Lidar operation was supported by Global Ocean Development Inc. (GODI).)

(2) Objectives

Objectives of the observations in this cruise is to study distribution and optical characteristics of ice/water clouds and marine aerosols using a two-wavelength polarization Mie lidar.

(3) Measured parameters

Vertical profiles of backscatter coefficient at 532nm
Vertical profiles of backscatter coefficient at 1064nm
Vertical profiles of depolarization ratio at 532nm

(4) Method

Vertical profiles of aerosols and clouds are measured with a two-wavelength polarization Mie lidar. The lidar employs a Nd:YAG laser as a light source which generates the fundamental output at 1064nm and the second harmonic at 532nm. Transmitted laser energy is typically 30mJ per pulse at both of 1064 and 532nm. The pulse repetition rate is 10Hz. The receiver telescope has a diameter of 20 cm. The receiver has three detection channels to receive the lidar signals at 1064 nm and the parallel and perpendicular polarization components at 532nm. An analog-mode avalanche photo diode (APD) is used as a detector for 1064nm, and photomultiplier tubes (PMTs) are used for 532 nm. The detected signals are recorded with a transient recorder and stored on a hard disk with a computer. The lidar system was installed in a container which has a glass window on the roof, and the lidar was operated continuously regardless of weather. Every 10 minutes vertical profiles of four channels (532 parallel, 532 perpendicular, 1064, 532 near range) are recorded.

(5) Results

The two wavelength polarization Mie lidar worked well for all the observation period and we succeeded in getting the lidar data. Examples of the measured data are depicted in Fig. 1. The figure indicates that the lidar can detect maritime aerosols in the planetary boundary layer (PBL) formed below 1km, water clouds formed at the top of the PBL, ice clouds in the upper layer and rain falling from clouds. Especially, it should be noted that the lidar could detect ice clouds (cirrus) up to very high altitude of 16km since optical and microphysical properties and distributions of cirrus are key parameters for evaluating climate change.

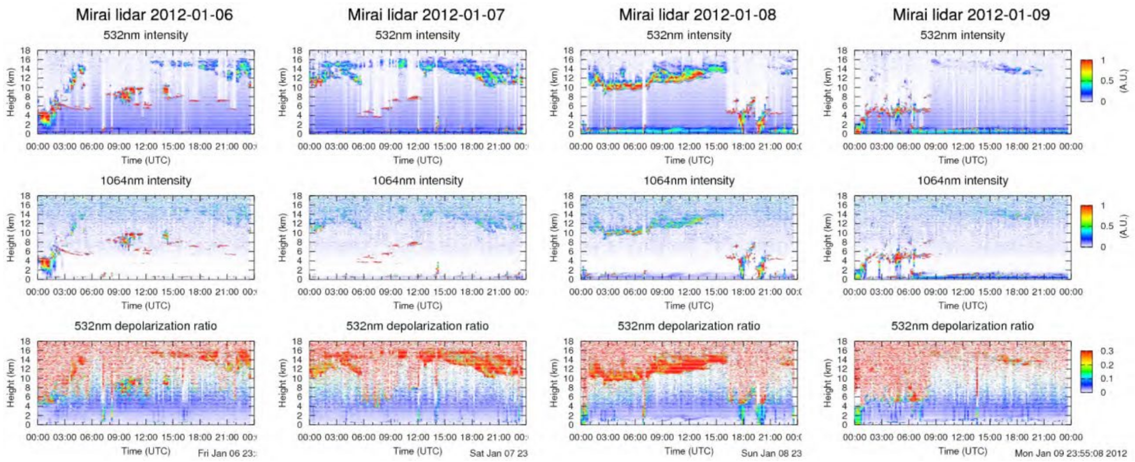

Figure 1: Time-height sections of backscatter intensities at 532nm and 1064nm and total depolarization ratios at 532nm measured from 6 January 2012 to 9 January 2012.

(6) Data archive

- raw data

lidar signal at 532 nm

lidar signal at 1064 nm

depolarization ratio at 532 nm

temporal resolution 10min/ vertical resolution 6 m

data period (UTC): Dec. 5, 2011 – Feb. 8, 2012

processed data (plan)

cloud base height, apparent cloud top height

phase of clouds (ice/water)

cloud fraction

boundary layer height (aerosol layer upper boundary height)

backscatter coefficient of aerosols

particle depolarization ratio of aerosols

(7) Data policy and Citation

Contact NIES lidar team (nsugimot/i-matsui/shimizua/nisizawa@nies.go.jp) to utilize lidar data for productive use.

2.10 Isotopes in rainfall and water vapor

(1) Personnel

Naoyuki Kurita (JAMSTEC) *Principal Investigator （not on-board）*

Operator

Katsuhisa Maeno (Global Ocean Development Inc.: GODI)

(2) Objective

It is well known that the variability of stable water isotopes (HDO and $H_2{}^{18}O$) reflects the integrated history of water mass exchange that occurs during transportation from the upstream region. Thus, water isotope tracer is recognized as the powerful tool to study of the hydrological cycles in the marine atmosphere. However, oceanic region is one of sparse region of the isotope data, it is necessary to fill the data to identify the moisture sources by using the isotope tracer. In this study, to fill this sparse observation area, intense water isotopes observation was conducted along the cruise track of MR11-07.

(3) Method

Following observation was carried out throughout this cruise.

- Atmospheric moisture sampling:

Ambient air sampling was conducted using both latest laser based water vapor isotope analyzer (WVIA) and conventional cryogenic cold trap method. We used different air-sampling tube lines for each sampling. Both air-sampling lines connected at the middle level (20m above the sea level) of the mast at the compass deck to the laboratory. Air was drawn by external pump at a flow rate of 2 Lmin-1 for laser instrument and 1.5-3.0 Lmin-1 for cold trap method (flow rate was adjustment depending on the concentration). As for laser based measurement, every 50 minutes, the 3-way valve in the instrument automatically switched from ambient inlet to WVISS reference air, and then reference air with a H2O mixing ratio of 10000 ppmv was introduced to the WVIA during 10 minutes. After finishing reference gas measurement, the valve switches back to ambient inlet and ambient air sampling is resumed. The WVIA can measure HDO and H218O in the water vapor every second.

As for collection of vapor samples in cold trap, sampled air was passed through a glass trap in an ethanol bath, which was thermoelectrically cooled to -100 degree C. It is collected every 12 hour during the cruise. Amount of cold-trapped vapor was between 5 and 30g. After collection, water in the trap was subsequently thawed and poured into the 6ml glass bottle.

- Rainwater sampling

Rainwater samples gathered in rain/snow collector were collected just after precipitation events have ended. The collected sample was then transferred into glass bottle (6ml) immediately after the measurement of precipitation amount.

- Surface seawater sampling

Seawater sample taken by the pump from 4m depth were collected in glass bottle (6ml) around the noon at the local time.

(4) Water samples for isotope analysis

Sampling of water vapor for isotope analysis is summarized in Table 2.10-1 (85 samples). The detail of rainfall sampling (32 samples) is summarized in Table 2.10-2. Described rainfall amount is calculated from the collected amount of precipitation. Sampling of surface seawater taken by pump from 4m depths is summarized in Table 2.10-3

(63 samples).

(5) Data archive

The isotopic data of water vapor can obtain from the laser based water vapor isotope analyzer on board. The archived raw observed data was submitted to JAMSTEC Data Management Group (DMG) after the cruise immediately. As for collected water samples, isotopes (HDO, $H_2{}^{18}O$) analysis will be done at RIGC/JAMSTEC, and then analyzed isotopes data will be submitted to JAMSTEC DMG.

Table 2.10-1 Summary of water vapor sampling for isotope analysis

	Start		End						
Sample	Date	Time (UT)	Date	Time (UT)	Lon	Lat	T.M. (m^3)	Sam. (ml)	H2O ppm
V-1	12.5	10:24	12.6	03:06	86-05.0E	1-10.8N	1.47	29.5	24974
V-2	12.6	03:09	12.6	15:00	87-57.3E	0-13.5S	1.05	22.0	26074
V-3	12.6	15:03	12.7	03:03	89-47.5E	1-36.3S	1.07	22.0	25587
V-4	12.7	03:06	12.7	15:00	91-28.9E	2-52.9S	1.07	20.0	23261
V-5	12.7	15:04	12.8	03:00	93-12.8E	4-11.3S	1.07	22.5	26168
V-6	12.8	03:03	12.8	15:00	95-00.6E	5-31.4S	1.07	23.0	26750
V-7	12.8	15:02	12.9	03:00	96-43.3E	6-48.1S	1.07	22.0	25587
V-8	12.9	03:03	12.9	15:00	98-26.8E	8-05.4S	1.06	23.0	27002
V-9	12.9	15:02	12.10	03:36	100-26.7E	9-12.3S	1.12	24.0	26667
V-10	12.10	03:38	12.10	08:30	101-21.8E	8-50.8S	0.54	12.5	28807
V-11	12.20	21:08	12.21	12:01	138-47.3E	11-53.6N	1.30	27.9	26708
V-13	12.23	19:42	12.24	00:00	149-20.6E	19-08.9N	0.38	6.2	20304
V-14	12.24	00:03	12.24	12:07	149-23.2E	17-50.8N	1.08	21.5	24774
V-15	12.24	12:11	12.25	00:00	149-35.0E	16-29.8N	1.06	18.5	21719
V-16	12.25	00:07	12.25	12:42	149-29.9E	15-10.1N	1.13	22.0	24228
V-17	12.25	12:46	12.26	00:00	149-20.0E	14-30.4N	1.02	20.0	24401
V-18	12.26	00:04	12.26	12:00	149-20.0E	13-17.6N	1.07	20.5	23842
V-19	12.26	12:03	12.27	00:00	149-19.6E	12-25.9N	1.07	21.5	25005
V-20	12.27	00:02	12.27	12:00	149-20.0E	11-09.3N	1.07	21.8	25354
V-21	12.27	12:03	12.28	00:00	149-20.1E	10-00.4N	1.07	22.2	25819
V-22	12.28	00:05	12.28	13:59	149-10.0E	9-29.4N	1.24	25.5	25591
V-23	12.28	14:00	12.29	00:00	149-19.8E	8-30.3N	0.89	18.0	25169
V-24	12.29	00:05	12.29	12:03	148-43.0E	7-02.8N	1.07	20.0	23261
V-25	12.29	12:06	12.30	00:00	148-16.4E	6-00.3N	1.07	19.8	23028
V-26	12.30	00:03	12.30	12:00	147-51.3E	5-00.1N	1.07	20.0	23261
V-27	12.30	12:02	12.31	00:00	147-26.7E	4-00.6N	1.07	21.5	25005

V-28	12.31	00:07	12.31	12:04	146-57.6E	2-51.7N	1.08	22.5	25926
V-29	12.31	12:07	1.1	00::09	146-47.0E	2-15.2N	1.08	23.0	26502
V-30	1.1	00:14	1.1	04:29	146-45.2E	2-16.2N	0.46	9.8	26512
V-31	1.3	14:07	1.4	00:00	144-55.3E	3-49.6S	0.14	2.0	17778
V-32	1.4	00:05	1.4	12:00	144-21.3E	2-45.7S	1.06	22.0	25828
V-33	1.4	12:03	1.5	00:00	145-34.1E	2-00.2S	1.07	22.6	26285
V-34	1.5	00:05	1.5	12:00	145-48.1E	1-11.6S	1.07	22.5	26168
V-35	1.5	12:05	1.6	00:00	146-00.2E	0-28.6S	1.07	22.5	26168
V-36	1.6	00:05	1.6	12:20	146-08.5E	0-00.0S	1.10	24.0	27152
V-37	1.6	12:24	1.7	00:01	146-21.3E	0-44.7N	1.03	22.0	26580
V-38	1.7	00:07	1.7	12:00	146-30.1E	01-14.8N	1.06	22.5	26415
V-39	1.7	12:03	1.8	00:00	146-38.6E	01-45.1N	1.07	22.2	25819
V-40	1.8	00:04	1.8	12:00	146-46.3E	03-18.3N	1.07	22.0	25587
V-41	1.8	12:05	1.9	00:00	146-43.3E	06-12.2N	1.06	20.0	23480
V-42	1.9	00:05	1.9	11:00	146-15.6E	08-42.8N	0.98	19.5	24762
V-43	1.9	11:04	1.9	23:08	145-29.7E	11-25.6N	1.08	20.4	23506
V-44	1.9	23:11	1.10	11:00	145-12.3E	12-43.2N	1.06	22.0	25828
V-45	1.10	11:05	1.10	13:55	145-07.2E	13-12.1N	0.43	7.5	21961
V-46	1.13	02:55	1.13	12:07	146-36.6E	15-30.1N	0.83	14.4	21590
V-47	1.13	12:10	1.14	00:03	148-19.7E	17-48.9N	1.06	16.4	19254
V-48	1.14	00:06	1.14	12:01	149-19.8E	19-10.8N	1.07	15.9	18492
V-49	1.14	12:04	1.15	02:18	149-19.8E	20-29.5N	1.27	15.2	14894
V-50	1.15	02:19	1.15	12:01	149-20.5E	21-10.8N	0.86	9.4	13602
V-51	1.15	12:03	1.16	00:00	149-20.1E	21-53.0N	1.08	11.9	13712
V-52	1.16	00:01	1.16	12:01	149-20.5E	23-10.7N	1.08	12.4	14288
V-53	1.16	12:05	1.17	00:00	149-02.3E	24-14.6N	1.07	13.8	16050
V-54	1.17	00:02	1.17	12:00	149-18.9E	24-29.1N	1.08	17.4	20049
V-55	1.17	12:03	1.18	00:04	149-19.6E	25-49.9N	1.08	14.6	16823
V-56	1.18	00:04	1.18	12:00	149-19.9E	26-29.9N	1.07	8.2	9537
V-57	1.18	12:03	1.19	00:00	149-19.9E	27-30.3N	1.07	6.4	7443
V-58	1.19	00:01	1.19	12:00	149-19.8E	28-29.9N	1.07	6.2	7211
V-59	1.19	12:04	1.20	00:00	149-20.0E	29-43.5N	1.07	6.2	7211
V-60	1.20	00:01	1.20	12:00	149-18.4E	29-56.9N	1.44	10.5	9074
V-61	1.20	12:02	1.21	00:00	149-20.2E	29-58.4N	1.99	15.8	9881
V-62	1.21	00:02	1.21	12:01	149-23.7E	30-10.2N	2.17	19.0	10896
V-63	1.21	12:06	1.22	00:00	149-15.1E	29-58.8N	2.15	17.8	10303
V-64	1.22	00:03	1.22	12:00	149-20.3E	30-58.4N	2.15	16.2	9377

V-65	1.22	12:03	1.23	00:00	149-19.7E	31-50.2N	2.13	21.8	12737
V-66	1.23	00:03	1.23	12:00	149-20.0E	32-29.6N	1.79	15.2	10567
V-67	1.23	12:03	1.24	00:18	149-21.1E	32-56.7N	1.85	14.4	9686
V-68	1.24	00:20	1.24	12:00	149-19.3E	33-11.7N	1.75	10.0	7111
V-69	1.24	12:02	1.25	00:00	149-20.2E	33-35.7N	1.78	8.2	5733
V-70	1.25	00:01	1.25	12:00	149-11.4E	34-12.9N	1.79	12.0	8343
V-71	1.25	12:04	1.26	00:01	149-19.2E	33-44.0N	2.16	12.4	7144
V-72	1.26	00:03	1.26	12:01	149-08.5E	34-14.6N	2.17	11.5	6595
V-73	1.26	12:03	1.27	00:01	148-50.3E	35-05.6N	2.14	6.2	3605
V-74	1.27	00:03	1.28	00:00	145-43.6E	34-31.9N	4.29	16.0	4641
V-75	1.28	00:03	1.29	00:24	145-50.2E	34-41.1N	4.36	16.0	4567
V-76	1.29	00:26	1.30	00:01	145-50.3E	34-50.1N	4.21	14.5	4286
V-77	1.30	00:02	1.31	00:08	148-30.5E	35-19.4N	4.32	13.2	3802
V-78	1.31	00:09	2.1	00:05	147-37.6E	36-44.5N	4.30	14.0	4052
V-79	2.1	00:06	2.2	00:57	147-13.6E	37-27.8N	4.42	16.0	4505
V-80	2.2	00:59	2.3	00:01	147-11.6E	37-25.2N	4.12	16.2	4893
V-81	2.3	00:02	2.4	00:02	145-53.7E	39-20.7N	4.28	11.2	3256
V-82	2.4	00:05	2.5	00:37	144-52.7E	40-46.8N	4.39	13.0	3685
V-83	2.5	00:39	2.6	00:00	143-27.5E	41-54.7N	4.17	9.8	2925
V-84	2.6	00:03	2.7	00:05	141-32.6E	40-31.8N	4.29	18.2	5279
V-85	2.7	00:08	2.8	00:03	141-16.8E	41-27.6N	4.31	15.2	4389

Table 2.10-2 Summary of precipitation sampling for isotope analysis.

	Date	Time (UT)	Lon	Lat	Date	Time (UT)	Lon	Lat	Rain (mm)	R/S
R-1	12.05	10:00	83-29.0E	03-08.0N	12.08	17:44	95-22.9E	05-49.0S	5.9	R
R-2	12.08	17:44	95-22.9E	05-49.0S	12.09	00:19	96-20.5E	06-30.5S	18.8	R
R-3	12.09	00:19	96-20.5E	06-30.5S	12.10	08:30	101-21.8E	08-50.8S	3.5	R
R-4	12.20	21:04	136-06.5E	09-50.8N	12.21	23:52	140-57.1E	13-33.4N	9.5	R
R-6	12.28	20:27	149-19.8E	08-50.2N	1.01	04:30	146-05.0E	02-17.0N	1.8	R
R-7	1.03	16:22	144-49.8E	03-59.7S	1.04	05:28	145-09.2E	03-18.6S	38.6	R
R-8	1.04	05:28	145-09.2E	03-18.6S	1.05	00:15	145-34.1E	02-00.2S	21.4	R
R-9	1.05	00:15	145-34.1E	02-00.2S	1.05	21:22	145-59.1E	00-33.5S	3.2	R
R-10	1.05	21:22	145-59.1E	00-33.5S	1.10	03:20	145-19.8E	12-02.0N	8.6	R
R-11	1.10	03:20	145-19.8E	12-02.0N	1.10	14:00	145-06.9E	13-13.5N	10.9	R
R-12	1.13	02:57	145-14.9E	13-45.1N	1.21	21:51	149-15.0E	29-58.8N	8.3	R

R-13	1.21	21:51	149-15.0E	29-59.8N	1.23	00:09	149-19.7E	31-50.1N	7.5	R
R-14	1.23	00:10	149-19.7E	31-50.1N	1.24	14:17	149-19.5E	33-09.3N	1.4	R
R-15	1.24	14:17	149-19.5E	33-09.3N	1.26	00:10	149-19.2E	33-44.0N	7.6	R
R-16	1.26	00:10	149-19.2E	33-44.0N	1.31	12:42	149-02.9E	36-04.8N	12.4	R
R-17	1.31	12:42	149-02.9E	36-04.8N	2.03	00:10	147-11.6E	37-25.2N	10.1	R
R-18	2.03	00:10	147-11.6E	37-25.18N	2.08	00:05	141-16.8E	41-27.6N	6.9	R

Table 2.10-3 Summary of sea surface water sampling for isotope analysis

Sampling No.		Date	Time	Position	
			(UTC)	LON	LAT
MR11-08 O-	1	12.6	06:06	86-32.4E	00-50.9N
MR11-08 O-	2	12.7	06:00	90-12.6E	01-55.5S
MR11-08 O-	3	12.8	06:00	93-40.2E	04-30.4S
MR11-08 O-	4	12.9	06:00	97-08.8E	07-04.6S
MR11-08 O-	5	12.10	06:07	100-50.9E	09-11.6S
MR11-08 O-	7	12.24	03:00	149-23.0E	18-30.0N
MR11-08 O-	8	12.25	03:00	149-34.9E	16-25.9N
MR11-08 O-	9	12.26	03:00	149-19.3E	13-50.0N
MR11-08 O-	10	12.27	03:00	149-19.5E	11-50.0N
MR11-08 O-	11	12.28	03:00	149-20.0E	10-00.2N
MR11-08 O-	12	12.29	03:00	149-14.1E	08-12.6N
MR11-08 O-	13	12.30	03:00	148-05.8E	05-34.5N
MR11-08 O-	14	12.31	03:00	147-13.0E	03-30.4N
MR11-08 O-	15	1.1	03:22	146-46.8E	02-16.1N
MR11-08 O-	16	1.4	03:00	145-00.8E	03-37.0S
MR11-08 O-	17	1.5	03:00	145-38.5E	01-45.0S
MR11-08 O-	18	1.6	03:00	146-04.2E	00-15.1S
MR11-08 O-	19	1.7	03:00	146-21.3E	00-45.0N
MR11-08 O-	20	1.8	03:00	146-42.5E	01-58.4N
MR11-08 O-	21	1.9	02:00	146-42.7E	06-39.1N
MR11-08 O-	22	1.10	02:00	145-21.7E	11-55.7N
MR11-08 O-	23	1.14	03:00	148-45.0E	18-22.9N
MR11-08 O-	24	1.15	03:01	149-19.7E	20-29.7N
MR11-08 O-	25	1.16	03:00	149-20.0E	22-29.8N
MR11-08 O-	26	1.17	02:58	149-02.0E	24-14.5N
MR11-08 O-	27	1.18	03:06	149-18.7E	25-49.8N
MR11-08 O-	28	1.19	03:00	149-19.7E	27-49.8N

MR11-08 O-	29	1.20	02:29	149-20.1E	29-50.2N
MR11-08 O-	30	1.21	03:01	149-30.1E	29-53.8N
MR11-08 O-	31	1.22	03:04	149-15.3E	30-01.1N
MR11-08 O-	32	1.23	03:03	149-19.7E	31-50.7N
MR11-08 O-	33	1.24	03:02	149-17.2E	33-11.2N
MR11-08 O-	34	1.25	03:12	149-19.7E	33-46.7N
MR11-08 O-	35	1.26	03:07	149-18.9E	33-52.4N
MR11-08 O-	36	1.27	03:00	148-49.0E	34-52.9N
MR11-08 O-	37	1.28	02:59	145-47.9E	34-40.2N
MR11-08 O-	38	1.29	03:00	145-52.9E	34-36.9N
MR11-08 O-	39	1.30	02:59	148-52.3E	34-43.5N
MR11-08 O-	40	1.31	03:01	148-27.3E	35-25.3N
MR11-08 O-	41	2.1	03:08	147-37.3E	36-44.6N
MR11-08 O-	42	2.2	03:06	147-10.7E	37-34.7N
MR11-08 O-	43	2.3	03:04	147-11.4E	37-25.0N
MR11-08 O-	44	2.4	03:00	145-50.7E	39-24.9N
MR11-08 O-	45	2.5	02:58	144-42.2E	40-59.9N

2.11 Ship-borne Sky radiometer

Kazuma Aoki (University of Toyama) Principal Investigator / not onboard
Tadahiro Hayasaka (Tohoku University) Co-worker / not onboard
Masataka Shiobara (NIPR) Co-worker / not onboard
Sky radiometer operation was supported by Global Ocean Development Inc.

(1) Objective

Objective of the observations in this aerosol is to study distribution and optical characteristics of marine aerosols by using a ship-borne sky radiometer (POM-01 MKII: PREDE Co. Ltd., Japan). Furthermore, collections of the data for calibration and validation to the remote sensing data were performed simultaneously.

(2) Methods and Instruments

Sky radiometer is measuring the direct solar irradiance and the solar aureole radiance distribution, has seven interference filters (0.34, 0.4, 0.5, 0.675, 0.87, 0.94, and 1.02 µm). Analysis of these data is performed by SKYRAD.pack version 4.2 developed by Nakajima *et al*. 1996.

@ Measured parameters

- Aerosol optical thickness at five wavelengths (400, 500, 675, 870 and 1020 nm)
- Ångström exponent
- Single scattering albedo at five wavelengths
- Size distribution of volume (0.01 µm – 20 µm)

GPS provides the position with longitude and latitude and heading direction of the vessel, and azimuth and elevation angle of sun. Horizon sensor provides rolling and pitching angles.

(3) Preliminary results

This study is not onboard. Data obtained in this cruise will be analyzed at University of Toyama.

(4) Data archives

Measurements of aerosol optical data are not archived so soon and developed, examined, arranged and finally provided as available data after certain duration. All data will archived at University of Toyama (K.Aoki, SKYNET/SKY: http://skyrad.sci.u-toyama.ac.jp/) after the quality check and submitted to JAMSTEC.

2.12 Tropospheric aerosol and gas observations by MAX-DOAS and auxiliary techniques

(1) Personnel

Hisahiro TAKASHIMA	(PI, JAMSTEC/RIGC, not on board)
Fumikazu TAKETANI	(JAMSTEC/RIGC, not on board)
Hitoshi IRIE	(JAMSTEC/RIGC, not on board)
Yugo KANAYA	(JAMSTEC/RIGC, not on board)

(2) Objectives

- To quantify typical background values of atmospheric aerosol and gas over the ocean
- To clarify transport processes from source over Asia to the ocean (and also clarify the gas emission from the ocean (including organic gas))
- To validate satellite measurements as well as chemical transport model
- To clarify aerosol/gas variation associated with equatorial waves/ISO/MJO.

(3) Methods

(3-1) MAX-DOAS

Multi-Axis Differential Optical Absorption Spectroscopy (MAX-DOAS) is a passive remote sensing technique designed for atmospheric aerosol and gas profile measurements using scattered visible and ultraviolet (UV) solar radiation at several elevation angles. Our MAX-DOAS instrument for R/V *Mirai* consists of two main parts: an outdoor telescope unit and an indoor spectrometer (Acton SP-2358 with Princeton Instruments PIXIS-400B). These two parts are connected by a 14-m bundle cable that consists of 12 cores with 100-mm radii. On the roof top of the anti-rolling system of R/V *Mirai*, the telescope unit was installed on a gimbal mount, which compensates for the pitch and roll of the ship. A sensor measuring pitch and roll of the telescope unit (10Hz) is used together to measure an offset of elevation angle due to incomplete compensation by the active-type gimbal. The line of sight was in directions of the starboard and portside of the vessel.

The MAX-DOAS system records spectra of scattered solar radiation every 0.2-0.4 second. Measurements were made at several elevation angles of 0, 1.5, 3, 5, 10, 20, 30, 70, 110, 150, 160, 170, 175, 177 and 178.5 degrees using a movable mirror, which repeated the same sequence of elevation angles every 30-min. The UV/visible spectra range was changed every minute (284-423 nm and 391-528 nm).

For the spectral analysis, spectra data were selected with a criterion for the elevation angle to be within ±0.2° of the target. For those spectra, DOAS spectral fitting was performed to quantify the slant column density (SCD), defined as the concentration integrated along the light path, for each elevation angle. In this analysis, SCDs of NO_2 (and other gases) and O_4 (O_2-O_2, collision complex of oxygen) were obtained together. Next, O_4 SCDs were converted to the aerosol optical depth (AOD) and the vertical profile of aerosol extinction coefficient (AEC) at a wavelength of 476 nm using an optimal estimation inversion method with a radiative transfer model. Using derived aerosol information, another inversion is performed to retrieve the tropospheric vertical column/profile of NO_2 and other gases.

(3-2) CO, O_3, and aerosol size distribution

Carbon monoxide (CO) and ozone (O_3) measurements were also continually conducted during the cruise. For CO and O_3 measurements, ambient air was continually sampled on the compass deck and drawn through ~20-m-long Teflon tubes connected to gas filter correlation CO analyzer (Model 48C, Thermo Fisher Scientific) and UV photometric based ozone analyzer (Model 49C, Thermo Fisher Scientific) in the *Research Information Center*. Aerosol size distribution measurements by optical particle counter (KR-12A, Rion) were not conducted due to instrument problems during the cruise.

(4) Preliminary results

These data for the whole cruise period will be analyzed.

(5) Data archives

The data will be submitted to the Data Management Group (DMG) of JAMSTEC after the full analysis of the raw spectrum data is completed, which will be <2 years after the end of the cruise.

2.13 Millimeter-wave radar

(1) Personnel

TAKANO Toshiaki (Chiba University)
NISHINO Daichi (Chiba University)
OHKURA Tetsuya (Chiba University)
TASHIRO Keisuke (Chiba University)
SUGIMOTO Nobuo (NIES)
NISHIZAWA Tomoaki (NIES)
MATSUI Ichiro (NIES)
OKAMOTO Hajime (Kyushu University)

(2) Objective

Main objective for the 95GHz cloud radar named FALCON-I is to detect vertical structure of cloud and precipitation and Doppler spectra of the observed targets. Combinational use of the radar and lidar is recognized to be a powerful tool to study vertical distribution of cloud microphysics, i.e., particle size and liquid/ice water content (LWC/IWC).

(3) Observations and products

Observation with FALCON-I was done continuously with 10 sec repetition cycle during the cruise. Basic output from data is cloud occurrence, radar reflectivity factor, and Doppler spectra. Sensitivity of FALCON-I is about -32 dBZ at 5 km height and its spatial resolution is about 15m. Doppler spectra were also obtained with 10 sec temporal resolution in the velocity range of ±3.1 m/s.

Detectabilities of clouds were degradated during the cruise MR11-07 in 10-20 dB because of decrease of radar output power. We fixed this problem at Colombo just before the cruise MR11-08 Leg1 and the sensitivity was good during the cruise. The data after Dec. 27th , middle of Leg2, howevere, had problem in data acquisition process and we do not obtain good data.

In order to derive reliable cloud amount and cloud occurrence, we need to have radar and lidar for the same record. Radar / lidar retrieval algorithm has been developed by H.Okamoto, Kyushu University. The algorithm is applied to water cloud in low level and also cirrus cloud in high altitude.

(4) Example of Data

An example of the time height cross-sections of radar reflectivity power obtained on December 9th, 2011, during MR11-08 Leg1 cruise are shown in Fig.2.13.1. The location of MIRAI was around 0N, 90E.

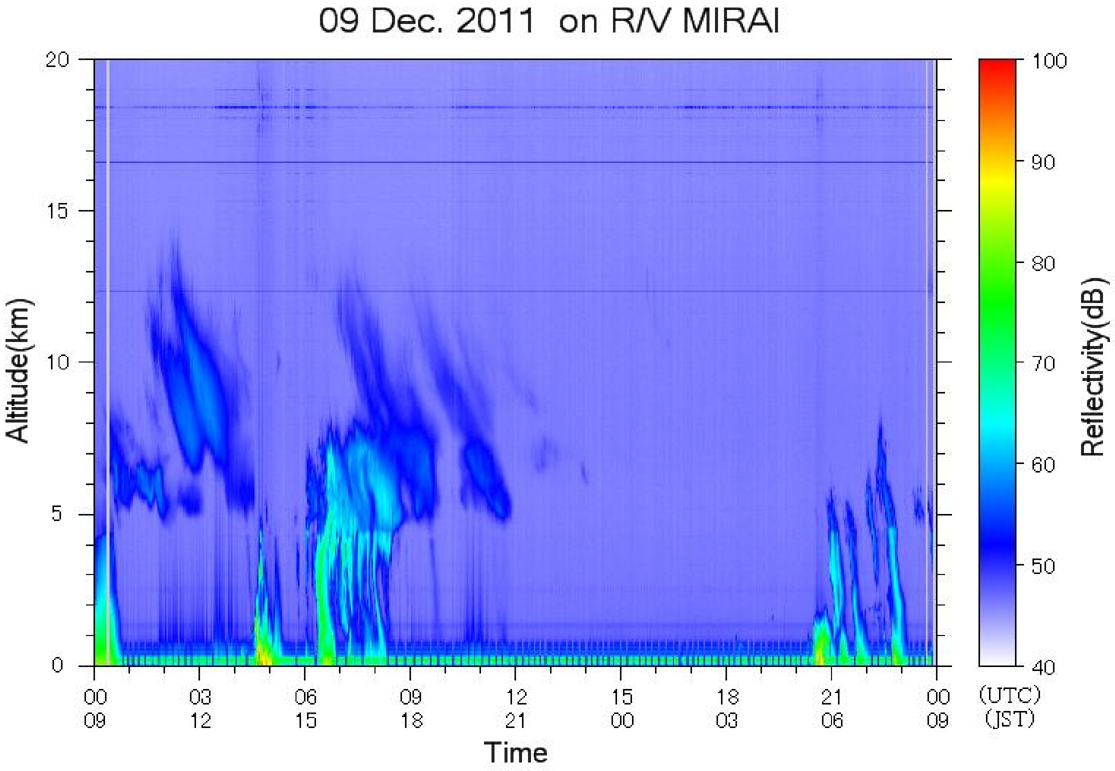

Fig 2.13.1. Time height cross section of radar reflectivity power in arbitral unit of dB on Dec. 9th, 2011 in Indian Ocean. We can recognize the melting layer at 4.5 km and thin clouds up to 14 km in height.

2.14 Sea surface gravity

(1) Personnel

Takeshi Matsumoto	***(University of the Ryukyus)***	***: Principal investigator (Not on-board)***
Naoto Hirano	***(Tohoku University)***	***: Principal investigator (Not on-board)***
Kazuho Yoshida	***(Global Ocean Development Inc., GODI)***	***-leg1, leg2-***
Ryo Kimura	***(GODI)***	***-leg1, leg2-***
Satoshi Okumura	***(GODI)***	***-leg2-***
Katsuhisa Maeno	***(GODI)***	***-leg3-***
Asuka Doi	***(GODI)***	***-leg3-***
Toshimitsu Goto	***(GODI)***	***-leg3-***
Ryo Ohyama	***(MIRAI Crew)***	***-leg1, leg2, leg3-***

(2) Introduction

The local gravity is an important parameter in geophysics and geodesy. We collected gravity data at the sea surface.

(3) Parameters

Relative Gravity [CU: Counter Unit]

[mGal] = (coef1: 0.9946) * [CU]

(4) Data Acquisition

We measured relative gravity using LaCoste and Romberg air-sea gravity meter S-116 (Micro-G LaCoste, LLC) during the MR11-08 cruise 4th December 2011 to 9th February 2012.

To convert the relative gravity to absolute one, we measured gravity, using portable gravity meter (CG-5, Scintrex), at Sekinehama as the reference point.

(5) Preliminary Results

Absolute gravity table is shown in Table 2.14-1.

Table 2.14-1. **Absolute gravity table MR11-08 cruise**

No.	Date	UTC	Port	Absolute Gravity (mGal)	Sea Level (cm)	Draft (cm)	Gravity at Sensor[*1] (mGal)	L&R[*2] (mGal)
1[*3]	13th/Aug./2011	01:13	Sekinehama	980371.93	302	646	980373.12	12656.80
2	9th/Feb./2012	04:05	Sekinehama	980371.94	265	605	980372.93	12616.45

*1: Gravity at Sensor= Absolute Gravity + Sea Level*0.3086/100 + (Draft-530)/100*0.2223

*2: Micro-g LaCoste air-sea gravity meter S-116

*3: MR11-06 cruise

(6) Data Archive

Surface gravity data obtained during this cruise will be submitted to the Data Management Group (DMG) in JAMSTEC, and will be archived there.

(7) Remarks (Times in UTC)

1) The observation was carried out within following periods,

Leg1: 10:00 5th Dec. 2011 to 08:30 10th Dec. 2011
Leg2: 22:10 21th Dec. 2011 to 00:00 22th Dec. 2011
19:30 23th Dec. 2011 to 04:30 1st Jan. 2012
14:00 3rd Jan 2012 to 15:03 10th Jan. 2012
Leg3: 02:45 13th Jan. 2012 to 00:00 09th Feb 2012.

2) Following periods, GRV data acquisition suspended due to the logging PC trouble.
10:09:54 to 10:18:45 30th Dec. 2011

3) Spring tension value was adjusted from 11235.7(cu) to 10824, when we replaced spring tension counter in Guam at 12th Jan. 2012.

2.15 On-board geomagnetic measurement

(1) Personnel

Takeshi Matsumoto	*(University of the Ryukyus)*	*: Principal investigator (Not on-board)*
Naoto Hirano	*(Tohoku University)*	*: Principal investigator (Not on-board)*
Kazuho Yoshida	*(Global Ocean Development Inc., GODI)*	*-leg1, leg2-*
Ryo Kimura	*(GODI)*	*-leg1, leg2-*
Satoshi Okumura	*(GODI)*	*-leg2-*
Katsuhisa Maeno	*(GODI)*	*-leg3-*
Asuka Doi	*(GODI)*	*-leg3-*
Toshimitsu Goto	*(GODI)*	*-leg3-*
Ryo Ohyama	*(MIRAI Crew)*	*-leg1, leg2, leg3-*

(2) Introduction

Measurement of magnetic force on the sea is required for the geophysical investigations of marine magnetic anomaly caused by magnetization in upper crustal structure. We measured geomagnetic field using a three-component magnetometer during the MR11-08 cruise 4th December 2011 to 9th February 2012.

(3) Principle of ship-board geomagnetic vector measurement

The relation between a magnetic-field vector observed on-board, $\mathbf{H}\mathrm{ob}$, (in the ship's fixed coordinate system) and the geomagnetic field vector, $\mathbf{F}$, (in the Earth's fixed coordinate system) is expressed as:

$$\mathbf{H}\mathrm{ob} = \widetilde{\mathbf{A}}\;\widetilde{\mathbf{R}}\;\widetilde{\mathbf{P}}\;\widetilde{\mathbf{Y}}\;\mathbf{F} + \mathbf{H}\mathrm{p} \qquad \text{(a)}$$

where $\widetilde{\mathbf{R}}$, $\widetilde{\mathbf{P}}$ and $\widetilde{\mathbf{Y}}$ are the matrices of rotation due to roll, pitch and heading of a ship, respectively. $\widetilde{\mathbf{A}}$ is a 3 x 3 matrix which represents magnetic susceptibility of the ship, and $\mathbf{H}\mathrm{p}$ is a magnetic field vector produced by a permanent magnetic moment of the ship's body. Rearrangement of Eq. (a) makes

$$\widetilde{\mathbf{R}}\;\mathbf{H}\mathrm{ob} + \mathbf{H}\mathrm{bp} = \widetilde{\mathbf{R}}\;\widetilde{\mathbf{P}}\;\widetilde{\mathbf{Y}}\;\mathbf{F} \qquad \text{(b)}$$

where $\widetilde{\mathbf{R}} = \widetilde{\mathbf{A}}^{-1}$, and $\mathbf{H}\mathrm{bp} = -\widetilde{\mathbf{R}}\;\mathbf{H}\mathrm{p}$. The magnetic field, $\mathbf{F}$, can be obtained by measuring $\widetilde{\mathbf{R}}$, $\widetilde{\mathbf{P}}$, $\widetilde{\mathbf{Y}}$ and $\mathbf{H}\mathrm{ob}$, if $\widetilde{\mathbf{R}}$ and $\mathbf{H}\mathrm{bp}$ are known. Twelve constants in $\widetilde{\mathbf{R}}$ and $\mathbf{H}\mathrm{bp}$ can be determined by measuring variation of $\mathbf{H}\mathrm{ob}$ with $\widetilde{\mathbf{R}}$, $\widetilde{\mathbf{P}}$ and $\widetilde{\mathbf{Y}}$ at a place where the geomagnetic field, $\mathbf{F}$, is known.

(4) Instruments on R/V MIRAI

A shipboard three-component magnetometer system (Tierra Tecnica SFG1214) is equipped on-board R/V MIRAI. Three-axes flux-gate sensors with ring-cored coils are fixed on the fore mast. Outputs from the sensors are digitized by a 20-bit A/D converter (1 nT/LSB), and sampled at 8 times per second. Ship's heading, pitch, and roll are measured by the Inertial Navigation System (INS) for controlling attitude of a Doppler radar. Ship's position (GPS) and speed data are taken from LAN every second.

(5) Data Archive

Surface gravity data obtained during this cruise will be submitted to the Data Management Group (DMG) in JAMSTEC, and will be archived there.

(6) Remarks (Times in UTC)

1) The observation was carried out within following periods,

Leg1: 10:00 5th Dec. 2011 to 08:30 10th Dec. 2011
Leg2: 22:10 21th Dec. 2011 to 00:00 22th Dec. 2011
19:30 23th Dec. 2011 to 04:30 1st Jan. 2012
14:00 3rd Jan 2012 to 15:03 10th Jan. 2012
Leg3: 02:45 13th Jan. 2012 to 00:00 9th Feb 2012.

2) For calibration of the ship's magnetic effect, we made a "figure-eight" turn (a pair of clockwise and anti-clockwise rotation). This calibration was carried out as below.

Leg1: 05:30 to 06:03 10th Dec. 2011 at 09-12.0S, 100-49.8E
Leg2: 03:55 to 04:28 1st Jan. 2012 at 02-16.0N, 146-46.4E
Leg3: 12:10 to 12:35 24th Jan. 2012 at 33-10.5N, 149-19.3E
01:10 to 01:44 6th Feb. 2012 at 41-45.6N, 143-11.7E

2.16 Radiosonde

(1) Personnel

Kunio Yoneyama	***(JAMSTEC)***	***not on-board***
Masaki Katsumata	***(JAMSTEC)***	***not on-board***
Kazuho Yoshida	***(GODI)***	
Ryo Kimura	***(GODI)***	
Ryo Ohyama	***(Mirai crew)***	

(2) Objectives

As part of the international field experiment “Cooperative Indian Ocean experiment on intraseasonal variability in the Year 2011 (CINDY2011)”, atmospheric sounding was carried out to measure the profiles of temperature, humidity, and wind speed/direction during the leg-1 cruise in the Indian Ocean.

(3) Apparatus

Atmospheric sounding by using GPS radiosonde was carried out. The GPS radiosonde sensor (RS92-SGPD) was launched with the balloons (Totex TA-200) from the sea-container (Vaisala ASAP) every 6 hours from December 5th, 12UTC to 10th, 06UTC. The on-board receiving/processing system consists of processor (Vaisala, SPS-311), processing and recording software (DigiCORA III/MW31, ver.3.64), GPS antenna (GA20), UHF antenna (RB21), and ground check kit (GC25). In the ground-check process, a barometer (Vaisala PTB-330) was used to provide reference values. For initial values, surface met station data taken at port-side were adopted (cf. Section 2.3).

(4) Results

Figure 2.16-1 is the time-height cross sections of equivalent potential temperature, relative humidity, zonal and meridional wind components.

(5) Remarks

Data were sent to the world meteorological community via Global Telecommunication System (GTS) through the Japan Meteorological Agency, immediately after each observation. Raw data have been archived as ASCII (tsv) every 2 seconds and binary (dc3db). These raw datasets have been submitted to JAMSTEC Data Research Center for Marine-Earth Sciences. The corrected datasets will be available from Mirai website (http://www.godac.jamstec.go.jp/cruisedata/mirai/e/), and CINDY website (http://www.jamstec.go.jp/iorgc/cindy/).

Table 2.16.1. Radiosonde launch log with surface values and maximum height.

No.	Date	Latitude	Longitude	Psfc	Tsfc	RHsfc	WD	Wsp	SST	Max height	
	YYYYMMDDHH	degN	degE	hPa	degC	%	deg	m/s	degC	hPa	m
1	2011120512	3.066	83.566	1005.0	28.1	72	7	2.4	29.5	31.1	23451
2	2011120518	2.349	84.490	1007.2	28.0	76	31	4.1	29.2	26.0	24588
3	2011120600	1.647	85.450	1005.3	27.7	76	18	2.5	29.0	29.6	23753
4	2011120606	0.950	86.397	1006.5	28.3	75	12	5.1	29.2	38.1	22222
5	2011120612	0.248	87.360	1004.9	27.4	79	11	3.2	29.5	31.2	23435
6	2011120618	−0.455	88.262	1006.9	28.0	76	333	3.1	29.4	43.6	21403
7	2011120700	−1.174	89.201	1004.5	26.8	82	29	4.2	29.2	36.5	22463
8	2011120706	−1.842	90.096	1006.0	28.0	71	10	2.2	29.3	25.6	24687
9	2011120712	−2.466	90.925	1003.8	28.0	75	286	2.2	29.5	30.2	23651
10	2011120718	−3.110	91.780	1006.9	28.1	76	287	3.6	29.3	42.2	21580
11	2011120800	−3.759	92.657	1005.6	27.4	79	277	4.1	29.2	30.6	23572
12	2011120806	−4.417	93.525	1006.2	28.2	75	303	4.8	29.3	27.5	24244
13	2011120812	−5.095	94.431	1004.1	28.2	74	308	6.2	29.4	34.3	22860
14	2011120818	−5.741	95.303	1005.2	26.4	88	5	6.3	29.0	37.6	22293
15	2011120900	−6.383	96.156	1004.0	26.3	84	334	7.0	28.6	45.0	21195
16	2011120906	−6.994	97.034	1004.5	26.7	86	316	8.9	28.5	36.4	22517
17	2011120912	−7.659	97.866	1003.7	27.6	81	307	7.0	28.4	28.9	23909
18	2011120918	−8.308	98.748	1005.5	27.5	82	316	6.8	28.0	38.9	22082
19	2011121000	−8.849	99.707	1004.9	26.4	84	300	12.2	28.1	38.9	22103
20	2011121006	−9.202	100.735	1005.9	26.3	84	328	4.4	28.4	43.9	21329

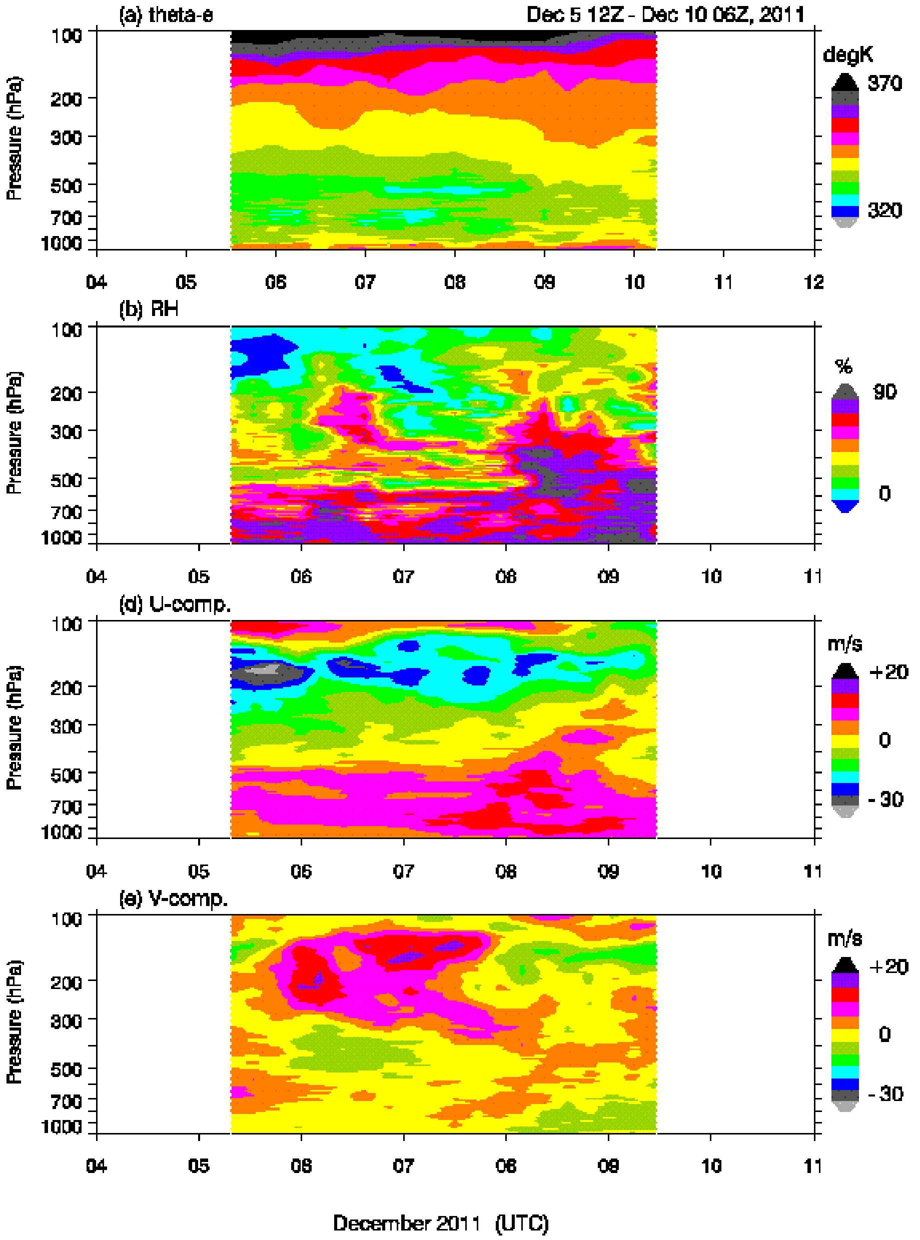

Fig. 2.16.1. Time-height cross sections of (a) equivalent potential temperature, (b) relative humidity, (c) zonal wind, and (d) meridional wind.

2.17 Doppler Radar

(1) Personnel

Masaki Katsumata	***(JAMSTEC)***	***not on-board***
Kunio Yoneyama	***(JAMSTEC)***	***not on-board***
Kazuho Yoshida	***(GODI)***	
Ryo Kimura	***(GODI)***	
Ryo Ohyama	***(Mirai crew)***	

(2) Objectives

As part of the international field experiment "Cooperative Indian Ocean experiment on intraseasonal variability in the Year 2011 (CINDY2011)", convective activity was monitored by operating Doppler radar during the leg-1 cruise in the Indian Ocean.

(3) Apparatus

The Doppler radar on board of Mirai is used. The specification of the radar is:

Frequency:	5290 MHz
Beam Width:	better than 1.5 degrees
Output Power:	250 kW (Peak Power)
Signal Processor:	RVP-7 (Vaisala Inc. Sigmet Product Line, U.S.A.)
Inertial Navigation Unit:	PHINS (Ixsea S.A.S., France)
Application Software:	IRIS/Open (Vaisala Inc. Sigmet Product Line, U.S.A.)

Parameters of the radar were checked and calibrated at the beginning/end of the cruise. In addition, daily checking was performed for (1) frequency, (2) mean output power, (3) pulse width, and (4) PRF (pulse repetition frequency). During the cruise, the volume scan consisting of 21 PPIs (Plan Position Indicator) was conducted every 10 minutes. A dual PRF mode with the maximum range of 160 km was used for the volume scan. Besides, surveillance PPI scan was performed every 30 minutes in a single PRF mode with the maximum range of 300 km. Detailed information for each observational mode is listed in Table 2.17.1.

(4) Results

Data were fully collected during the Leg-1 in the Indian Ocean. Data will be converted into the Cartesian coordinate after applying several noise filters.

(5) Remarks

All data datasets will be submitted to JAMSTEC Data Research Center for Marine-Earth Sciences. In addition, corrected data will be archived and released at CINDY project office at http://www.jamstec.go.jp/iorgc/cindy/.

Table 2.17.1. Parameters for each observational mode.

	Surveillance PPI	Volume Scan
Pulse Width	2 (microsec)	0.5 (microsec)
Scan Speed	18 (deg/sec)	18 (deg/sec)
PRF	260 (Hz)	900/720 (Hz)
Sweep Integration	32 samples	50 samples
Ray Spacing	1.0 (deg)	1.0 (deg)
Bin Spacing	250 (m)	250 (m)
Elevation Angle	0.5	0.5, 1.0, 1.8, 2.6, 3.4, 4.2, 5.0, 5.8, 6.7, 7.7, 8.9, 10.3, 12.3, 14.5, 17.1, 20.0, 23.3, 27.0, 31.0, 35.4, 40.0
Azimuth	Full Circle	Full Circle
Range	300 (km)	160 (km)

3. Station Observation

3.1 CTDO$_2$ Measurements

May 16, 2012

(1) Personnel

Hiroshi Uchida (JAMSTEC)
Leg 2
Shinsuke Toyoda (MWJ)
Hirokatsu Uno (MWJ)
Shungo Oshitani (MWJ)
Kenichi Kato (MWJ)
Satoshi Ozawa (MWJ)
Leg 3
Kenichi Katayama (MWJ)
Toru Idai (MWJ)
Naoko Miyamoto (MWJ)
Takami Mori (MWJ)

(2) Winch arrangements

The CTD package was deployed by using 4.5 Ton Traction Winch System (Dynacon, Inc., Bryan, Texas, USA), which was installed on the R/V Mirai in April 2001 (Fukasawa et al., 2004). Primary system components include a complete CTD Traction Winch System with up to 8000 m of 9.53 mm armored cable (Rochester Wire & Cable).

(3) Overview of the equipment

The CTD system was SBE 911plus system (Sea-Bird Electronics, Inc., Bellevue, Washington, USA). The SBE 911plus system controls 36-position SBE 32 Carousel Water Sampler. The Carousel accepts 12-litre Niskin-X water sample bottles (General Oceanics, Inc., Miami, Florida, USA). The SBE 9plus was mounted horizontally in a 36-position carousel frame. SBE's temperature (SBE 3) and conductivity (SBE 4) sensor modules were used with the SBE 9plus underwater unit. The pressure sensor is mounted in the main housing of the underwater unit and is ported to outside through the oil-filled plastic capillary tube. A modular unit of underwater housing pump (SBE 5T) flushes water through sensor tubing at a constant rate independent of the CTD's motion, and pumping rate (3000 rpm) remain nearly constant over the entire input voltage range of 12-18 volts DC. Flow speed of pumped water in standard TC duct is about 2.4 m/s. Two sets of temperature and conductivity modules were used. An SBE's dissolved oxygen sensor (SBE 43) was placed between the primary conductivity sensor and the pump module. Auxiliary sensors, a Deep Ocean Standards Thermometer (SBE 35), an altimeter (PSA-916T; Teledyne Benthos, Inc., North Falmous, Massachusetts, USA), two oxygen optodes (RINKO-III; JFE Alec Co., Ltd, Kobe Hyogo, Japan), a fluorometer (Seapoint sensors, Inc., Kingston, New Hampshire, USA), a transmissometer (C-Star Transmissometer; WET Labs, Inc., Philomath, Oregon, USA), and a Photosynthetically Active Radiation (PAR) sensor (Satlantic, LP, Halifax, Nova Scotia, Canada) were also used with the SBE 9plus underwater unit. To minimize motion of the CTD package, a heavy stainless frame (total weight of the CTD package without sea water in the bottles is about 1000 kg) was used with an aluminum plate (54 × 90 cm).

An additional set of SBE 911plus CTD system with 12-position SBE 32 was also used for some deep casts in leg 3 because weight of the armored cable used was too heavy to operate deep casts safely deeper than 5700 dbar within the load rating (3 ton) of the winch system.

Summary of the system used in this cruise

36-position CWS system

Deck unit:

SBE 11plus, S/N 0272

Under water unit:

SBE 9plus, S/N 117457 (Pressure sensor: S/N 1027)

Temperature sensor:

SBE 3plus, S/N 4815 (primary)

SBE 3plus, S/N 5329 (secondary, leg 2)

SBE 3plus, S/N 4811 (secondary, leg 3)

Conductivity sensor:

SBE 4, S/N 2854 (primary)

SBE 4, S/N 3036 (secondary)

Oxygen sensor:

SBE 43, S/N 0394

JFE Advantech RINKO-III, S/N 0024 (foil batch no. 144002A)

JFE Advantech RINKO-III, S/N 0079 (foil batch no. 160002A)

Pump:

SBE 5T, S/N 4598 (primary)

SBE 5T, S/N 4595 (secondary)

Altimeter:

PSA-916T, S/N 1100 (leg 2)

PSA-916T, S/N 1157 (leg 3)

Deep Ocean Standards Thermometer:

SBE 35, S/N 0045

Fluorometer:

Seapoint Sensors, Inc., S/N 3054

Transmissometer:

C-Star, S/N CST-1363DR

PAR:

Satlantic LP, S/N 0049

Carousel Water Sampler:

SBE 32, S/N 0391 (36-position)

SBE 32, S/N 0389 (12-position)

Water sample bottle:

12-litre Niskin-X model 1010X (no TEFLON coating)

12-position CWS system

Deck unit:

SBE 11plus, S/N 0272

Under water unit:

SBE 9plus, S/N 94766 (Pressure sensor: S/N 0786)

Temperature sensor:

SBE 3plus, S/N 1359 (primary)

SBE 3plus, S/N 1525 (secondary)

Conductivity sensor:

SBE 4, S/N 1203 (primary)

SBE 4, S/N 2435 (secondary)

Oxygen sensor:

SBE 43, S/N 0205

JFE Advantech RINKO-III, S/N 0037 (foil batch no. 144005A)

Pump:

SBE 5T, S/N 3118 (primary)

SBE 5T, S/N 3293 (secondary)

Altimeter:

PSA-916T, S/N 1100

Deep Ocean Standards Thermometer:

SBE 35, S/N 0022

Carousel Water Sampler:

SBE 32, S/N 0389

Water sample bottle:

12-litre Niskin-X model 1010X (no TEFLON coating)

(4) Pre-cruise calibration

i. Pressure

The Paroscientific series 4000 Digiquartz high pressure transducer (Model 415K: Paroscientific, Inc., Redmond, Washington, USA) uses a quartz crystal resonator whose frequency of oscillation varies with pressure induced stress with 0.01 per million of resolution over the absolute pressure range of 0 to 15000 psia (0 to 10332 dbar). Also, a quartz crystal temperature signal is used to compensate for a wide range of temperature changes at the time of an observation. The pressure sensor has a nominal accuracy of 0.015 % FS (1.5 dbar), typical stability of 0.0015 % FS/month (0.15 dbar/month), and resolution of 0.001 % FS (0.1 dbar). Since the pressure sensor measures the absolute value, it inherently includes atmospheric pressure (about 14.7 psi). SEASOFT subtracts 14.7 psi from computed pressure automatically.

Pre-cruise sensor calibrations for linearization were performed at SBE, Inc.

S/N 1027, 4 February 2011

S/N 0786, 17 November 2009

The time drift of the pressure sensor is adjusted by periodic recertification corrections against a dead-weight piston gauge (Model 480DA, S/N 23906; Piston unit, S/N 079K; Weight set, S/N 3070; Bundenberg Gauge Co. Ltd., Irlam, Manchester, UK). The corrections are performed at JAMSTEC, Yokosuka, Kanagawa, Japan by Marine Works Japan Ltd. (MWJ), Yokohama, Kanagawa, Japan, usually once in a year in order to monitor sensor time drift and linearity.

S/N 1027, 19 May 2011

slope = 1.00017335

offset = 0.16281

S/N 0786, 27 May 2011

slope = 0.99988759

offset = 0.05087

ii. Temperature (SBE 3)

The temperature sensing element is a glass-coated thermistor bead in a stainless steel tube, providing a pressure-free measurement at depths up to 10500 (6800) m by titanium (aluminum) housing. The SBE 3 thermometer has a nominal accuracy of 1 mK, typical stability of 0.2 mK/month, and resolution of 0.2 mK at 24 samples per second. The premium temperature sensor, SBE 3plus, is a more rigorously tested and calibrated version of standard temperature sensor (SBE 3).

Pre-cruise sensor calibrations were performed at SBE, Inc.

S/N 4815, 25 January 2011

S/N 5329, 11 February 2011

S/N 4811, 9 February 2011

S/N 1359, 18 May 2011

S/N 1525, 10 June 2011

Pressure sensitivities of SBE 3s were corrected according to a method by Uchida et al. (2007), for the following sensors.

S/N 4815, –3.45974716e–7 [°C/dbar]

S/N 4811, –2.7192e–7 [°C/dbar]

S/N 1359, –1.8386e–7 [°C/dbar]

Pressure sensitivities were not yet determined for S/N 5329 and 1525.

iii. Conductivity (SBE 4)

The flow-through conductivity sensing element is a glass tube (cell) with three platinum electrodes to provide in-situ measurements at depths up to 10500 (6800) m by titanium (aluminum) housing. The SBE 4 has a nominal accuracy of 0.0003 S/m, typical stability of 0.0003 S/m/month, and resolution of 0.00004 S/m at 24 samples per second. The conductivity cells have been replaced to newer style cells for deep ocean measurements.

Pre-cruise sensor calibrations were performed at SBE, Inc.

S/N 2854, 1 June 2011
S/N 3036, 1 June 2011
S/N 1203, 25 May 2011
S/N 2435, 2 March 2011

The value of conductivity at salinity of 35, temperature of 15 °C (IPTS-68) and pressure of 0 dbar is 4.2914 S/m.

iv. Oxygen (SBE 43)

The SBE 43 oxygen sensor uses a Clark polarographic element to provide in-situ measurements at depths up to 7000 m. The range for dissolved oxygen is 120 % of surface saturation in all natural waters, nominal accuracy is 2 % of saturation, and typical stability is 2 % per 1000 hours.

Pre-cruise sensor calibration was performed at SBE, Inc.

S/N 0394, 25 October 2011
S/N 0205, 27 May 2011

v. Deep Ocean Standards Thermometer

Deep Ocean Standards Thermometer (SBE 35) is an accurate, ocean-range temperature sensor that can be standardized against Triple Point of Water and Gallium Melt Point cells and is also capable of measuring temperature in the ocean to depths of 6800 m. The SBE 35 was used to calibrate the SBE 3 temperature sensors in situ (Uchida et al., 2007).

Pre-cruise sensor linearization was performed at SBE, Inc.

S/N 0045, 27 September 2002
S/N 0022, 4 March 2009

Then the SBE 35 is certified by measurements in thermodynamic fixed-point cells of the TPW (0.01 °C) and GaMP (29.7646 °C). The slow time drift of the SBE 35 is adjusted by periodic recertification corrections. Pre-cruise sensor calibration was performed at SBE, Inc.

S/N 0045, 10 February 2011 (slope and offset correction)
S/N 0022, 23 January 2011 (slope and offset correction)

The time required per sample = 1.1 × NCYCLES + 2.7 seconds. The 1.1 seconds is total time per an acquisition cycle. NCYCLES is the number of acquisition cycles per sample and was set to 4. The 2.7 seconds is required for converting the measured values to temperature and storing average in EEPROM.

vi. Altimeter

Benthos PSA-916T Sonar Altimeter (Teledyne Benthos, Inc.) determines the distance of the target from the unit by generating a narrow beam acoustic pulse and measuring the travel time for the pulse to bounce back from the target surface. It is rated for operation in water depths up to 10000 m. The PSA-916T uses the nominal speed of sound of 1500 m/s.

vii. Oxygen optode (RINKO)

RINKO (JFE Alec Co., Ltd.) is based on the ability of selected substances to act as dynamic fluorescence quenchers. RINKO model III is designed to use with a CTD system which accept an auxiliary analog sensor, and is designed to operate down to 7000 m.

Outputs from RINKO are the raw phase shift data. The RINKO can be calibrated by the Stern-Volmer equation, according to a method by Uchida et al. (2010):

$$O_2\ (\mu\text{mol/l}) = [(V_0 / V) - 1] / K_{sv}$$

where V is voltage, V_0 is voltage in the absence of oxygen and K_{sv} is Stern-Volmer constant. The V_0 and the K_{sv} are assumed to be functions of temperature as follows.

$$K_{sv} = C_0 + C_1 \times T + C_2 \times T^2$$

$$V_0 = 1 + C_3 \times T$$

$$V = C_4 + C_5 \times V_b$$

where T is CTD temperature (°C) and V_b is raw output (volts). V_0 and V are normalized by the output in the absence of oxygen at 0°C. The oxygen concentration is calculated using accurate temperature data from the CTD temperature sensor instead of temperature data from the RINKO. The pressure-compensated oxygen concentration O_{2c} can be calculated as follows.

$$O_{2c} = O_2\ (1 + C_p p / 1000)^{1/3}$$

where p is CTD pressure (dbar) and C_p is the compensation coefficient. Since the sensing foil of the optode is permeable only to gas and not to water, the optode oxygen must be corrected for salinity. The salinity-compensated oxygen can be calculated by multiplying the factor of the effect of salt on the oxygen solubility (García and Gordon, 1992). García and Gordon (1992) have recommended the use of the solubility coefficients derived from the data of Benson and Krause.

Pre-cruise sensor calibrations were performed at RIGC/JAMSTEC.

S/N 0024, 20 June 2011
S/N 0079, 6 December 2011

viii. Fluorometer

The Seapoint Chlorophyll Fluorometer (Seapoint Sensors, Inc., Kingston, New Hampshire, USA) provides in-situ measurements of chlorophyll-a at depths up to 6000 m. The instrument uses modulated blue LED lamps and a blue excitation filter to excite chlorophyll-a. The fluorescent light emitted by the chlorophyll-a passes through a red emission filter and is detected by a silicon photodiode. The low level signal is then processed using synchronous demodulation circuitry, which generates an output voltage proportional to chlorophyll-a concentration.

ix. Transmissometer

The C-Star Transmissometer (WET Labs, Inc., Philomath, Oregon, USA) measures light transmittance at a single wavelength over a know path. In general, losses of light propagating through water can be attributed to two primary causes: scattering and absorption. By projecting a collimated beam of light through the water and placing a focused receiver at a known distance away, one can quantify these losses. The ratio of light gathered by the receiver to the amount originating at the source is known as the beam transmittance. Suspended particles, phytoplankton, bacteria and dissolved organic matter contribute to the losses sensed by the instrument. Thus, the instrument provides information both for an indication of the total concentrations of matter in the water as well as for a value of the water clarity.

x. PAR

Satlantic's Photosynthetically Active Radiation (PAR) sensors provide highly accurate measurements of PAR (400 – 700 nm) for a wide range of aquatic and terrestrial applications. The ideal spectral response for a PAR sensor is one that gives equal emphasis to all photons between 400 – 700 nm. Satlantic PAR sensors use a high quality filtered silicon photodiode to provide a near equal spectral response across the entire wavelength range of the measurement.

Pre-cruise sensor calibration was performed at Satlantic, LP.

22 January 2009

(5) Data collection and processing

i. Data collection

CTD system was powered on at least 20 minutes in advance of the data acquisition to stabilize the pressure sensor and was powered off at least two minutes after the operation in order to acquire pressure data on the ship's deck.

The package was lowered into the water from the starboard side and held 10 m beneath the surface in order to activate the pump. After the pump was activated, the package was lifted to the surface and lowered at a rate of 1.0 m/s to 200 m (or 300 m when significant wave height is high) then the package was stopped to operate the heave compensator of the crane. The package was lowered again at a rate of 1.2 m/s to the bottom. For the up cast, the package was lifted at a rate of 1.1 m/s except for bottle firing stops. At each bottle firing stops, the bottle was fired after waiting from the stop for 30 seconds (or 20 seconds from station P10_78_1 to save time) and the package was stayed at least 5 seconds for measurement of the SBE 35. At 200 m (or 300 m) from the surface, the package was stopped to stop the heave compensator of the crane.

Water samples were collected using a 36-bottle (or 12-bottles) SBE 32 Carousel Water Sampler with 12-litre Niskin-X bottles. Before a cast taken water for CFCs, the bottle frame and Niskin-X bottles were wiped with acetone.

Data acquisition software

SEASAVE-Win32, version 7.18c

ii. Data collection problems

(a) Miss trip and miss fire

Niskin bottles did not trip correctly at the following stations.

Miss trip	Miss fire
P10_46_1, #11	P10N_106_2, #31

iii. Data processing

SEASOFT consists of modular menu driven routines for acquisition, display, processing, and archiving of oceanographic data acquired with SBE equipment. Raw data are acquired from instruments and are stored as unmodified data. The conversion module DATCNV uses instrument configuration and calibration coefficients to create a converted engineering unit data file that is operated on by all SEASOFT post processing modules. The following are the SEASOFT and original software data processing module sequence and specifications used in the reduction of CTD data in this cruise.

Data processing software

SBEDataProcessing-Win32, version 7.21d

DATCNV converted the raw data to engineering unit data. DATCNV also extracted bottle information where scans were marked with the bottle confirm bit during acquisition. The duration was set to 4.4 seconds, and the offset was set to 0.0 second. When the bottle was fired without bottle firing stop, the duration was set to 1.0 second and the offset was set to 0.0 second, and a quality flag of 4 (bad) was set to the SBE 35 data. The hysteresis correction for the SBE 43 data (voltage) was applied for both profile and bottle information data.

TCORP (original module, version 1.1) corrected the pressure sensitivity of the SBE 3 for both profile and bottle information data.

RINKOCOR (original module, version 1.0) corrected the time-dependent, pressure-induced effect (hysteresis) of the RINKO for both profile data.

RINKOCORROS (original module, version 1.0) corrected the time-dependent, pressure-induced effect (hysteresis) of the RINKO for bottle information data by using the hysteresis-corrected profile data.

BOTTLESUM created a summary of the bottle data. The data were averaged over 4.4 seconds (or 1 second for the bottle fired without stop).

ALIGNCTD converted the time-sequence of sensor outputs into the pressure sequence to ensure that all calculations were made using measurements from the same parcel of water. For a SBE 9plus CTD with the ducted temperature and conductivity sensors and a 3000-rpm pump, the typical net advance of the conductivity relative to the temperature is 0.073 seconds. So, the SBE 11plus deck unit was set to advance the primary and the secondary conductivity for 1.73 scans (1.75/24 = 0.073 seconds). Oxygen data are also systematically delayed with respect to depth mainly because of the long time constant of the oxygen sensor and of an additional delay from the transit time of water in the pumped plumbing line. This delay was compensated by 6 seconds advancing the SBE 43 oxygen sensor output (voltage) relative to the temperature data. Delay of the RINKO data was also compensated by 1 second advancing sensor output (voltage) relative to the temperature data. Delay of the transmissometer data was also compensated by 2 seconds advancing sensor output (voltage) relative to the temperature data.

WILDEDIT marked extreme outliers in the data files. The first pass of WILDEDIT obtained an accurate estimate of the true standard deviation of the data. The data were read in blocks of 1000 scans. Data greater than 10 standard deviations were flagged. The second pass computed a standard deviation over the same 1000 scans excluding the flagged values. Values greater than 20 standard deviations were marked bad. This process was applied to pressure, temperature, conductivity and SBE 43 output.

CELLTM used a recursive filter to remove conductivity cell thermal mass effects from the measured conductivity. Typical values used were thermal anomaly amplitude alpha = 0.03 and the time constant 1/beta = 7.0.

FILTER performed a low pass filter on pressure with a time constant of 0.15 seconds. In order to produce zero phase lag (no time shift) the filter runs forward first then backwards.

WFILTER performed as a median filter to remove spikes in fluorometer and transmissometer data. A median value was determined by 49 scans of the window.

SECTIONU (original module, version 1.1) selected a time span of data based on scan number in order to reduce a file size. The minimum number was set to be the start time when the CTD package was beneath the sea-surface after activation of the pump. The maximum number was set to be the end time when the depth of the package was 1 dbar below the surface. The minimum and maximum numbers were automatically calculated in the module.

LOOPEDIT marked scans where the CTD was moving less than the minimum velocity of 0.0 m/s (traveling backwards due to ship roll).

DESPIKE (original module, version 1.0) removed spikes of the data. A median and mean absolute deviation was calculated in 1-dbar pressure bins for both down- and up-cast, excluding the flagged values. Values greater than 4 mean absolute deviations from the median were marked bad for each bin. This process was performed 2 times for temperature, conductivity, SBE 43, and RINKO output.

DERIVE was used to compute oxygen (SBE 43).

BINAVG averaged the data into 1-dbar pressure bins. The center value of the first bin was set equal to the bin size. The bin minimum and maximum values are the center value plus and minus half the bin size. Scans with pressures greater than the minimum and less than or equal to the maximum were averaged. Scans were interpolated so that a data record exist every dbar.

DERIVE was re-used to compute salinity, potential temperature, and density (σ_θ).

SPLIT was used to split data into the down cast and the up cast.

Remaining spikes in the CTD data were manually eliminated from the 1-dbar-averaged data. The data gaps resulting from the elimination were linearly interpolated with a quality flag of 6.

References

Fukasawa, M., T. Kawano and H. Uchida (2004): Blue Earth Global Expedition collects CTD data aboard Mirai, BEAGLE 2003 conducted using a Dynacon CTD traction winch and motion-compensated crane, *Sea Technology*, 45, 14–18.

García, H. E. and L. I. Gordon (1992): Oxygen solubility in seawater: Better fitting equations. *Limnol. Oceanogr.*, 37 (6), 1307–1312.

Uchida, H., G. C. Johnson, and K. E. McTaggart (2010): CTD oxygen sensor calibration procedures, The GO-SHIP Repeat Hydrography Manual: A collection of expert reports and guidelines, IOCCP Rep., No. 14, ICPO Pub. Ser. No. 134.

Uchida, H., K. Ohyama, S. Ozawa, and M. Fukasawa (2007): In situ calibration of the Sea-Bird 9plus CTD thermometer, *J. Atmos. Oceanic Technol.*, 24, 1961–1967.

3.2 Bottle Salinity

May 10, 2012

(1) Personnel

Hiroshi Uchida (JAMSTEC)
Fujio Kobayashi (MWJ) (Leg 1)
Tatsuya Tanaka (MWJ) (Leg 2)
Hiroki Ushiromura (MWJ) (Leg 1)
Tamami Ueno (MWJ) (Leg 2)

(2) Objectives

Bottle salinities were measured to correct CTD salinity data.

(3) Instrument and Method

i. Salinity Sample Collection

Samples for salinity measurement were collected and stored in 250-mL brown borosilicate glass bottles with GL32 screw caps with PTFE liners (without cones). Each bottle and cap was rinsed three times with sample water, and the water was allowed to overflow the bottle. Excess water was poured out until the water was level with the shoulder of the bottle. The bottles were stored at least 12 hours in a laboratory where the salinity was to be measured for temperature equilibration with upside down in a carrying case.

ii. Instruments and Method

The salinity analysis was carried out using Guildline Autosal salinometer model 8400B (S/N 62556 in leg 2 and S/N 62827 in leg 3), which was modified by adding an Ocean Scientific International Ltd. peristaltic-type sample intake pump and two Guildline platinum thermometers model 9450. One thermometer monitored an ambient temperature and the other monitored a bath temperature of the salinometer. The resolution of the thermometer was 0.001°C. The measurement system was almost same as Aoyama *et al*. (2002) and the measurements were basically made according to the salinity measurement manual (Kawano, 2010). The salinometer was operated in the air-conditioned room of the ship at a bath temperature of 24°C.

An ambient temperature varied from approximately 20°C to 24°C, while a bath temperature is stable and varied within ±0.002°C. A measure of a double conductivity ratio of a sample is taken as a median of 31 readings. Data collection was started after 10 seconds and it took about 10 seconds to collect 31 readings by a personal computer. Data were sampled for the sixth and seventh filling of the cell. In case where the difference between the double conductivity ratio of this two fillings is smaller than 0.00002, the average value of the two double conductivity ratios is used to calculate the bottle salinity with the algorithm for practical salinity scale, 1978 (UNESCO, 1981). If the difference is grater than or equal to the 0.00003, we measure another additional filling of the cell. In case where the double conductivity ratio of the additional filling does not satisfy the criteria above, we measure other additional fillings of the cell within 10 fillings in total. In case where the number of fillings is 10 and those fillings do not satisfy the criteria above, the median of the double conductivity ratios of the last five fillings are used to calculate the bottle salinity.

The measurement was conducted about from 6 to 23 hours per day and the cell was cleaned with soap after the measurement of the day. We measured about 4,000 samples in total.

(4) Preliminary Result

i. Standard Seawater

Leg 2

Standardization control was set to 796 during leg 2. The value of STANDBY was 5602 ± 0002 and that of ZERO was 0.00000 ± 0.00001. We used IAPSO Standard Seawater batch P153 which conductivity ratio was 0.99979 (double conductivity ratio is 1.99958) as the standard for salinity. We measured 90 bottles of P153 during routine measurement. Fig. 3.2.1 shows the history of double conductivity ratio of the Standard Seawater batch P153 during leg 2.

As the repeatability of this salinometer was not stable, drifts were calculated by fitting data from P153 to the average of P153 obtained each day. Correction for the double conductivity ratio of the sample was made to compensate for the drift. After correction, the average of double conductivity ratio became 1.99958 and the standard deviation was 0.00002, which is equivalent to 0.0003 in salinity.

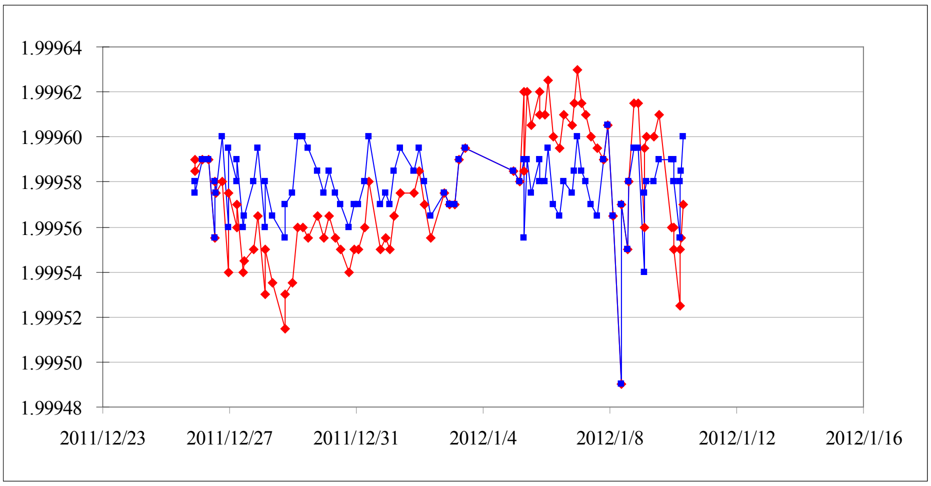

Figure 3.2.1. History of Double conductivity ratio of P153 during leg 2. Horizontal and vertical axes represents date and double conductivity ratio, respectively. Red dots are raw data and blue dots are corrected data.

Leg 3

As the repeatability of the salinometer (S/N 62556) was not stable in leg 2, the salinity analysis was carried out the salinometer (S/N 62827) in leg 3, and standardization control was set to 482 during leg 3. The value of STANDBY was 5408 ± 0002 and that of ZERO was 0.00000 ± 0.00001. We used IAPSO Standard Seawater batch P153 as the standard for salinity. We measured 85 bottles of P153 during routine measurement. Fig.3.2.2 shows the history of double conductivity ratio of the Standard Seawater batch P153 during leg 3.

Drifts were calculated by fitting data from P153 to the equation obtained by the least square method (solid lines). Correction for the double conductivity ratio of the sample was made to compensate for the drift. After correction, the average of double conductivity ratio became 1.99958 and the standard deviation was 0.00001, which is equivalent to 0.0002 in salinity.

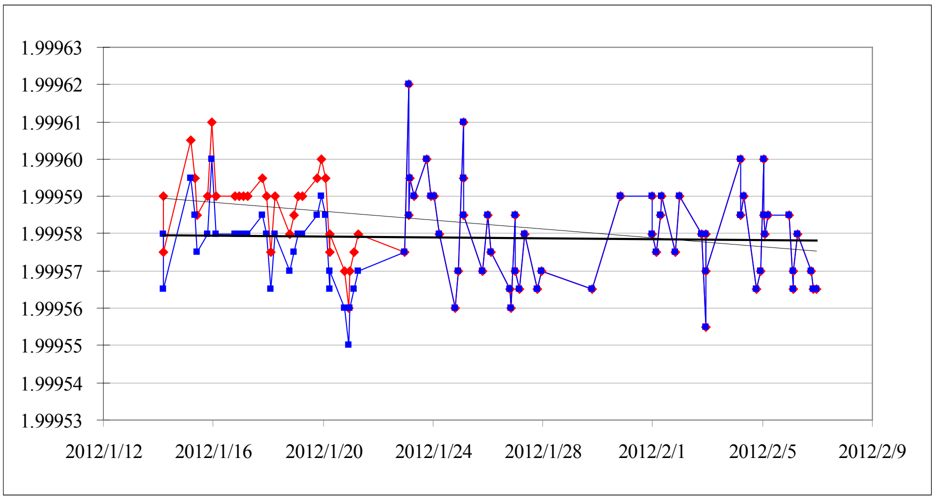

Figure 3.2.2. Same as Fig. 3.2.1, but for leg 2.

ii. Sub-Standard Seawater

We also used sub-standard seawater which was deep-sea water filtered by pore size of 0.45 micrometer and stored in a 20 liter cubitainer made of polyethylene and stirred for at least 24 hours before measurement. It was measured every six water samples in order to check the possible sudden drift of the salinometer. In this cruise, no remarkable sudden drift was detected for the salinometers.

iii. Replicate Samples

We took 325 and 248 pairs of replicate samples during legs 2 and 3, respectively. Figures 3.2.3 and 3.2.4 show the histogram of the absolute difference between replicate samples. The standard deviations of the absolute deference of salinity were 0.00083 and 0.00017 for leg 2 and leg 3, respectively.

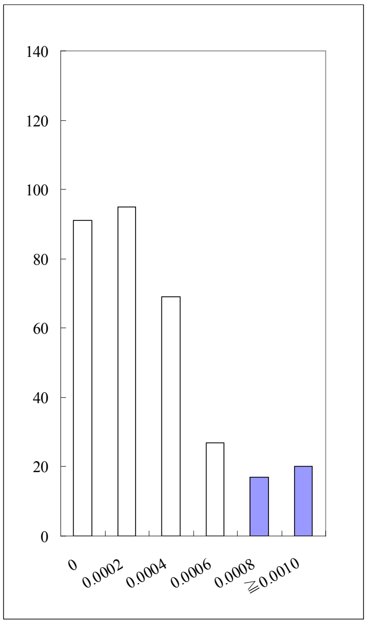

Figure 3.2.3. The histogram of the absolute difference between replicate samples in leg 2. Horizontal axis is absolute difference in salinity and vertical axis is frequency.

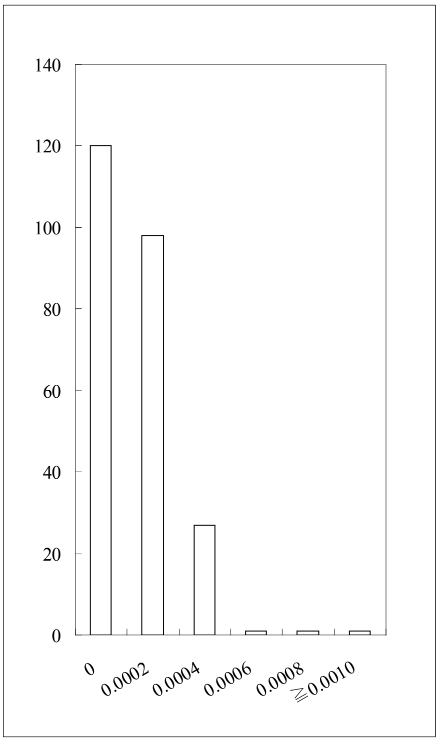

Figure 3.2.4. Same as Fig. 3.2.3, but for leg 3.

(5) Reference

Aoyama, M., T. Joyce, T. Kawano and Y. Takatsuki (2002): Standard seawater comparison up to P129. Deep-Sea

Research, I, 49, 1103–1114.

Kawano, T. (2010): Method for salinity (conductivity ratio) measurement. The GO-SHIP Repeat Hydrography Manual: A Collection of Expert Reports and Guidelines, IOCCP Rep. 14, ICPO Publication series 134, Version 1.

UNESCO (1981): Tenth report of the Joint Panel on Oceanographic Tables and Standards. UNESCO Tech. Papers in Mar. Sci., 36, 25 pp.

3.3 Density

March 5, 2012

(1) Personnel

Hiroshi Uchida (JAMSTEC)

(2) Objectives

The objective of this study is to collect absolute salinity (also called "density salinity") data, and to evaluate an algorithm to estimate absolute salinity provided along with TEOS-10 (the International Thermodynamic Equation of Seawater 2010) (IOC et al., 2010).

(3) Materials and methods

Seawater densities were measured during the cruise or will be measured after the cruise with an oscillation-type density meter (DMA 5000M, serial no. 80570578, Anton-Paar GmbH, Graz, Austria) with a sample changer (Xsample 122, serial no. 80548492, Anton-Paar GmbH). The sample changer was used to load samples automatically from up to ninety-six 12-mL glass vials. AC power was supplied to the density meter through a frequency conversion AC power supply unit (AA500F, Takasago, Ltd., Japan).

The water samples were collected in 100-mL PFA bottles (Sanplatec Co., Japan), 100-mL or 50-mL I-BOY polypropylene bottles (AS ONE, Co., Japan), and vacuum sealed with an aluminum bag (HRS, MAL or ALH, Meiwa Sanshou Co., Ltd, Japan). Densities of the samples were measured at 20 ºC by the density meter from two to six times for each bottle.

Time drift of the density meter was monitored by periodically measuring the density of ultra-pure water (Milli-Q water, Millipore, Billerica, Massachusetts, USA) prepared from Yokosuka (Japan) tap water in July 2010. The true density at 20 ºC of the Milli-Q water was estimated to be 998.2038 kg m^{-3} from the isotopic composition and International Association for the Properties of Water and Steam (IAPWS)-95 standard. An offset correction was applied to the measured density by using the Milli-Q water measurements ($\rho_{\text{Milli-Q}}$) with a slight modification of the density dependency (Uchida et al., 2011). The offset (ρ_{offset}) of the measured density (ρ) was estimated from the following equation:

$$\rho_{\text{offset}} = (\rho_{\text{Milli-Q}} - 998.2038) - (\rho - 998.2038) \times 0.000241 \text{ [kg m}^{-3}\text{]}.$$

The offset correction was verified by measuring Reference Material for Nutrients in Seawater (RMNS) lot BF (Kanso Technos Co., Ltd., Osaka, Japan) along with the Milli-Q water. Mean density of 11 bottles of the RMNS measured during the cruise was 1024.4824 ± 0.0021 kg m^{-3}. Density salinity can be back calculated from measured density and temperature with TEOS-10.

The water samples collected at stations 56, 53, 49, 45, 41, 37, 34, 31, 27, 1, 5, 10, 15, and 21 were vacuum sealed with the HRS aluminum bag and measured within a few days after the collection. The rest of water samples were vacuum sealed with the HRS or ALH aluminum bag and stored in a refrigerator to measure in the laboratory after the cruise since the density meter was broken.

(4) Reference

IOC, SCOR and IAPSO (2010): The international thermodynamic equation of seawater – 2010: Calculation and use of thermodynamic properties. Intergovernmental Oceanographic Commission, Manuals and Guides No. 56, United Nations Educational, Scientific and Cultural Organization (English), 196 pp.

Uchida, H., T. Kawano, M. Aoyama and A. Murata (2011): Absolute salinity measurements of standard seawaters for conductivity and nutrients. *La mer*, 49, 237-244.

3.4 Oxygen

May 01, 2012

Yuichiro Kumamoto

Japan Agency for Marine-Earth Science and Technology

(1) Personnel

Yuichiro Kumamoto [1], ***Miyo Ikeda*** [2], ***Misato Kuwahara*** [2], ***Shin'ichiro Yokogawa*** [2], ***Kanako Yoshida*** [2], **and** ***Yuki Miyajima*** [2]

1) Japan Agency for Marine-Earth Science and Technology
2) Marine Works Japan Co. Ltd

(2) Objectives

Dissolved oxygen is one of good tracers for the ocean circulation. Recent studies indicated that the oxygen minimum layers in the tropical region have expanded (Stramma et al., 2008). Climate models predict a decline in oceanic dissolved oxygen concentration and a consequent expansion of the oxygen minimum layers under global warming conditions, which results mainly from decreased interior advection and ongoing oxygen consumption by remineralization. The mechanism of the decrease, however, is still unknown. During MR11-08 cruise, we measured dissolved oxygen concentration from surface to bottom layers at all the hydrocast stations along approximately 149°E in the western Pacific. These stations reoccupied the WOCE Hydrographic Program P10 and P10N stations in 1993 and 2005, respectively. Our purpose is to evaluate temporal change in dissolved oxygen concentration in the western Pacific between the 1993/2005 and 2011/12.

(3) Reagents

Pickling Reagent I: Manganous chloride solution (3M)

Pickling Reagent II: Sodium hydroxide (8M) / sodium iodide solution (4M)

Sulfuric acid solution (5M)

Sodium thiosulfate (0.025M)

Potassium iodate (0.001667M): Wako Pure Chemical Industries, Ltd., volumetric standard, reference material for iodometry, Lot No.EPR3227, Purity: 99.96±0.01%

CSK standard of potassium iodate: Lot EPJ3885, Wako Pure Chemical Industries Ltd., 0.0100N

(4) Instruments

Burette for sodium thiosulfate and potassium iodate;

APB-620 and APB-510 manufactured by Kyoto Electronic Co. Ltd. / 10 cm^3 of titration vessel

Detector;

Automatic photometric titrator, DOT-01X manufactured by Kimoto Electronic Co. Ltd.

(5) Seawater sampling

Following procedure is based on a determination method in the WHP Operations Manual (Dickson, 1996). Seawater samples were collected from 12-liters Niskin sampler bottles attached to the CTD-system. Seawater for bottle oxygen measurement was transferred from the Niskin sampler bottle to a volume calibrated glass flask (ca. 100 cm^3). Three times volume of the flask of seawater was overflowed. Sample temperature was measured by a thermometer during the overflowing. Then two reagent solutions (Reagent I, II) of 0.5 cm^3 each were added immediately into the sample flask and the stopper was inserted carefully into the flask. The sample flask was then shaken vigorously to mix the contents and to disperse the precipitate finely throughout. After the precipitate has settled at least halfway down the flask, the flask was shaken again to disperse the precipitate. The sample flasks containing pickled samples were stored in a laboratory until they were titrated.

(6) Sample measurement

At least two hours after the re-shaking, the pickled samples were measured on board. A magnetic stirrer bar and 1 cm^3 sulfuric acid solution were added into the sample flask and stirring began. Samples were titrated by sodium thiosulfate solution whose molarity was determined by potassium iodate solution. Temperature of sodium thiosulfate during titration was recorded by a thermometer. We measured dissolved oxygen concentration using two sets of the titration apparatus, named DOT-7 and DOT-8. Dissolved oxygen concentration ($\mu mol\ kg^{-1}$) was calculated by the sample temperature during the sampling, bottle salinity, flask volume, and titrated volume of the sodium thiosulfate solution. When the bottle salinity data is flagged to be 3 (questionable), 4 (bad), or 5 (missing), CTD salinity (primary) data is referred in the calculation alternatively.

(7) Standardization

Concentration of sodium thiosulfate titrant (ca. 0.025M) was determined by potassium iodate solution. Pure potassium iodate was dried in an oven at 130°C. 1.7835 g potassium iodate weighed out accurately was dissolved in deionized water and diluted to final volume of 5 dm^3 in a calibrated volumetric flask (0.001667M). 10 cm^3 of the standard potassium iodate solution was added to a flask using a volume-calibrated dispenser. Then 90 cm^3 of deionized water, 1 cm^3 of sulfuric acid solution, and 0.5 cm^3 of pickling reagent solution II and I were added into the flask in order. Amount of titrated volume of sodium thiosulfate (usually 5 times measurements average) gave the molarity of the sodium thiosulfate titrant. Table 3.4.1 shows result of the standardization during this cruise. Error (C.V.) of the standardization was 0.02±0.01 %, c.a. 0.05 $\mu mol\ kg^{-1}$.

(8) Determination of the blank

The oxygen in the pickling reagents I (0.5 cm^3) and II (0.5 cm^3) was assumed to be 3.8×10^{-8} mol (Murray *et al.*, 1968). The blank from the presence of redox species apart from oxygen in the reagents (the pickling reagents I, II, and the sulfuric acid solution) was determined as follows. 1 and 2 cm^3 of the standard potassium iodate solution were added to two flasks respectively. Then 100 cm^3 of deionized water, 1 cm^3 of sulfuric acid solution, and 0.5 cm^3 of pickling reagent solution II and I each were added into the two flasks in order. The blank was determined by difference between the two times of the first (1 cm^3 of KIO_3) titrated volume of the sodium thiosulfate and the second (2 cm^3 of KIO_3) one. The results of 3 times blank determinations were averaged (Table 3.4.1). The averaged blank values for DOT-7 and DOT-8 were -0.001 ± 0.002 (S.D., n=21) and 0.001 ± 0.001 (S.D., n=21) cm^3, respectively.

Table 3.4.1 Results of the standardization and the blank determinations during MR11-08.

	KIO_3 No.		$Na_2S_2O_3$ No.	DOT-7		DOT-8		Stations
(UTC)	#	ID No.		E.P.	blank	E.P.	blank	
2011/12/22	05	20110523-05-02	20110602-01	3.953	-0.002	3.957	-0.001	P10-059,058,057,056,055,054,053,052,051,050,049,048,047,046,045
2011/12/28		20110523-05-01	20110602-01	3.952	-0.001	3.956	0.001	P10-044,043,042,041,040,039
2011/12/29		20110523-05-07	20110602-02	3.956	-0.003	3.961	-0.001	P10-038,037,036,035,034,033,032,031,030,029,028,027
2012/01/03		20110523-05-08	20110602-02	3.963	0.000	3.964	0.003	P10-001,002,003,004,005,006,007,008,009,010,011,012,013,014,015,016,017,018,019,020,021,022
2012/1/7		20110523-05-05	20110602-03	3.959	-0.001	3.961	0.001	P10-023,024,025,026
2012/1/14	06	20110524-06-03	20110602-03	3.963	-0.001	3.964	0.001	P10-059,060,061,062,063,064,065,066,067,068,069,070,071,072,073
2012/1/19		20110524-06-05	20110602-04	4.075	-0.004	4.076	0.000	P10-074,P10N-075,076,077,078,079,080,081,082,083,084,085,088,086,087,090,092,094,096
2012/2/1		20110524-06-01	20110602-05	3.957	-0.002	3.959	0.001	P10N-098,100,102,104,106,110,112,114,115

(9) Replicate sample measurement

From a single routine CTD cast, a pair of replicate samples was collected at three layers of 10, 1800, and 3750 dbar. In order to estimate uncertainty including instrumental error, two samples of a replicate pair were measured using DOT-7 and DOT-8 separately. Total amount of the replicate sample pairs of good measurement (flagged 2) was 331. The standard deviation of the replicate measurement was 0.13 $\mu mol\ kg^{-1}$ that was calculated by a procedure (SOP23) in DOE (1994). A difference between measurements of a replicate pair is slightly large in samples from low-oxygen layers (Fig. 3.4.1), which is probably due to sampling error on the deck. In the hydrographic data sheet, a mean of replicate sample pairs will be presented with the flag 2 (see section 12).

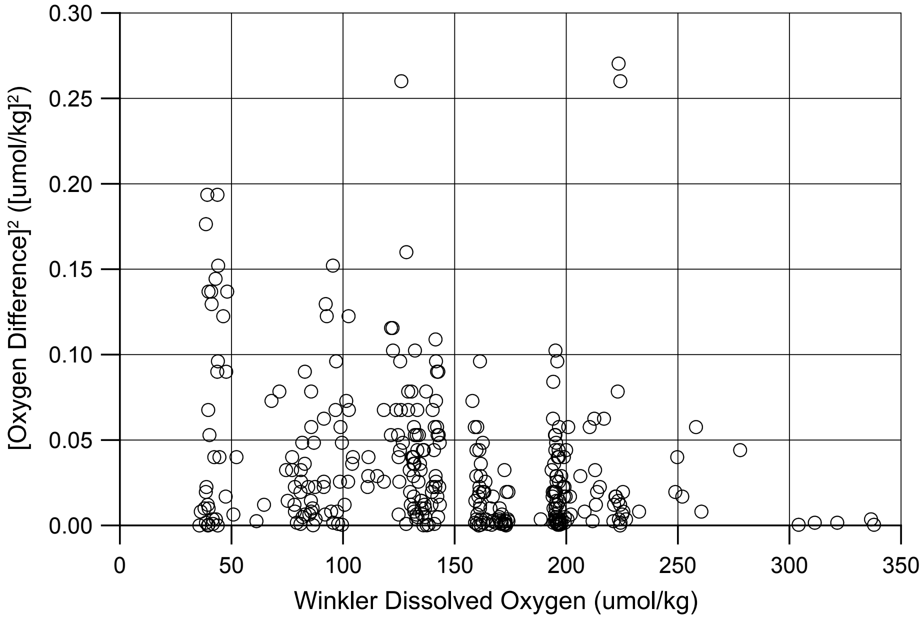

Figure 3.4.1 Oxygen difference between measurements of a replicate pair against oxygen concentration.

(10) Duplicate sample measurement

Duplicate samples were taken from 35 CTD casts during this cruise. Niskin numbers and sampling pressure of the duplicate pairs at the 35 stations are shown in Table 3.4.2. Two samples of a duplicate pair were measured using DOT-7 and DOT-8 separately in the same way of the replicate sample measurements. The standard deviation of the duplicate measurements was calculated to be 0.14 μmol kg^{-1} that was equivalent with that of the replicate measurements (0.13 μmol kg^{-1}, see section 9).

(11) CSK standard measurements

The CSK standard is a commercial potassium iodate solution (0.0100 N) for analysis of dissolved oxygen. We titrated the CSK standard solutions (Lot EPJ3885) against our KIO_3 standards as samples before and during this cruise (Table 3.4.3). A good agreement among them confirms that there was no systematic shift in our oxygen analyses from preparation of our KIO_3 standards onshore to sample measurements on board.

(12) Quality control flag assignment

Quality flag values were assigned to oxygen measurements using the code defined in Table 0.2 of WHP Office Report WHPO 91-1 Rev.2 section 4.5.2 (Joyce *et al.*, 1994). Measurement flags of 2 (good), 3 (questionable), 4 (bad), and 5 (missing) have been assigned (Table 3.4.4). The replicate data were averaged and flagged 2 if both of them were flagged 2. If either of them was flagged 3 or 4, a datum with "younger" flag was selected. Thus we did not use flag of 6 (replicate measurements). For the choice between 2, 3, or 4, we basically followed a flagging procedure as listed below:

Table 3.4.2 Results of the duplicate sample measurements during MR11-08.

	Leg	Stations	Pres.(db)	#1 Niskin		#1 Oxygen [umol/kg]	#2 Niskin		#2 Oxygen [umol/kg]	Difference [(umol/kg)^2]
1	2	P10-59	5656	1	X12J01	176.21	2	X12J02	176.25	0.002
2	2	P10-58	5500	2	X12J02	174.49	3	X12J03	174.42	0.005
3	2	P10-57	5170	2	X12J02	173.25	4	X12J04	173.33	0.006
4	2	P10-56	5080	2	X12J02	172.65	5	X12J05	172.50	0.023
5	2	P10-55	4750	2	X12J02	164.09	6	X12J06	164.11	0.000
6	2	P10-54	4420	2	X12J02	164.89	7	X12J07	164.94	0.003
7	2	P10-53	4330	2	X12J02	163.54	8	X12J08	163.61	0.005
8	2	P10-52	4000	2	X12J02	155.00	9	X12J09	154.90	0.010
9	2	P10-44	3830	2	X12J02	155.70	10	X12J10	155.56	0.020
10	2	P10-43	3500	2	X12J02	149.74	11	X12J11	149.56	0.032
11	2	P10-42	3170	5	X12102	143.09	12	X12J12	143.07	0.000
12	2	P10-41	3080	2	X12103	139.96	13	X12101	140.13	0.029
13	2	P10-38	2870	4	X12104	138.17	14	X12J14	138.00	0.029
14	2	P10-37	2600	2	X12103	129.87	15	X12J15	129.92	0.002
15	2	P10-36	2330	2	X12103	119.45	16	X12J16	119.35	0.010
16	2	P10-35	2270	2	X12103	117.47	17	X12J17	116.93	0.292
17	2	P10-34	2000	2	X12103	113.64	18	X12J18	113.39	0.063
18	2	P10-33	1730	2	X12103	103.02	19	X12J19	102.90	0.014
19	2	P10-32	1670	2	X12103	101.57	20	X12001	101.45	0.014
20	2	P10-31	1400	2	X12103	96.37	21	X12J21	96.64	0.073
21	2	P10-30	1130	2	X12103	92.36	22	X12J22	92.70	0.116
22	2	P10-4	1400	2	X12103	109.34	21	X12J36	109.40	0.004
23	2	P10-5	1670	2	X12103	110.04	20	X12J35	109.89	0.023
24	2	P10-6	1730	2	X12103	109.66	19	X12J34	109.45	0.044
25	2	P10-12	1930	2	X12103	116.36	18	X12J33	116.08	0.078
26	2	P10-13	2200	2	X12103	125.37	17	X12J32	125.40	0.001
27	2	P10-15	2330	2	X12103	128.02	16	X12046	128.23	0.044
28	2	P10-16	2600	2	X12103	135.43	15	X12J30	135.42	0.000
29	2	P10-17	2870	2	X12103	139.94	14	X12J29	139.56	0.144
30	2	P10-18	2930	2	X12103	140.07	13	X12J28	139.79	0.078
31	2	P10-19	3250	2	X12103	144.23	12	X12J27	143.98	0.063

32	2	P10-21	3920	2	X12103	152.71	9	X12J25	152.57	0.020
33	2	P10-22	4500	2	X12103	156.23	7	X12J23	156.01	0.048
34	2	P10-23	4330	2	X12103	155.42	8	X12J24	155.31	0.012
35	2	P10-24	3670	2	X12103	148.59	10	X12J26	148.72	0.017

Table 3.4.3 Results of the CSK standard (Lot EPJ3885) measurements on board.

Date (UTC)	KIO$_3$ ID No.	DOT-7		DOT-8		Remarks
		Conc. (N)	error (N)	Conc. (N)	error (N)	
2011/12/22	20110523-05-02	0.010008	0.000003	0.010008	0.000007	MR11-08 Leg-2
2012/01/14	20110524-06-07	0.010009	0.000002	0.010005	0.000009	MR11-08 Leg-3

Date (UTC)	KIO$_3$ ID No.	DOT-1		–		Remarks
		Conc. (N)	error (N)	–	–	
2011/5/27	20100630-01-11	0.010008	0.000005	–	–	before cruise
2011/5/30	20110524-07-12	0.010007	0.000004	–	–	before cruise
2011/5/31	20110523-05-12	0.010006	0.000007	–	–	before cruise
2011/6/1	20110523-01-12	0.010006	0.000010			before cruise

a. Bottle oxygen concentration at the sampling layer was plotted against sampling pressure. Any points not lying on a generally smooth trend were noted.

b. Difference between bottle oxygen and CTD oxygen (OPTODE sensor) was then plotted against sampling pressure. If a datum deviated from a group of plots, it was flagged 3.

c. Vertical sections against pressure and potential density were drawn. If a datum was anomalous on the section plots, datum flag was degraded from 2 to 3, or from 3 to 4.

d. If there was problem in the measurement, the datum was flagged 4.

e. If the bottle flag was 4 (did not trip correctly), a datum was flagged 4 (bad). In case of the bottle flag 3 (leaking) or 5 (unknown problem), a datum was flagged based on steps a, b, c, and d.

Table 3.4.4 Summary of assigned quality control flags.

Flag	Definition	
2	Good	3080
3	Questionable	4
4	Bad	4
5	Not report (missing)	0
Total		3088

(13) Preliminary Results

i. Comparison with oxygen measurements at the cross point.

During this cruise, we compared vertical profiles of oxygen concentration at a cross point (24°N/149°E) between from our past cruise (MR05-05) and this cruise (MR11-08). The first and second hydrocasts were conducted on 30-Dec.-2005 (MR05-05_P03-X10, 24.486°N/149.356°E) and 17-January-2012 (MR11-08_P10-067, 24.241°N/149.033°E), respectively. Below about 2000 dbar, the first and second measurements agree well (Fig. 3.4.2).

ii. Distribution of dissolved oxygen along WHP-P10/P10N in 2011/12

Figure 3.4.3 shows that a tongue-shaped oxygen minima is lying under the thermocline around 500 – 1500 m depth. The highest concentration was measured in surface waters of the northernmost stations off Hokkaido. Another high-oxygen water was found in bottom waters of the north of 10°N, which corresponds the Circumpolar Deep Water (CDW). The basin-scale distribution of dissolved oxygen in 2011/12 well agrees with those obtained in 1993 and 2005.

iii. Decadal changes in dissolved oxygen along WHP-P10/P10N from 2005 and 2011/12

Along the P10 line, temporal variation of dissolved oxygen between 2005 and 2011/12 was large (< about 10 umol/kg) above 1000 m depth where the vertical gradient of dissolved oxygen is sharp. Below that depth dissolved oxygen changes less than 10 umol/kg were also observed in some regions, implying influence of heaving and internal waves. In addition, we found 1~2 umol/kg of oxygen decrease in near bottom waters between 10 and 30°N that corresponds CDW.

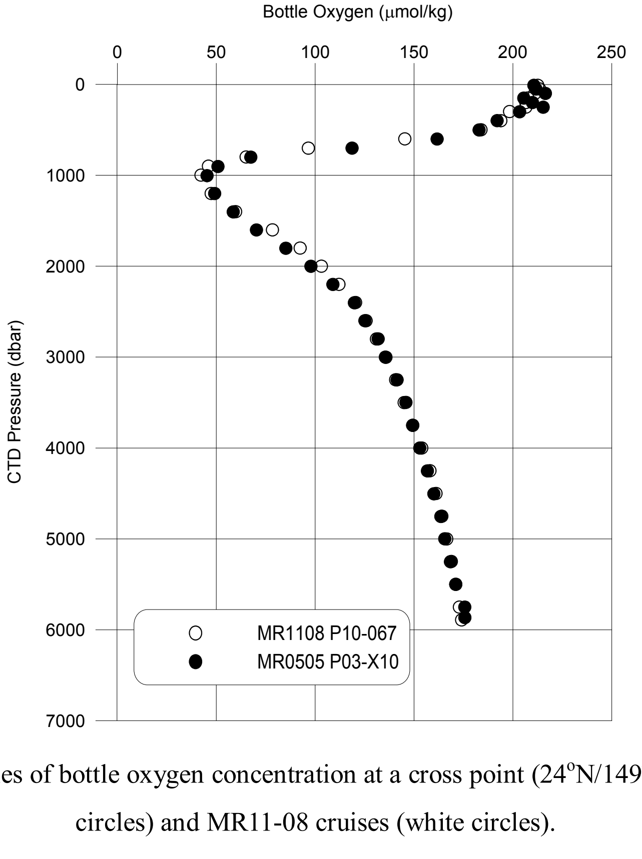

Figure 3.4.2 Vertical profiles of bottle oxygen concentration at a cross point (24°N/149°E) during MR05-05 (black circles) and MR11-08 cruises (white circles).

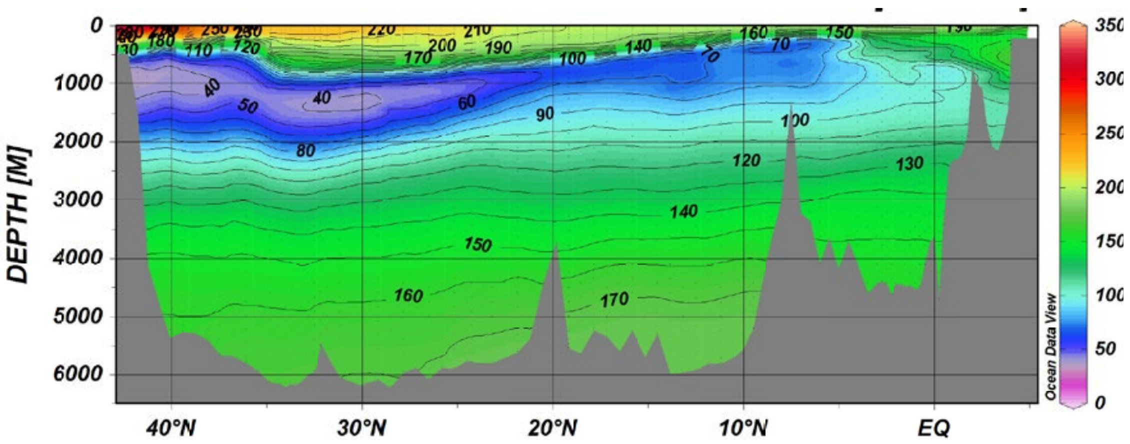

Figure 3.4.3 Transect of bottle oxygen concentration along the cruse track of MR11-08 in the winter of 2011-2012.

References

Dickson, A. (1996) Determination of dissolved oxygen in sea water by Winkler titration, in WHPO Pub. 91-1 Rev. 1, November 1994, Woods Hole, Mass., USA.

DOE (1994) Handbook of methods for the analysis of the various parameters of the carbon dioxide system in sea water; version 2. A.G. Dickson and C. Goyet (eds), ORNL/CDIAC-74.

Joyce, T., and C. Corry, eds., C. Corry, A. Dessier, A. Dickson, T. Joyce, M. Kenny, R. Key, D. Legler, R. Millard, R. Onken, P. Saunders, M. Stalcup (1994) Requirements for WOCE Hydrographic Programme Data Reporting, WHPO Pub. 90-1 Rev. 2, May 1994 Woods Hole, Mass., USA.

Murray, C.N., J.P. Riley, and T.R.S. Wilson (1968) The solubility of oxygen in Winkler reagents used for determination of dissolved oxygen, Deep-Sea Res., 15, 237-238.

Stramma, L., G. C. Johnson, J. Sprintall, V. Mohrholz (2008) Expanding Oxygen-Minimum Zones in the Tropical Oceans, Science, 320, 655-668.

3.5 Nutrients

13 June 2012 ver2.0

(1) Personnel

Michio AOYAMA (Meteorological Research Institute / Japan Meteorological Agency, Principal Investigator)

LEG 2

Minoru KAMATA (Department of Marine Science, Marine Works Japan Ltd.)
Kenichiro SATO (Department of Marine Science, Marine Works Japan Ltd.)
Masanori ENOKI (Department of Marine Science, Marine Works Japan Ltd.)

LEG 3

Minoru KAMATA (Department of Marine Science, Marine Works Japan Ltd.)
Kenichiro SATO (Department of Marine Science, Marine Works Japan Ltd.)
Yasuhiro ARII (Department of Marine Science, Marine Works Japan Ltd.)

(2) Objectives

The objectives of nutrients analyses during the R/V Mirai MR11-08 cruise, WOCE P10 revisited cruise in 2011/2012, in the western Pacific Ocean are as follows;

- Describe the present status of nutrients concentration with excellent comparability.
- The determinants are nitrate, nitrite, silicate and phosphate.
- Study the temporal and spatial variation of nutrients concentration based on the previous high quality experiments data of WOCE previous P10 cruises in 1993 and 2005, GOESECS, IGY and so on.
- Study of temporal and spatial variation of nitrate: phosphate ratio, so called Redfield ratio.
- Obtain more accurate estimation of total amount of nitrate, silicate and phosphate in the interested area.
- Provide more accurate nutrients data for physical oceanographers to use as tracers of water mass movement.

(3) Summary of nutrients analysis

We made 95 QuAAtro 2-HR runs for the samples at 101 stations in MR11-08. The total amount of layers of the seawater sample reached up to 3091 for MR11-08. We made duplicate measurement at all layers.

(4) Instrument and Method

(4.1) Analytical detail using QuAAtro 2-HR systems (BL-Tech)

Nitrate + nitrite and nitrite were analyzed according to the modification method of Grasshoff (1970). The sample nitrate was reduced to nitrite in a cadmium tube inside of which was coated with metallic copper. The sample streamed with its equivalent nitrite was treated with an acidic, sulfanilamide reagent and the nitrite forms nitrous acid which reacted with the sulfanilamide to produce a diazonium ion. N-1-Naphthylethylene-diamine added to the sample stream then coupled with the diazonium ion to produce a red, azo dye. With reduction of the nitrate to nitrite, both nitrate and nitrite reacted and were measured; without reduction, only nitrite reacted. Thus, for the nitrite analysis, no reduction was performed and the alkaline buffer was not necessary. Nitrate was computed by difference.

The silicate method was analogous to that described for phosphate. The method used was essentially that of Grasshoff et al. (1983), wherein silicomolybdic acid was first formed from the silicate in the sample and added molybdic acid; then the silicomolybdic acid was reduced to silicomolybdous acid, or "molybdenum blue" using ascorbic acid as the reductant. The analytical methods of the nutrients, nitrate, nitrite, silicate and phosphate, during this cruise were same as the methods used in (Kawano et al. 2009).

The phosphate analysis was a modification of the procedure of Murphy and Riley (1962). Molybdic acid was added to the seawater sample to form phosphomolybdic acid which was in turn reduced to phosphomolybdous acid using L-ascorbic acid as the reductant.

The details of modification of analytical methods used in this cruise are also compatible with the methods described in nutrients section in GO-SHIP repeat hydrography manual (Hydes et al., 2010). The flow diagrams and reagents for each parameter are shown in Figures 3.5.1 to 3.5.4.

(4.2) Nitrate Reagents

Imidazole (buffer), 0.06 M (0.4 % w/v)

Dissolve 4 g imidazole, $C_3H_4N_2$, in ca. 1000 ml DIW; add 2 ml concentrated HCl. After mixing, 1 ml Triton(R)X-100 (50 % solution in ethanol) is added.

Sulfanilamide, 0.06 M (1 % w/v) in 1.2M HCl

Dissolve 10 g sulfanilamide, $4\text{-}NH_2C_6H_4SO_3H$, in 900 ml of DIW, add 100 ml concentrated HCl. After mixing, 2 ml Triton(R)X-100 (50 %f solution in ethanol) is added.

N-1-Napthylethylene-diamine dihydrochloride, 0.004 M (0.1 %f w/v)

Dissolve 1 g NEDA, $C_{10}H_7NHCH_2CH_2NH_2 \cdot 2HCl$, in 1000 ml of DIW and add 10 ml concentrated HCl. After mixing, 1 ml Triton(R)X-100 (50 %f solution in ethanol) is added.
Stored in a dark bottle.

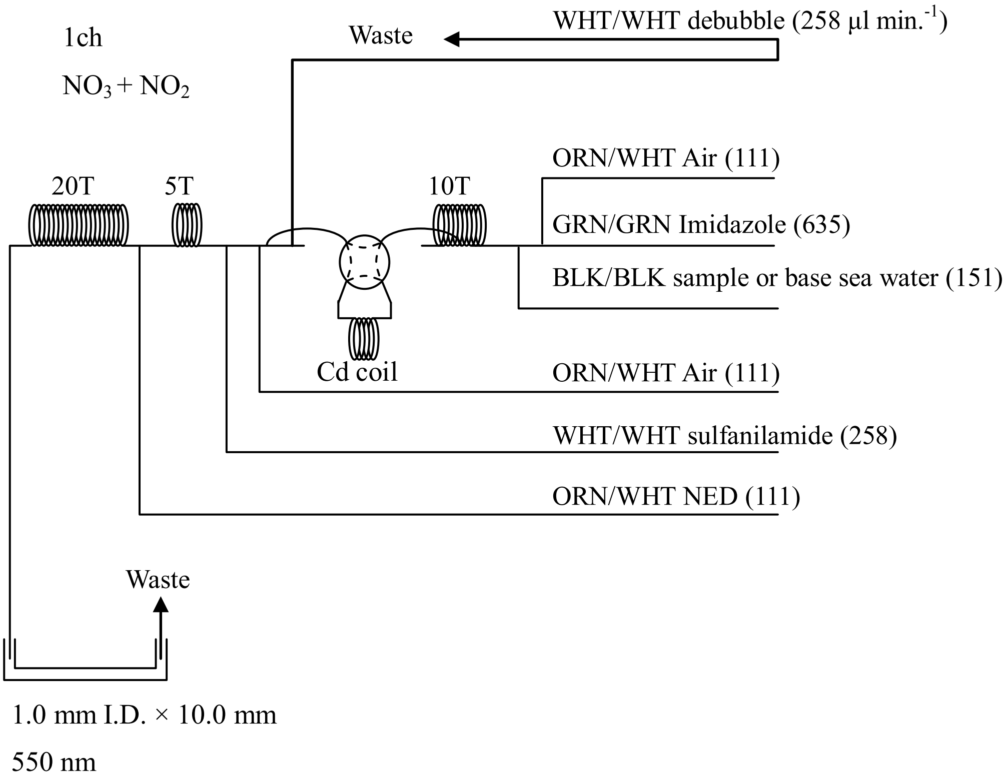

Figure 3.5.1 NO_3+NO_2 (1ch.) Flow diagram.

(4.3) Nitrite Reagents

Sulfanilamide, 0.06 M (1 % w/v) in 1.2 M HCl

Dissolve 10g sulfanilamide, 4-$NH_2C_6H_4SO_3H$, in 900 ml of DIW, add 100 ml concentrated HCl. After mixing, 2 ml Triton(R)X-100 (50 % solution in ethanol) is added.

N-1-Napthylethylene-diamine dihydrochloride, 0.004 M (0.1 % w/v)

Dissolve 1 g NEDA, $C_{10}H_7NHCH_2CH_2NH_2 \cdot 2HCl$, in 1000 ml of DIW and add 10 ml concentrated HCl. After mixing, 1 ml Triton(R)X-100 (50 %f solution in ethanol) is added. This reagent was stored in a dark bottle.

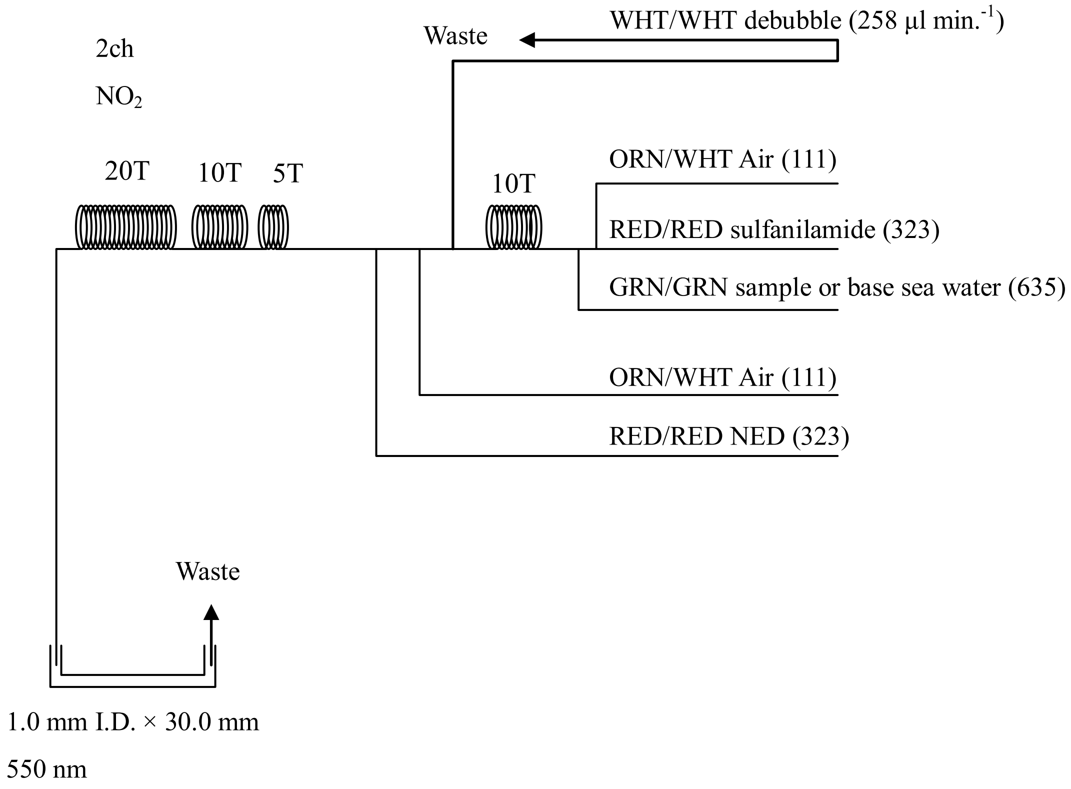

Figure 3.5.2 NO_2 (2ch.) Flow diagram.

(4.4) Silicate Reagents

Molybdic acid, 0.06 M (2 % w/v)

Dissolve 15 g disodium Molybdate(VI) dihydrate, $Na_2M_oO_4 \cdot 2H_2O$, in 980 ml DIW, add 8 ml concentrated H_2SO_4. After mixing, 20 ml sodium dodecyl sulphate (15 % solution in water) is added.

Oxalic acid, 0.6 M (5 % w/v)

Dissolved 50 g oxalic acid anhydrous, HOOC:COOH, in 950 ml of DIW.

Ascorbic acid, 0.01M (3 % w/v)

Dissolved 2.5g L (+)-ascorbic acid, $C_6H_8O_6$, in 100 ml of DIW. This reagent was freshly prepared before every measurement.

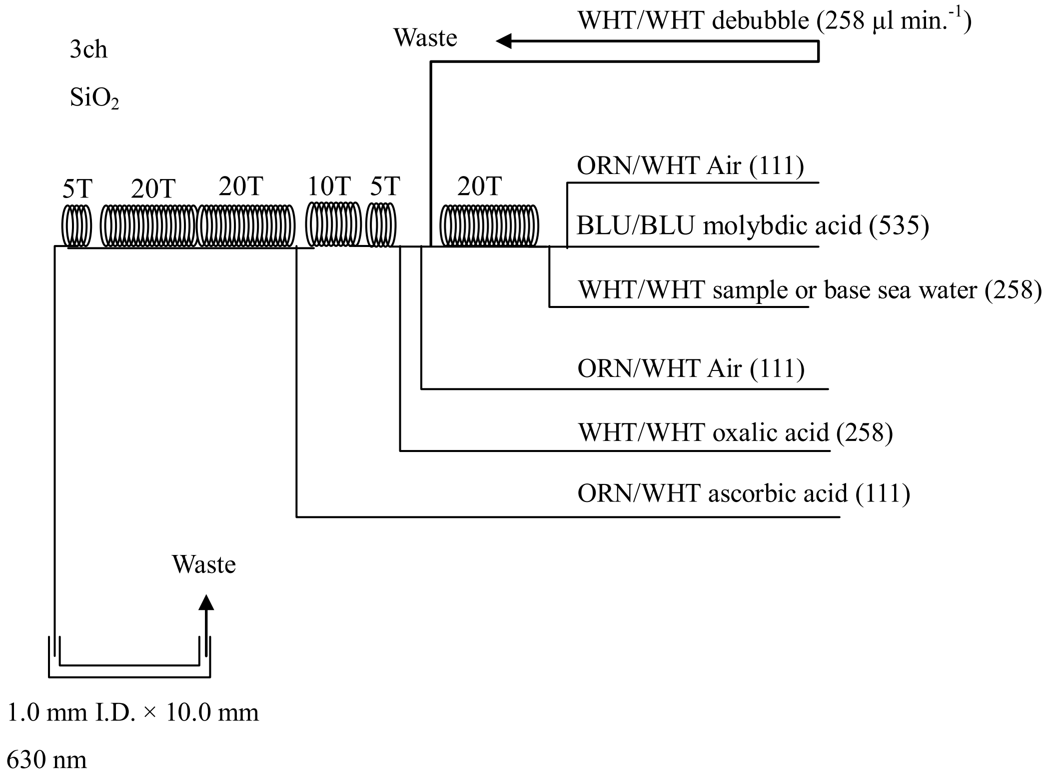

Figure 3.5.3 SiO_2 (3ch.) Flow diagram.

(4.5) Phosphate Reagents

Stock molybdate solution, 0.03M (0.8 % w/v)

Dissolved 8 g disodium molybdate (VI) dihydrate, $Na_2M_oO_4$•$2H_2O$, and 0.17 g antimony potassium tartrate, $C_8H_4K_2O_{12}Sb_2$•$3H_2O$, in 950 ml of DIW and added 50 ml concentrated H_2SO_4.

Mixed Reagent

Dissolved 1.2 g L (+)-ascorbic acid, $C_6H_8O_6$, in 150 ml of stock molybdate solution. After mixing, 3 ml sodium dodecyl sulphate (15 % solution in water) was added in leg3 of this cruise, 4mL sodium dodecyl sulphate (15 % solution in water) was added in leg2 because to reduce relatively noisy signals. This reagent was freshly prepared before every measurement.

Reagent for sample dilution

Dissolved sodium chloride, NaCl, 10 g in ca. 950 ml of DIW, added 50 ml acetone and 4 ml concentrated H_2SO_4. After mixing, 5 ml sodium dodecyl sulphate (15 % solution in water) was added.

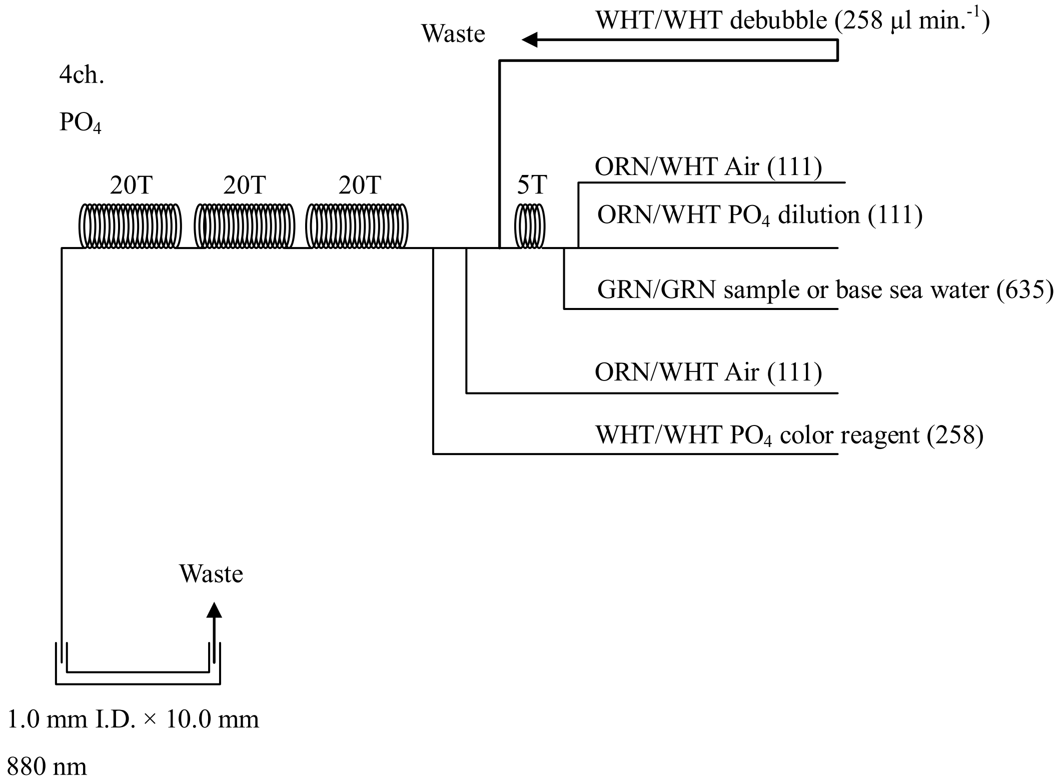

Figure 3.5.4 PO_4 (4ch.) Flow diagram.

(4.6) Sampling procedures

Sampling of nutrients followed that oxygen, salinity and trace gases. Samples were drawn into two of virgin 10 ml polyacrylates vials without sample drawing tubes. These were rinsed three times before filling and vials were capped immediately after the drawing. The vials were put into water bath adjusted to ambient temperature, 24 ± 2 deg. C, in about 30 minutes before use to stabilize the temperature of samples in MR11-08.

No transfer was made and the vials were set an auto sampler tray directly. Samples were analyzed after collection basically within 24 hours in MR11-08.

(4.7) Data processing

Raw data from QuAAtro 2-HR was treated as follows:

- Checked baseline shift.
- Checked the shape of each peak and positions of peak values taken, and then changed the positions of peak values taken if necessary.
- Carry-over correction and baseline drift correction were applied to peak heights of each samples followed by sensitivity correction.
- Baseline correction and sensitivity correction were done basically using liner regression.
- Loaded pressure and salinity from CTD data to calculate density of seawater.

- Calibration curves to get nutrients concentration were assumed second order equations.

(5) Nutrients standards

(5.1) Volumetric laboratory ware of in-house standards

All volumetric glass ware and polymethylpentene (PMP) ware used were gravimetrically calibrated. Plastic volumetric flasks were gravimetrically calibrated at the temperature of use within 0 to 4 K.

Volumetric flasks

Volumetric flasks of Class quality (Class A) are used because their nominal tolerances are 0.05 % or less over the size ranges likely to be used in this work. Class A flasks are made of borosilicate glass, and the standard solutions were transferred to plastic bottles as quickly as possible after they are made up to volume and well mixed in order to prevent excessive dissolution of silicate from the glass. High quality plastic (polymethylpentene, PMP, or polypropylene) volumetric flasks were gravimetrically calibrated and used only within 0 to 4 K of the calibration temperature.

The computation of volume contained by glass flasks at various temperatures other than the calibration temperatures were done by using the coefficient of linear expansion of borosilicate crown glass.

Because of their larger temperature coefficients of cubical expansion and lack of tables constructed for these materials, the plastic volumetric flasks were gravimetrically calibrated over the temperature range of intended use and used at the temperature of calibration within 0 to 4 K. The weights obtained in the calibration weightings were corrected for the density of water and air buoyancy.

Pipettes and pipettors

All pipettes have nominal calibration tolerances of 0.1 % or better. These were gravimetrically calibrated in order to verify and improve upon this nominal tolerance.

(5.2) Reagents, general considerations

Specifications

For nitrate standard, “potassium nitrate 99.995 suprapur®” provided by Merck, CAS No. : 7757-91-1, was used.

For nitrite standard, “sodium nitrate” provided by Wako, CAS No. : 7632-00-0, was used. The assay of nitrite salts was determined according JIS K8019 were 98.31%. We use that value to adjust the weights taken.

For the silicate standard, we use “Silicon standard solution SiO_2 in NaOH 0.5 mol/l CertiPUR®” provided by Merck, CAS No. : 1310-73-2, of which lot number is HC097572 is used. The silicate concentration is certified by NIST-SRM3150 with the uncertainty of 0.5 %. Factor of HC097572 was signed 1.000, however we reassigned the factor as 0.976 from the result of comparison among RMNS in MR11-E02 cruise.

For phosphate standard, “potassium dihydrogen phosphate anhydrous 99.995 suprapur®” provided by Merck, CAS No. : 7778-77-0, was used.

Ultra pure water

Ultra pure water (MilliQ water) freshly drawn was used for preparation of reagents, standard solutions and for measurement of reagent and system blanks.

Low-Nutrient Seawater (LNSW)

Surface water having low nutrient concentration was taken and filtered using 0.45 μm pore size membrane filter. This water is stored in 20 liter cubitainer with paper box. The concentrations of nutrient of this water were measured carefully in Jan 2011.

Treatment of silicate standard due to high alkalinity

Since the silicon standard solution Merck CertiPUR® is in NaOH 0.5 mol/l, we need to dilute and neutralize to avoid make precipitation of $MgOH_2$ etc. When we make B standard, silicon standard solution is diluted by factor 12 with pure water and neutralized by HCl 1.0 mol/l to be about 7. After that B standard solution is used to prepare C standards.

(5.3) Concentrations of nutrients for A, B and C standards

Concentrations of nutrients for A, B and C standards are set as shown in Table 3.5.1. The C standard is prepared according recipes as shown in Table 3.5.2. All volumetric laboratory tools were calibrated prior the cruise as stated in chapter (i). Then the actual concentration of nutrients in each fresh standard was calculated based on the ambient, solution temperature and determined factors of volumetric lab. wares.

The calibration curves for each run were obtained using 6 levels, C-1, C-2, C-3, C-4, C-5 and C-6.

Table 3.5.1 Nominal concentrations of nutrients for A, B and C standards.

	A	B	C-1	C-2	C-3	C-4	C-5	C-6
NO_3(µM)	45000	900	BS	BU	BT	BD	BF	55
NO_2(µM)	4000	20	BS	BU	BT	BD	BF	1.2
SiO_2(µM)	36000	2880	BS	BU	BT	BD	BF	167
PO_4(µM)	3000	60	BS	BU	BT	BD	BF	3.6

Table 3.5.2 Working calibration standard recipes.

C Std.	B-1 Std.	B-2 Std.
C-6	30 ml	30 ml

B-1 Std.: Mixture of nitrate, silicate and phosphate

B-2 Std.: Nitrite

(5.4) Renewal of in-house standard solutions.

In-house standard solutions as stated in (iii) were renewed as shown in Table 3.5.3(a) to (c).

Table 3.5.3(a) Timing of renewal of in-house standards.

NO_3, NO_2, SiO_2, PO_4	Renewal
A-1 Std. (NO_3)	maximum 1 month
A-2 Std. (NO_2)	maximum 1 month
A-3 Std. (SiO_2)	commercial prepared solution
A-4 Std. (PO_4)	maximum 1 month
B-1 Std.	
(mixture of NO_3, SiO_2, PO_4)	8 days
B-2 Std. (NO_2)	8 days

Table 3.5.3(b) Timing of renewal of in-house standards.

Working standards	Renewal
C-6 Std. (mixture of B-1 and B-2 Std.)	24 hours

Table 3.5.3(c) Timing of renewal of in-house standards for reduction estimation.

Reduction estimation	Renewal
D-1 Std. (3600µM NO_3)	8 days
43µM NO_3	when C Std. renewed
47µM NO_2	when C Std. renewed

(6) Reference material of nutrients in seawater

To get the more accurate and high quality nutrients data to achieve the objectives stated above, huge numbers of the bottles of the reference material of nutrients in seawater (hereafter RMNS) are prepared (Aoyama et al., 2006, 2007, 2008, 2009). In the previous worldwide expeditions, such as WOCE cruises, the higher reproducibility and precision of nutrients measurements were required (Joyce and Corry, 1994). Since no standards were available for the measurement of nutrients in seawater at that time, the requirements were described in term of reproducibility. The required reproducibility was 1 %, 1 to 2 %, 1 to 3 % for nitrate, phosphate and silicate, respectively. Although nutrient data from the WOCE one-time survey was of unprecedented quality and coverage due to much care in sampling and measurements, the differences of nutrients concentration at crossover points are still found among the expeditions (Aoyama and Joyce, 1996, Mordy et al., 2000, Gouretski and Jancke, 2001). For instance, the mean offset of nitrate concentration at deep waters was 0.5 μmol kg^{-1} for 345 crossovers at world oceans, though the maximum was 1.7 μmol kg^{-1} (Gouretski and Jancke, 2001). At the 31 crossover points in the Pacific WHP one-time lines, the WOCE standard of reproducibility for nitrate of 1 % was fulfilled at about half of the crossover points and the maximum difference was 7 % at deeper layers below 1.6 deg. C in potential temperature (Aoyama and Joyce, 1996).

During the period from 2003 to 2010, RMNS were used to keep comparability of nutrients measurement among the 8 cruises of CLIVAR project (Sato et al., 2010) , MR10-05 cruise for Arctic research (Aoyama et al., 2010) and MR10-06 cruise for “Change in material cycles and ecosystem by the climate change and its feedback” (Aoyama et al., 2011).

(6.1) RMNSs for this cruise

RMNS lots BS, BU, BT, BD and BF, which cover full range of nutrients concentrations in the western Pacific Ocean are prepared. 80 sets of BS, BU, BT, BD and BF are prepared.

One hundred forty bottles of RMNS lot BE are prepared for MR11-08. Lot BE was used all stations. These RMNS assignment were completely done based on random number. The RMNS bottles were stored at a room in the ship, REAGENT STORE, where the temperature was maintained around 13-24 deg. C.

(6.2) Assigned concentration for RMNSs

We assigned nutrients concentrations for RMNS lots BS, BU, BT, BD, BE, and BF as shown in Table 3.4.4.

Table 3.4.4 Assigned concentration of RMNSs.

unit: μmol kg^{-1}

	Nitrate	Phosphate	Silicate	Nitrite
BS*	0.07	0.064	1.61	0.02
BU*	3.97	0.379	20.30	0.07
BT*	18.21	1.320	41.00	0.47

BD*	29.86	2.194	64.39	0.05
BE**	36.70	2.662	99.20	0.03
BF***	41.39	2.809	150.23 †	0.02

* The values are assigned for this cruise on 27 July 2011.

** The values are assigned for this cruise on 4 April 2009 (Table3.4.4 in WHP P21 REVISIT DATA BOOK).

*** The values are assigned for this cruise on 10 October 2007 (Table3.4.4 in WHP P1, P14 REVISIT DATA BOOK).

. † This value is changed in MR11-03 cruise.

(6.3) The homogeneity of RMNSs

The homogeneity of lot BE used in MR11-08 cruise and analytical precisions are shown in Table 3.5.5. These are for the assessment of the magnitude of homogeneity of the RMNS bottles those are used during the cruise. As shown in Table 3.5.5 homogeneity of RMNS lot BE for nitrate, phosphate and silicate are the same magnitude of analytical precision derived from fresh raw seawater in January 2009.

Table 3.5.5 Homogeneity of lot BE derived from simultaneous 209 samples measurements and analytical precision onboard R/V Mirai in MR11-08.

	Nitrate	**Phosphate**	**Silicate**
	CV %	**CV %**	**CV %**
BE	**0.17**	**0.28**	**0.17**
Precision	**0.12**	**0.20**	**0.14**

BE: N=209

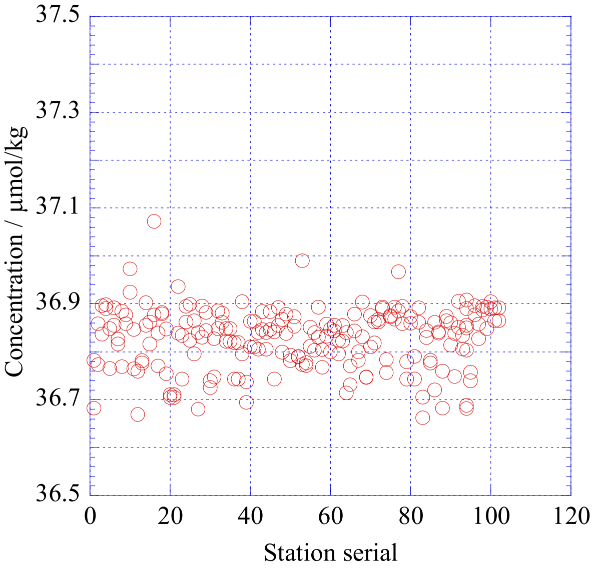

Figure 3.5.5 Time series of RMNS-BE of nitrate for MR11-08.

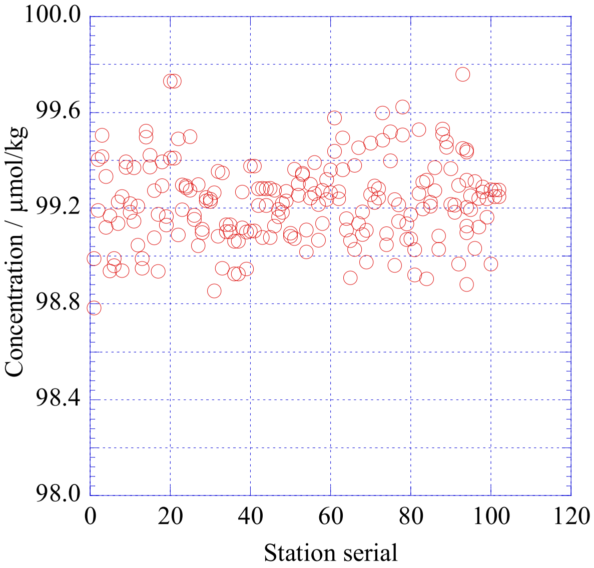

Figure 3.5.6 Time series of RMNS-BE of silicate for MR11-08.

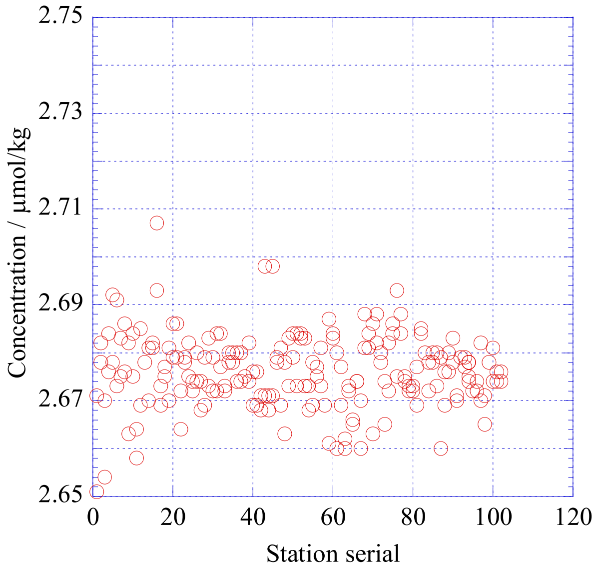

Figure 3.5.7 Time series of RMNS-BE of phosphate for MR11-08.

(6.4) Comparability of RMNSs during the periods from 2003 to 2011

Cruise-to-cruise comparability has examined based on the results of the previous results of RMNSs measurements obtained among cruises, and RMNS international comparison experiments in 2003 and 2009. The uncertainties for each value were obtained similar method described in 7.1 in this chapter at the measurement before each cruise and inter-comparison study, shown as precruise and intercomparison, and mean of uncertainties during each cruise, only shown cruise code, respectively. As shown in Table 3.5.7, the nutrients concentrations of RMNSs were in good agreement among the measurements during the period from 2003 to 2011. For the silicate measurements, we show lot numbers and chemical company names of each cruise/measurement in the footnote. As shown in Table 3.4.7, there shows less comparability among the measurements due to less comparability among the standard solutions provided by chemical companies in the silicate measurements.

Table 3.5.7 (a) Comparability for nitrate.

unit: µmol kg^{-1}

Cruise / Lab.	RM Lots													
	AH	unc.	AZ	unc.	BA	unc.	AX	unc.	AV	unc.	BC	unc.	BE	unc.
							Nitrate							
2003														
2003intercomp_reported	35.23	0.06					21.39							
MR03-K04 Leg1	35.25													
MR03-K04 Leg2	35.37													
MR03-K04 Leg4	35.37													
MR03-K04 Leg5	35.34													

Cruise / Lab.	RM Lots													
	AH	unc.	AZ	unc.	BA	unc.	AX	unc.	AV	unc.	BC	unc.	BE	unc.
2005														
MR05-02			42.30		0.07	0.02	21.45	0.07	33.35	0.06	40.70	0.06		
MR05-05_1 precruise	35.65	0.05	42.30	0.10	0.07	0.00	21.41	0.01	33.41	0.02	40.76	0.03		
MR05-05_1			42.33		0.07	0.01	21.43	0.05	33.36	0.05	40.73	0.85		
MR05-05_2 precruise			42.33		0.08	0.00	21.39	0.02	33.36	0.05	40.72	0.03		
MR05-05_2			42.34		0.07	0.01	21.44	0.05	33.36	0.05	40.73	0.06		
MR05-05_3 precruise			42.35		0.06	0.00	21.49	0.01	33.39	0.01	40.79	0.01		
MR05-05_3			42.36		0.07	0.01	21.44	0.04	33.37	0.05	40.75	0.05		
2006														
2006intercomp			42.24	0.04	0.04	0.00	21.40	0.02	33.32	0.03	40.63	0.04		
2003intercomp_revisit	35.40	0.03												
2007														
MR07-04_1 precruise	35.74	0.03			0.07	0.00	21.59	0.02	33.49	0.03	40.83	0.03		
MR07-04_2 precruise	35.80	0.01			0.08	0.00	21.60	0.01	33.47	0.01	40.92	0.02		
MR07-04					0.08	0.01	21.41	0.06	33.38	0.05	40.77	0.05		
MR07-06_1 precruise	35.61	0.02			0.07	0.00	21.44	0.01	33.43	0.02	40.79	0.02		
MR07-06_2 precruise	35.61	0.04			0.06	0.00	21.43	0.02	33.54	0.04	40.79	0.05		
MR07-06_1					0.08	0.01	21.44	0.03	33.41	0.05	40.81	0.04		
MR07-06_2					0.09	0.01	21.44	0.03	33.39	0.06	40.81	0.04		
							Nitrate							
2008														
2008intercomp_report					0.08	0.00	21.44	0.02						
2006intercomp_revisit			42.27	0.04	0.07	0.00	21.47	0.02	33.34	0.03				
2003intercomp_revisit	35.35	0.04												
2009														
MR09-01_0 precruise			42.36	0.02	0.07	0.00	21.43	0.01	33.42	0.02	40.81	0.02	36.70	0.02
MR09-01_1			42.42	0.06	0.11	0.01	21.51	0.04	33.53	0.04	40.82	0.11	36.74	0.04
MR09-01_2			42.43	0.05			21.54	0.03	33.53	0.03			36.74	0.03
INSS stability test_1	35.76	0.22			0.08	0.01	21.49	0.02	33.45	0.03				
2010														
SGONS stability test_2			42.46	0.05	0.10	0.00	21.51	0.02	33.52				36.76	0.02
SGONS stability test_3			42.48		0.09		21.52		33.63				36.77	
2011														
SGONS stability test_4			42.56	0.07	0.08	0.01	21.62	0.01	33.65	0.07			36.83	0.03

SGONS stability test_5			42.49	0.05	0.06	0.00							36.87	0.06
MR11-08_2													36.83	0.07
SGONS stability test_6														
MR11-08_3													36.83	0.06

Table 3.5.7 (b) Comparability for Phosphate.

unit: µmol kg^{-1}

Cruise / Lab.	RM Lots													
	AH	unc.	AZ	unc.	BA	unc.	AX	unc.	AV	unc.	BC	unc.	BE	unc.
							Phosphate							
2003														
2003intercomp	2.141	0.001												
MR03-K04 Leg1	2.110													
MR03-K04 Leg2	2.110													
MR03-K04 Leg4	2.110													
MR03-K04 Leg5	2.110													
2005														
MR05-02			3.010		0.061	0.010	1.614	0.008	2.515	0.008	2.778	0.010		
MR05-05_1 precruise	2.148	0.006	3.020	0.010	0.045	0.000	1.620	0.001	2.517	0.002	2.781	0.002		
MR05-05_1			3.016		0.063	0.007	1.615	0.006	2.515	0.007	2.778	0.033		
MR05-05_2 precruise			3.015		0.066	0.000	1.608	0.001	2.510	0.001	2.784	0.002		
MR05-05_2			3.018		0.064	0.005	1.614	0.004	2.515	0.005	2.782	0.006		
MR05-05_3 precruise			3.020		0.060	0.000	1.620	0.001	2.517	0.002	2.788	0.002		
MR05-05_3			3.016		0.061	0.004	1.618	0.005	2.515	0.004	2.779	0.008		
2006														
2006intercomp			3.018	0.002	0.071	0.000	1.623	0.001	2.515	0.001	2.791	0.001		
2003intercomp_revisit	2.141	0.001												
2007														
MR07-04_1 precruise	2.140	0.002			0.062	0.000	1.620	0.001	2.512	0.002	2.782	0.002		
MR07-04_2 precruise	2.146	0.002			0.056	0.000	1.620	0.001	2.517	0.002	2.788	0.002		
MR07-04					0.066	0.004	1.617	0.005	2.513	0.004	2.781	0.007		
MR07-06_1 precruise	2.144	0.001			0.066	0.000	1.617	0.001	2.517	0.001	2.790	0.001		

MR07-06_2 precruise	**2.146**	**0.002**			**0.067**	**0.000**	**1.620**	**0.001**	**2.517**	**0.002**	**2.789**	**0.002**		
MR07-06_1					**0.064**	**0.004**	**1.620**	**0.003**	**2.515**	**0.003**	**2.783**	**0.005**		
MR07-06_2					**0.066**	**0.004**	**1.619**	**0.005**	**2.515**	**0.003**	**2.785**	**0.006**		
2008														
2008intercomp_report					**0.068**	**0.000**	**1.615**	**0.005**						
2006intercomp_revisit			**3.014**	**0.008**	**0.065**	**0.000**	**1.627**	**0.005**	**2.513**	**0.007**				
2003intercomp_revisit	**2.131**	**0.006**												
2009														
MR09-01_0 precruise			**3.017**	**0.001**	**0.074**	**0.000**	**1.619**	**0.001**	**2.520**	**0.001**	**2.790**	**0.001**	**2.662**	**0.001**
MR09-01_1			**3.019**	**0.005**	**0.072**	**0.002**	**1.623**	**0.004**	**2.528**	**0.003**	**2.783**	**0.004**	**2.668**	**0.005**
MR09-01_2			**3.018**	**0.004**			**1.625**	**0.003**	**2.527**	**0.003**			**2.668**	**0.003**
INSS stability test_1	**2.134**	**0.008**			**0.069**	**0.001**	**1.606**	**0.001**	**2.512**	**0.003**				
2010														
SGONS stability test_2			**3.012**	**0.008**	**0.059**	**0.001**	**1.618**	**0.004**	**2.520**	**0.008**			**2.663**	**0.006**
SGONS stability test_3			**3.024**		**0.055**		**1.617**		**2.528**				**2.666**	
2011														
SGONS stability test_4			**3.017**	**0.006**	**0.066**	**0.004**	**1.624**	**0.005**	**2.533**	**0.030**			**2.668**	**0.006**
SGONS stability test_5			**3.011**	**0.004**	**0.003**								**2.665**	**0.002**
MR11-08_2													**2.676**	**0.008**
SGONS stability test_6														
MR11-08_3													**2.676**	**0.007**

Table 3.5.7 (C) Comparability for Silicate.

unit: µmol kg^{-1}

Cruise	**RM Lots**													
	AH	**unc.**	**AZ**	**unc.**	**BA**	**unc.**	**AX**	**unc.**	**AV**	**unc.**	**BC**	**unc.**	**BE**	**unc.**
			Silicate											
2003														
2003intercomp[*]	**130.51**	**0.20**												
MR03-K04 Leg1[**]	**132.01**													
MR03-K04 Leg2[**]	**132.26**													
MR03-K04 Leg4[**]	**132.28**													
MR03-K04 Leg5[**]	**132.19**													
2005														
MR05-02[#]			**133.69**		**1.61**	**0.05**	**58.04**	**0.11**	**153.92**	**0.19**	**155.93**	**0.19**		
MR05-05_1 precruise[##]	**132.49**	**0.13**	**133.77**	**0.02**	**1.51**	**0.00**	**58.06**	**0.03**	**153.97**	**0.09**	**15.65**	**0.09**		

MR05-05_1 [##]			**133.79**		**1.59**	**0.07**	**58.01**	**0.12**	**154.01**	**0.26**	**156.08**	**0.36**		
MR05-05_2 precruise [##]			**133.78**		**1.58**	**0.00**	**57.97**	**0.04**	**154.07**	**0.09**	**156.21**	**0.10**		
MR05-05_2 [##]			**133.88**		**1.59**	**0.06**	**58.00**	**0.09**	**154.05**	**0.16**	**156.14**	**0.15**		
MR05-05_3 precruise [##]			**134.02**		**1.57**	**0.00**	**58.05**	**0.05**	**154.07**	**0.14**	**156.11**	**0.14**		
MR05-05_3 [##]			**133.79**		**1.60**	**0.05**	**57.98**	**0.09**	**153.98**	**0.18**	**156.08**	**0.13**		
2006														
2006intercomp [\$]			**133.83**	**0.07**	**1.64**	**0.00**	**58.20**	**0.03**	**154.16**	**0.08**	**156.31**	**0.08**		
2003intercomp_revisit [\$]	**132.55**	**0.07**												
2007														
MR07-04_1 precruise [\$\$]	**133.38**	**0.06**			**1.61**	**0.00**	**58.46**	**0.03**	**154.82**	**0.07**	**156.98**	**0.07**		
MR07-04_2 precruise [\$\$]	**133.15**	**0.12**			**1.69**	**0.00**	**58.44**	**0.05**	**154.87**	**0.14**	**156.86**	**0.14**		
MR07-04 [\$\$]					**1.62**	**0.07**	**58.11**	**0.11**	**154.45**	**0.21**	**156.62**	**0.48**		
MR07-06_1 precruise [\$\$]	**133.02**	**0.09**			**1.64**	**0.00**	**58.50**	**0.04**	**155.06**	**0.11**	**156.33**	**0.11**		
MR07-06_2 precruise [\$\$]	**132.70**	**0.07**			**1.56**	**0.00**	**58.25**	**0.03**	**154.39**	**0.08**	**156.57**	**0.08**		
MR07-06_1 [\$\$]					**1.61**	**0.04**	**58.13**	**0.08**	**154.48**	**0.13**	**156.64**	**0.08**		
MR07-06_2 [\$\$]					**1.58**	**0.07**	**58.04**	**0.10**	**154.38**	**0.16**	**156.61**	**0.13**		
2008														
2008intercomp [¥]					**1.64**	**0.00**	**58.17**	**0.05**						
2006intercomp_re [¥]			**134.11**	**0.11**	**1.65**	**0.00**	**58.26**	**0.05**	**154.36**	**0.12**				
2003intercomp_re [¥]	**132.11**	**0.11**												

	RM Lots													
Cruise	**AH**	**unc.**	**AZ**	**unc.**	**BA**	**unc.**	**AX**	**unc.**	**AV**	**unc.**	**BC**	**unc.**	**BE**	**unc.**
							Silicate							
2009														
MR09-01_0 precruise [¥]			**133.93**	**0.04**	**1.57**	**0.00**	**58.06**	**0.02**	**154.23**	**0.05**	**156.16**	**0.05**	**99.20**	**0.03**
MR09-01_1 [¥]			**133.97**	**0.11**	**1.34**	**0.11**	**58.15**	**0.08**	**154.48**	**0.09**	**155.89**	**0.13**	**99.24**	**0.08**
MR09-01_2 [¥]			**133.96**	**0.11**			**58.19**	**0.08**	**154.42**	**0.12**			**99.23**	**0.08**
INSS stability test_1 [¥¥]	**132.40**	**0.35**			**1.69**	**0.02**	**58.18**	**0.02**	**154.43**	**0.09**				
2010														
SGONS stability test_2 [¥¥]			**133.89**	**0.12**	**1.58**	**0.02**	**58.15**	**0.04**	**154.43**	**0.21**			**99.20**	**0.07**
SGONS stability test_3 [¥¥]			**134.20**		**1.58**		**58.10**		**154.90**				**99.18**	
2011														
SGONS stability test_4 [+]			**134.16**	**0.09**	**1.68**	**0.04**	**58.26**	**0.05**	**154.56**	**0.05**			**99.30**	**0.07**
SGONS stability test_5 [+]			**133.27**	**0.21**	**1.49**	**0.02**							**98.82**	**0.18**
MR11-08_2 [++]													**99.21**	**0.17**

SGONSstability test_6^{++}		
MR11-08_3^{++}	**99.25**	**0.18**

List of lot numbers: *: Kanto 306F9235; **: Kanto 402F9041; #: Kanto 507F9205; ##: Kanto 609F9157; $: Merck OC551722; $$: Merck HC623465; ¥: Merck HC751838; ¥¥: HC814662; +: HC074650;
++: HC097572

(7) Quality control

(7.1) Precision of nutrients analyses during the cruise

Precision of nutrients analyses during the cruise was evaluated based on the 9 to 11 measurements, which are measured every 10 to 13 samples, during a run at the concentration of C-6 std. Summary of precisions are shown as shown in Table 3.5.8 and Figures 3.5.8 to 3.5.10, the precisions for each parameter are generally good considering the analytical precisions estimated from the simultaneous analyses of 14 samples in January 2009 as shown in Table 3.4.6. Analytical precisions previously evaluated were 0.18 % for nitrate, 0.14 % for phosphate and 0.08 % for silicate, respectively. During this cruise, analytical precisions were 0.12 % for nitrate, 0.20 % for phosphate and 0.14 % for silicate in terms of median of precision, respectively. Then we can conclude that the analytical precisions for nitrate, phosphate and silicate throughout this cruise became relatively bad. The reasons of the phenomenon is discussed in chapter (8).

Table 3.5.8 Summary of precision based on the replicate analyses.

	Nitrate	**Phosphate**	**Silicate**
	CV %	**CV %**	**CV %**
Median	0.12	0.20	0.14
Mean	0.13	0.21	0.13
Maximum	0.4	0.4	0.25
Minimum	0.04	0.05	0.05
N	102	102	102

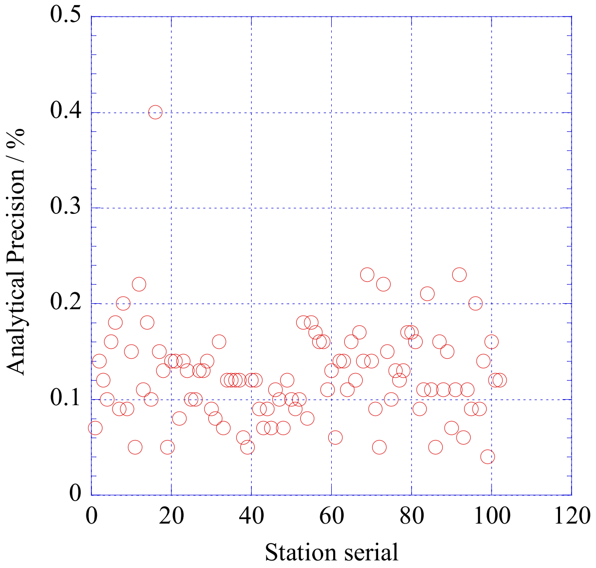

Figure 3.5.8 Time series of precision of nitrate for MR11-08.

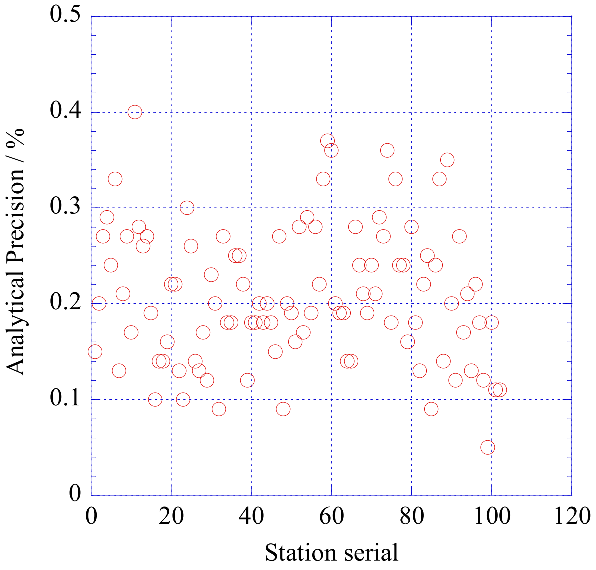

Figure 3.5.9 Time series of precision of phosphate for MR11-08.

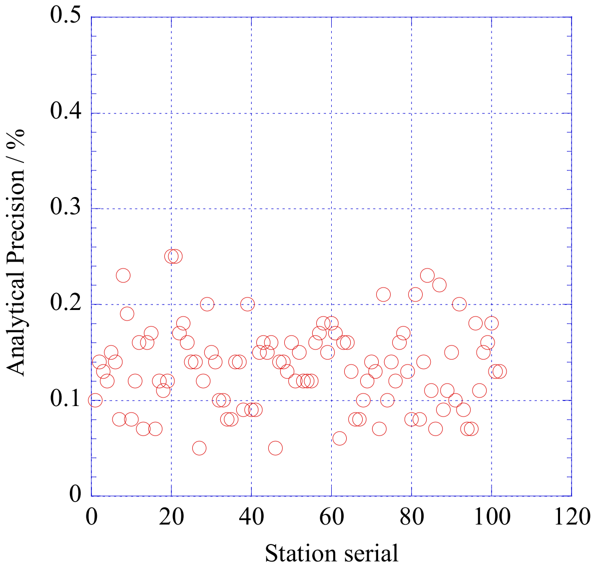

Figure 3.5.10 Time series of precision of silicate for MR11-08.

(7.2) Carry over

We also summarize the magnitudes of carry over throughout the cruise. These are small enough within acceptable levels as shown in Table 3.4.10 and Figures 3.5.11 – 3.5.13..

Table 3.4.10 Summary of carry over through out MR11-08 cruise.

	Nitrate **CV %**	**Phosphate** **CV %**	**Silicate** **CV %**
Median	**0.11**	**0.19**	**0.10**
Mean	**0.12**	**0.21**	**0.10**
Maximum	**0.33**	**0.8**	**0.28**
Minimum	**0.00**	**0.00**	**0.00**
N	**102**	**102**	**102**

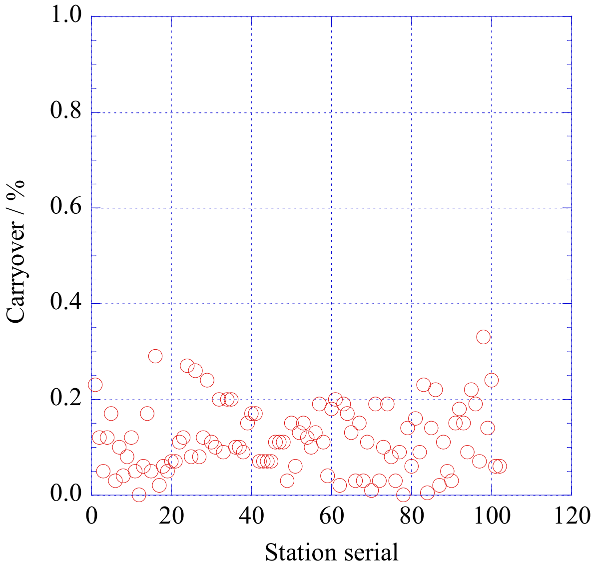

Figure 3.5.11 Time series of carryover of nitrate for MR11-08.

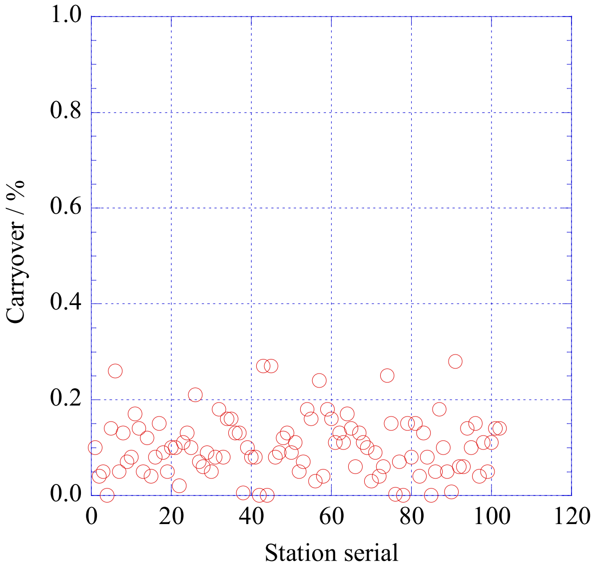

Figure 3.5.12 Time series of carryover of silicate for MR11-08.

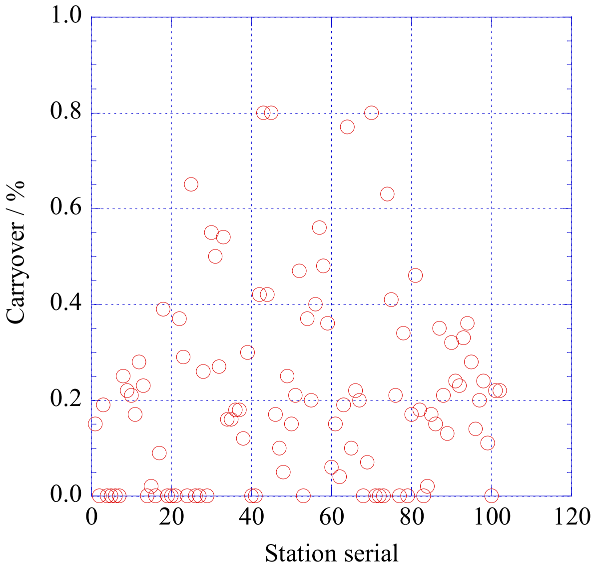

Figure 3.5.13 Time series of carryover of phosphate for MR11-08.

(7.2) Estimation of uncertainty of phosphate, nitrate and silicate concentrations

Empirical equations, eq. (1), (2) and (3) to estimate uncertainty of measurement of phosphate, nitrate and silicate are used based on measurements of 140 sets of RMNSs during the this cruise. These empirical equations are as follows, respectively.

Phosphate Concentration Cp in µmol kg^{-1}:

Uncertainty of measurement of phosphate (%) =

0.14871+ 0.61128 *(1/Cp) + 0.02228 * (1/Cp) *(1/Cp) --- (1)

where Cp is phosphate concentration of sample.

Nitrate Concentration Cn in µmol kg^{-1}:

Uncertainty of measurement of nitrate (%) =

0.14629 + 2.5141 *(1/Cn) + 0.056725 * (1/Cn) * (1/Cn) --- (2)

where Cn is nitrate concentration of sample.

Silicate Concentration Cs in µmol kg^{-1}:

Uncertainty of measurement of silicate (%) =

0.12394+ 9.9377 * (1/Cs) + 7.6725 * (1/Cs) * (1/Cs) --- (3)

where Cs is silicate concentration of sample.

(8) Problems/improvements occurred and solutions.

During this cruse, we observed noisy signals in output of QuAAtro 2-HR systems. After this cruise we investigated on this and confirmed that noisy signals were originated from Kr-lamps of the colorimeters. We did fix this problem by using LED lamps instead of Kr-lamps.

(9) Data archive

All data will be submitted to JAMSTEC Data Management Group (DMG) and is currently under its control.

References

Aminot, A. and Kerouel, R. 1991. Autoclaved seawater as a reference material for the determination of nitrate and phosphate in seawater. Anal. Chim. Acta, 248: 277-283.

Aminot, A. and Kirkwood, D.S. 1995. Report on the results of the fifth ICES intercomparison exercise for nutrients in sea water, ICES coop. Res. Rep. Ser., 213.

Aminot, A. and Kerouel, R. 1995. Reference material for nutrients in seawater: stability of nitrate, nitrite, ammonia and phosphate in autoclaved samples. Mar. Chem., 49: 221-232.

Aoyama M., and Joyce T.M. 1996, WHP property comparisons from crossing lines in North Pacific. In Abstracts, 1996 WOCE Pacific Workshop, Newport Beach, California.

Aoyama, M., 2006: 2003 Intercomparison Exercise for Reference Material for Nutrients in Seawater in a Seawater Matrix, Technical Reports of the Meteorological Research Institute No.50, 91pp, Tsukuba, Japan.

Aoyama, M., Susan B., Minhan, D., Hideshi, D., Louis, I. G., Kasai, H., Roger, K., Nurit, K., Doug, M., Murata, A., Nagai, N., Ogawa, H., Ota, H., Saito, H., Saito, K., Shimizu, T., Takano, H., Tsuda, A., Yokouchi, K., and Agnes, Y. 2007. Recent Comparability of Oceanographic Nutrients Data: Results of a 2003 Intercomparison Exercise Using Reference Materials. Analytical Sciences, 23: 1151-1154.

Aoyama M., J. Barwell-Clarke, S. Becker, M. Blum, Braga E. S., S. C. Coverly,E. Czobik, I. Dahllof, M. H. Dai, G. O. Donnell, C. Engelke, G. C. Gong, Gi-Hoon Hong, D. J. Hydes, M. M. Jin, H. Kasai, R. Kerouel, Y. Kiyomono, M. Knockaert, N. Kress, K. A. Krogslund, M. Kumagai, S. Leterme, Yarong Li, S. Masuda, T. Miyao, T. Moutin, A. Murata, N. Nagai, G.Nausch, M. K. Ngirchechol, A. Nybakk, H. Ogawa, J. van Ooijen, H. Ota, J. M. Pan, C. Payne, O. Pierre-Duplessix, M. Pujo-Pay, T. Raabe, K. Saito, K. Sato, C. Schmidt, M. Schuett, T. M. Shammon, J. Sun, T. Tanhua, L. White, E.M.S. Woodward, P. Worsfold, P. Yeats, T. Yoshimura, A.Youenou, J. Z. Zhang, 2008: 2006 Intercomparison Exercise for Reference Material for Nutrients in Seawater in a Seawater Matrix, Technical Reports of the Meteorological Research Institute No. 58, 104pp.

Aoyama, M., Nishino, S., Nishijima, K., Matsushita, J., Takano, A., Sato, K., 2010a. Nutrients, In: R/V Mirai Cruise Report MR10-05. JAMSTEC, Yokosuka, pp. 103-122.

Aoyama, M., Matsushita, J., Takano, A., 2010b. Nutrients, In: MR10-06 preliminary cruise report. JAMSTEC, Yokosuka, pp. 69-83

Gouretski, V.V. and Jancke, K. 2001. Systematic errors as the cause for an apparent deep water property variability:

global analysis of the WOCE and historical hydrographic data・REVIEW ARTICLE, Progress In Oceanography, 48: Issue 4, 337-402.

Grasshoff, K., Ehrhardt, M., Kremling K. et al. 1983. Methods of seawater analysis. 2nd rev. Weinheim: Verlag Chemie, Germany, West.

Hydes, D.J., Aoyama, M., Aminot, A., Bakker, K., Becker, S., Coverly, S., Daniel, A., Dickson, A.G., Grosso, O., Kerouel, R., Ooijen, J. van, Sato, K., Tanhua, T., Woodward, E.M.S., Zhang, J.Z., 2010. Determination of Dissolved Nutrients (N, P, Si) in Seawater with High Precision and Inter-Comparability Using Gas-Segmented Continuous Flow Analyzers, In: GO-SHIP Repeat Hydrography Manual: A Collection of Expert Reports and Guidelines. IOCCP Report No. 14, ICPO Publication Series No 134.

Joyce, T. and Corry, C. 1994. Requirements for WOCE hydrographic programmed data reporting. WHPO Publication, 90-1, Revision 2, WOCE Report No. 67/91.

Kawano, T., Uchida, H. and Doi, T. WHP P01, P14 REVISIT DATA BOOK, (Ryoin Co., Ltd., Yokohama, 2009).

Kirkwood, D.S. 1992. Stability of solutions of nutrient salts during storage. Mar. Chem., 38 : 151-164.

Kirkwood, D.S. Aminot, A. and Perttila, M. 1991. Report on the results of the ICES fourth intercomparison exercise for nutrients in sea water. ICES coop. Res. Rep. Ser., 174.

Mordy, C.W., Aoyama, M., Gordon, L.I., Johnson, G.C., Key, R.M., Ross, A.A., Jennings, J.C. and Wilson. J. 2000. Deep water comparison studies of the Pacific WOCE nutrient data set. Eos Trans-American Geophysical Union. 80 (supplement), OS43.

Murphy, J., and Riley, J.P. 1962. Analytica chim. Acta 27, 31-36.

Sato, K., Aoyama, M., Becker, S., 2010. RMNS as Calibration Standard Solution to Keep Comparability for Several Cruises in the World Ocean in 2000s. In: Aoyama, M., Dickson, A.G., Hydes, D.J., Murata, A., Oh, J.R., Roose, P., Woodward, E.M.S., (Eds.), Comparability of nutrients in the world's ocean. Tsukuba, JAPAN: MOTHER TANK, pp 43-56.

Uchida, H. & Fukasawa, M. WHP P6, A10, I3/I4 REVISIT DATA BOOK Blue Earth Global Expedition 2003 1, 2, (Aiwa Printing Co., Ltd., Tokyo, 2005).

3.6 Chlorofluorocarbons and Sulfur hexafluoride

Ken’ichi Sasaki[1], Katsunori Sagishima[2], Shoko Tatamisashi[2], Hironori Satoh[2], and Masahiro Ohrui[2]

1) Mutsu Institute for Oceanography, Japan Agency for Marine Earth Science and Technology

2) Marine Works Japan Co. Ltd

3.6.1 Objectives

Chlorofluorocarbons (CFCs) and sulfur hexafluoride (SF_6) are man-made stable gases. These atmospheric gases can slightly dissolve in sea surface water by air-sea gas exchange and then are spread into the ocean interior. So dissolved these gases could be used as chemical tracers for the ocean circulation. We measured concentrations of three chemical species of CFCs, CFC-11 (CCl_3F), CFC-12 (CCl_2F_2), and CFC-113 ($C_2Cl_3F_3$), and SF_6 in seawater on board.

3.6.2 Apparatus

We use three measurement systems. One is SF_6/CFCs simultaneous analyzing system. Other two are CFCs analyzing system. Both systems are basically purging and trapping gas chromatography.

Table 3-6-1 Instruments

SF_6/CFCs simultaneous analyzing system	
Gas Chromatograph:	GC-14B (Shimadzu Ltd.)
Detector 1:	ECD-14 (Shimadzu Ltd)
Detector 2	ECD-14 (Shimadzu Ltd)
Analytical Column:	
Pre-column:	Silica Plot capillary column [OD: 0.32 mm, length: 10 m, film thickness: 4 μm]
Main column 1:	Connected two columns (MS 5A packed column [1/16” OD, 10 cm length stainless steel tubing packed the section of 7 cm with 80/100 mesh Molecular Sieve 5A] followed by Gas Pro [OD: 0.32 mm, length: 35 m])
Main column2:	Silica Plot capillary column [OD: 0.32mm, length: 30 m, film thickness: 4 μm]
Purging & trapping:	Developed in JAMSTEC. Cold trap columns are 30 cm length stainless steel tubing packed the section of 5cm with 100/120 mesh Porapak T and followed by the section of 5cm of 100/120 mesh Carboxen 1000. OD of the main and focus trap columns are 1/8” and 1/16”, respectively.
CFCs analyzing system	
Gas Chromatograph:	GC-14B (Shimadzu Ltd.)
Detector:	ECD-14 (Shimadzu Ltd)
Analytical Column:	

Pre-column:	Silica Plot capillary column [OD: 0.53mm, length: 8 m, film thickness: 6μm]
Main column:	Connected two capillary columns (Pola Bond-Q [OD: 0.53mm, length: 9 m, film thickness: 10 m] followed by Silica Plot [OD: 0.53mm, length: 14 m, film thickness: 6μm])
Purging & trapping:	Developed in JAMSTEC. Cold trap columns are 1/16" OD stainless steel tubing packed the section of 5cm with Porapak T.

3.6.3 Procedures

3.6.3.1 Sampling

Seawater sub-samples were collected from 12 litter Niskin bottles to 250 ml and 400 ml of glass bottles for CFC and SF_6 measurements, respectively. The bottles were filled by nitrogen gas before sampling. Two times of the bottle volumes of seawater sample were overflowed. The bottles filled by seawater sample were kept in water bathes controlled at 7ºC. The samples were taken to determination as soon as possible after sampling (usually within 24 hours).

In order to confirm CFC/SF_6 concentrations of standard gases and their stabilities and also to check saturation levels in sea surface water, mixing ratios in background air were periodically analyzed. Air samples were continuously led into laboratory by 10 mm OD Dekaron tubing. The end of the tubing was put on a head of the compass deck and another end was connected onto an air pump in the laboratory. The tubing was relayed by a T-type union which had a small stop cock. Air sample was collected from the flowing air into a 200ml glass cylinder attached on the cock.

3.6.3.2 Analysis

SF6/CFCs simultaneous analyzing system

Constant volume of sample water (200 ml) is taken into a sample loop. The sample is send into stripping chamber and dissolved SF_6 and CFCs are de-gassed by N_2 gas purging for 9 minutes. The gas sample is dried by magnesium perchlorate desiccant and concentrated on a main trap column cooled down to -80 ºC. Stripping efficiencies are frequently confirmed by re-stripping of surface layer samples and more than 99 % of dissolved SF_6 and CFCs are extracted on the first purge. Following purging & trapping, the main trap column is isolated and moved into slit of heater block electrically heated to 170 ºC. After 1 minute, the desorbed gases are sent onto focus trap cooled down to -80 ºC for 30 seconds. Gaseous sample on the focus trap are desorbed by same manner of the main trap, and lead into the pre-column. Sample gases are roughly separated in the pre-column. SF_6 and CFC-12 are sent on to main column 1 (MC 1) and CFC-11 and CFC-113 still remain on the pre-column. Main column connected on pre-column is switched to the main column 2 (MC 2). Another carrier gas line is connected to MC 1 and SF6 and CFC-12 are further separated and detected by an electron capture detector, ECD 1. CFC-11 and CFC-113 lead to MC 2 are detected by ECD 2. When CFC-113 eluted from pre-column onto MC 2, the pre-column is switched onto another line and flushed by counter flow of pure nitrogen gas.

CFCs analyzing system

Constant volume of sample water (50 ml) is taken into a sample loop. The sample is send into stripping chamber and dissolved CFCs are de-gassed by N_2 gas purging for 8 minutes. The gas sample is dried by magnesium perchlorate desiccant and concentrated on a main trap column cooled down to -50 ºC. Stripping efficiencies are frequently confirmed by re-stripping of surface layer samples and more than 99.5 % of dissolved CFCs are extracted on the first purge. Following purging & trapping, the trap column is isolated and electrically heated to 140 ºC. The desorbed gases are lead into the pre-column. Sample gases are roughly separated in the pre-column. When CFC-113 eluted from pre-column onto main column, the pre-column is switched onto another line and flushed by counter flow of pure nitrogen gas.

Nitrogen gases used in these system was filtered by gas purifier tube packed with Molecular Sieve 13X (MS-13X).

Table 3-6-2 Analytical conditions

SF_6/CFCs simultaneous analyses

Temperature
Analytical Column: 95 ºC
Detector (ECD): 300 ºC
Trap column: -80 ºC (at adsorbing) & 170 ºC (at desorbing)

Mass flow rate of nitrogen gas (99.99995%)
Carrier gas 1: 5 ml/min
Carrier gas 2: 5 ml/min
Detector make-up gas 1: 35 ml/min
Detector make-up gas 2: 35 ml/min
Back flush gas: 7 ml/min
Sample purge gas: 200 ml/min

CFCs analyses

Temperature
Analytical Column: 95 ºC
Detector (ECD): 240 ºC
Trap column: -50 ºC (at adsorbing) & 140 ºC (at desorbing)

Mass flow rate of nitrogen gas (99.99995%)
Carrier gas : 13 ml/min

Detector make-up gas : 24 ml/min
Back flush gas: 20 ml/min
Sample purge gas: 130 ml/min

Standard gas (Japan Fine Products co. ltd.)

Cylinder No.	Base gas	CFC-11	CFC-12	CFC113	SF_6	N_2O	remarks
		ppt	ppt	ppt	ppt	ppb	
CPB23379	Air	501	251	40.3	5.02	198	SF_6/CFC, Leg 2
CPB17172	Air	998	519	90.0	10.0	300	SF_6/CFC, Leg 3
CPB17174	Air	1499	750	130	10.0	502	SF_6/CFC, Leg 3
CPB26826	N_2	299	160	30.1	0.0	0	CFC, Leg 2,3
CPB15674	N_2	299	160	30.0	0.0	0	CFC, Leg 2,3
CPB15651	N_2	299	159	30.2	0.0	0	CFC, Leg 2

3.6.3.3 Performance

The analytical precisions are estimated from replicate sample analyses. The estimated preliminary precisions were ± 0.005 pmol/kg (n =201), ± 0.004 pmol/kg (n = 201), ± 0.003 pmol/kg (n = 166), ± 0.03 fmol/kg (n = 103) for CFC-11, CFC-12, CFC-113 and SF_6, respectively.666666

3.6.4 Data archive

All data will be submitted to JAMSTEC Data Management Group (DMG) and under its control.

3.7. Carbon items

(1) Personnel

Akihiko Murata (JAMSTEC)
Yoshiko Ishikawa (MWJ)
Tomonori Watai (MWJ)
Ayaka Hatsuyama (MWJ)
Hatsumi Aoyama (MWJ)
Makoto Takada (MWJ)
Yasumi Yamada (MWJ)

(2) Objectives

Concentrations of CO_2 in the atmosphere are now increasing at a rate of 1.9 ppmv yr^{-1} owing to human activities such as burning of fossil fuels, deforestation, and cement production. It is an urgent task to estimate as accurately as possible the absorption capacity of the oceans against the increased atmospheric CO_2, and to clarify the mechanism of the CO_2 absorption, because the magnitude of the anticipated global warming depends on the levels of CO_2 in the atmosphere, and because the ocean currently absorbs 1/3 of the 6 Gt of carbon emitted into the atmosphere each year by human activities.

In this cruise, we were aimed at quantifying how much anthropogenic CO_2 absorbed in the ocean are transported and redistributed in the western Pacific. For the purpose, we measured CO_2-system parameters such as dissolved inorganic carbon (C_T), total alkalinity (A_T) and pH.

(3) Apparatus

i. C_T

Measurement of C_T was made with two total CO_2 measuring systems (called as Systems C and D, respectively; Nippon ANS, Inc.), which were slightly different from each other. The systems comprised of a seawater dispensing system, a CO_2 extraction system and a coulometer. In this cruise, we used coulometers, Seacat2000 and Model23000 for Systems C and D, respectively, both of which were constructed by Nippon ANS. Each of the two systems had almost a same specification as follows:

The seawater dispensing system has an auto-sampler (6 ports), which dispenses seawater from a 300 ml borosilicate glass bottle into a pipette of about 20 ml volume by PC control. The pipette is kept at 20 °C by a water jacket, in which water from a water bath set at 20 °C is circulated. CO_2 dissolved in a seawater sample is extracted in a stripping chamber of the CO_2 extraction system by adding phosphoric acid (10 % v/v) of about 2 ml. The stripping chamber is approx. 25 cm long and has a fine frit at the bottom. The acid is added to the stripping chamber from the bottom of the chamber by pressurizing an acid bottle for a given time to push out the right amount of acid. The pressurizing is made with nitrogen gas (99.9999 %). After the acid is transferred to the stripping chamber, a seawater sample kept in a pipette is introduced to the stripping chamber by the same method as in adding an acid. The seawater reacted with phosphoric acid is stripped of CO_2 by bubbling the nitrogen gas through a fine frit at the bottom of the stripping chamber. The CO_2

stripped in the chamber is carried by the nitrogen gas (flow rates is 140 ml min^{-1}) to the coulometer through a dehydrating module. The modules of Systems C and D consist of two electric dehumidifiers (kept at 1 - 2 °C) and a chemical desiccant ($Mg(ClO_4)_2$).

The measurement sequence such as system blank (phosphoric acid blank), 2 % CO_2 gas in a nitrogen base, sea water samples (6) is programmed to repeat. The measurement of 2 % CO_2 gas is made to monitor response of coulometer solutions purchased from UIC, Inc. or laboratory-made.

ii. A_T

Measurement of A_T was made based on spectrophotometry using a custom-made system (Nippon ANS, Inc.). The system comprises of a water dispensing unit, an auto-burette (765 Dosimat, Metrohm), and a spectrophotometer (Carry 50 Bio, Varian), which are automatically controlled by a PC. The water dispensing unit has a water-jacketed pipette and a water-jacketed titration cell. The spectrophotometer has a water-jacketed quartz cell, length and volume of which are 8 cm and 13 ml, respectively. To circulate sample seawater between the titration and the quartz cells, PFA tubes are connected to the cells.

A seawater of approx. 42 ml is transferred from a sample bottle (borosilicate glass bottle; 130 ml) into the water-jacketed (25 ºC) pipette by pressurizing the sample bottle (nitrogen gas), and is introduced into the water-jacketed (25 ºC) titration cell. The seawater is circulated between the titration and the quartz cells by a peristaltic pump to rinse the route. Then, Milli-Q water is introduced into the titration cell, and is circulated in the route twice to rinse the route. Next, a seawater of approx. 42 ml is weighted again by the pipette, and is transferred into the titration cell. The weighted seawater is introduced into the quartz cell. Then, for seawater blank, absorbances are measured at three wavelengths (750, 616 and 444 nm). After the measurement, an acid titrant, which is a mixture of approx. 0.05 M HCl in 0.65 M NaCl and bromocresol green (BCG) is added (about 2 ml) into the titration cell. The seawater + acid titrant solution is circulated for 6 minutes between the titration and the quartz cells, with stirring by a stirring tip and bubbling by wet nitrogen gas in the titration cell. Then, absorbances at the three wavelengths are measured again.

Calculation of A_T is made by the following equation:

$$A_T = (-[H^+]_T V_{SA} + M_A V_A) / V_S,$$

where M_A is the molarity of the acid titrant added to the seawater sample, $[H^+]_T$ is the total excess hydrogen ion concentration in the seawater, and V_S, V_A and V_{SA} are the initial seawater volume, the added acid titrant volume, and the combined seawater plus acid titrant volume, respectively. $[H^+]_T$ is calculated from the measured absorbances based on the following equation (Yao and Byrne, 1998):

$$\begin{aligned} pH_T = -\log[H^+]_T &= 4.2699 + 0.002578(35 - S) + \log((R - 0.00131)/(2.3148 - 0.1299R)) \\ &\quad - \log(1 - 0.001005S), \end{aligned}$$

where S is the sample salinity, and R is the absorbance ratio calculated as:

$$R = (A_{616} - A_{750})/(A_{444} - A_{750}),$$

where A_i is the absorbance at wavelength i nm.

The HCl in the acid titrant is standardized on land. The concentrations of BCG were estimated to be approx. 2.0×10^{-6} M in the sample seawater, respectively.

iii. pH

Measurement of pH was made by a pH measuring system (Nippon ANS, Inc.). For the detection of pH, spectrophotometry was adopted. The system comprises of a water dispensing unit and a spectrophotometer (Carry 50 Scan, Varian). For an indicator, *m*-cresol purple (2 mM) was used.

Seawater is transferred from borosilicate glass bottle (300 ml) to a sample cell in the spectrophotometer. The length and volume of the cell are 8 cm and 13 ml, respectively, and the sample cell is kept at 25.00 ± 0.05 ºC in a thermostated compartment. First, absorbances of seawater only are measured at three wavelengths (730, 578 and 434 nm). Then the indicator is injected and circulated for about 4 minutes to mix the indicator and seawater sufficiently. After the pump is stopped, the absorbances of seawater + indicator are measured at the same wavelengths. The pH is calculated based on the following equation (Clayton and Byrne, 1993):

$$\mathrm{pH} = \mathrm{p}K_2 + \log\left(\frac{A_1/A_2 - 0.00691}{2.2220 - 0.1331(A_1/A_2)}\right),$$

where A_1 and A_2 indicate absorbances at 578 and 434 nm, respectively, and $\mathrm{p}K_2$ is calculated as a function of water temperature and salinity.

(4) Performances

i. C_T

The two systems worked well without a major malfunction. Replicate analysis was made approximately on every about 9th seawater sample. During the leg 2, the repeatability for Systems C and D were estimated to be 0.72 ± 0.64 (n = 58 pairs) and 0.72 ± 0.64 (n = 38 pairs) μmol kg^{-1}, respectively. During the leg 3, they were 0.78 ± 0.73 (n = 33 pairs) and 0.57 ± 0.51 (n = 52 pairs) μmol kg^{-1}, respectively.

ii. A_T

The system showed a very good precision compared to systems used in previous studies. A few replicate samples were taken on every station. During the leg 2, the repeatability was estimated to be 0.48 ± 0.43 µmol kg^{-1} (n = 94 pairs), while during the leg 3, it was estimated to be 0.51 ± 0.45 µmol kg^{-1} (n = 87 pairs).

iii. pH

The system worked well with no troubles. The average of absolute differences between replicate samples were 0.0005 ± 0.0005 (n = 112 pairs) and 0.0007 ± 0.0006 (n = 104) pH unit for legs 2 and 3, respectively.

(5) Results

Cross sections of C_T, pH, and A_T along WOCE P10 line are illustrated in Figs. 3.9.1, 3.9.2 and 3.9.3, respectively.

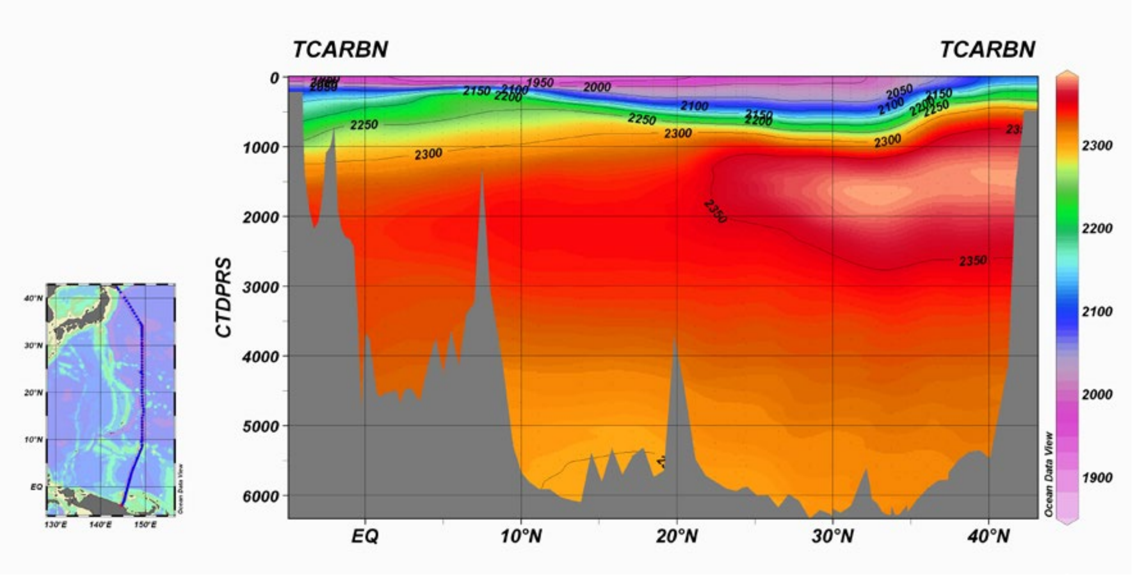

Fig. 3.7.1. Distributions of C_T along the P10 line.

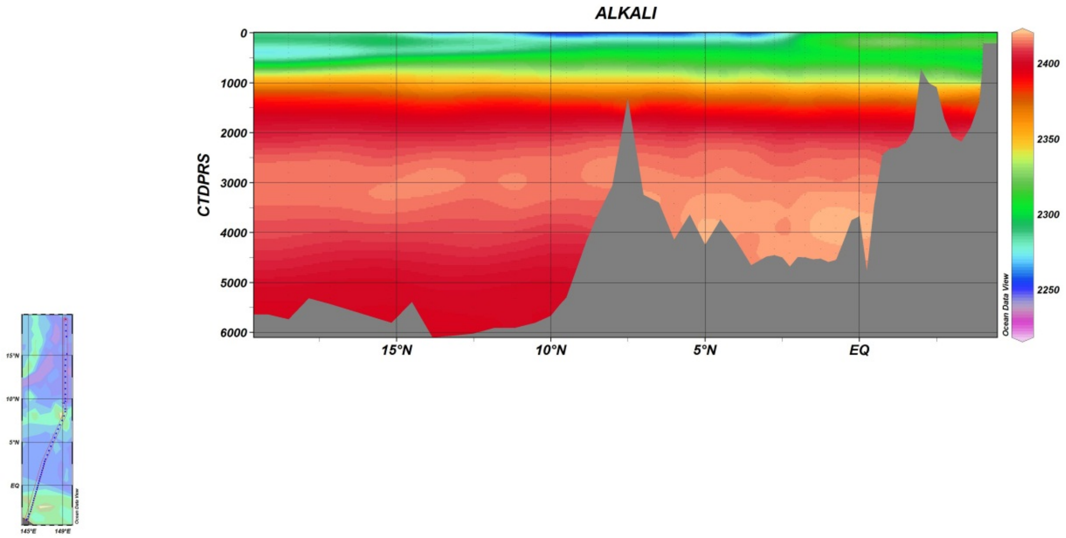

Fig. 3.7.2. Distributions of A_T along the P10 line.

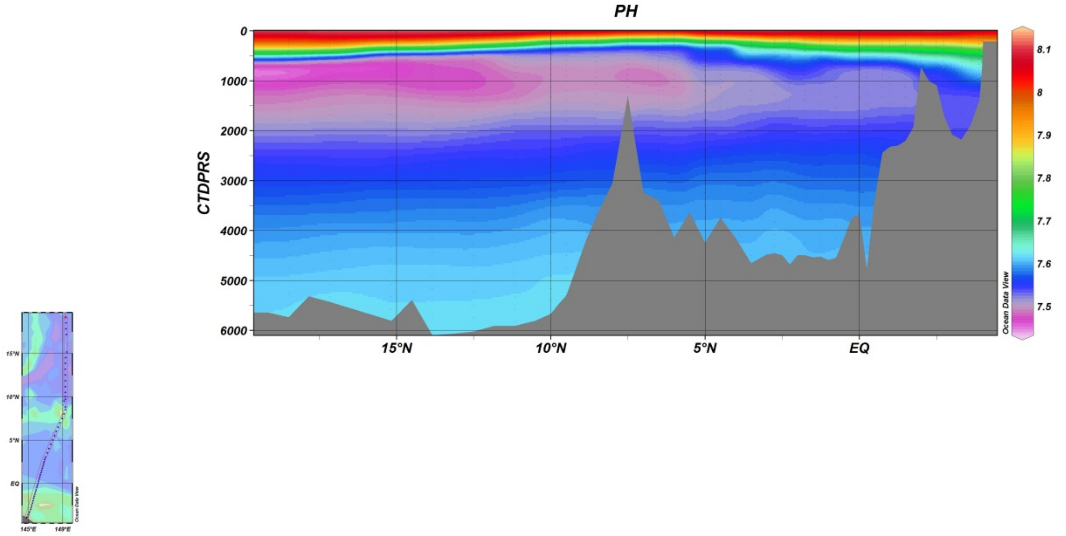

Fig. 3.7.3. Distributions of pH along the P10 line.

References

Clayton T.D. and R.H. Byrne (1993) Spectrophotometric seawater pH measurements: total hydrogen ion concentrtaion scale calibration of m-cresol purple and at-sea results. Deep-Sea Research 40, 2115-2129.

Yao W. and R. H. Byrne (1998) Simplified seawater alkalinity analysis: Use of linear array spectrometers. Deep-Sea Research I 45, 1383-1392.

3.8 Chlorophyll *a*

February 29, 2012

(1) Personnel

Osamu Yoshida[1,2,3], Hiroshi Uchida[4], Yuki Okazaki[3], Shinichi Oikawa[2], Hikari Shimizu[2], Chisato Yoshikawa[5,6], Shoko Tatamisashi[7], Masahiro Orui[7], and Naohiro Yoshida[5]*

[1] *College of Agriculture, Food and Environment Sciences, Rakuno Gakuen University*

[2] *Faculty of Environment Systems, Rakuno Gakuen University*

[3] *Graduate School of Dairy Science, Rakuno Gakuen University*

[4] *Research Institute for Global Change, Japan Agency for Marine-Earth Science and Technology*

[5] *Interdisciplinary Graduate School of Science and Engineering, Tokyo Institute of Technology*

[6] ***Japan Society for the Promotion of Science***

[7] *Department of Marine Science, Marine Works Japan LTD.*

* *Principal Investigator*

(2) Sampling elements

All sampling stations of RGU group and JAMSTEC are listed below.

Table 1. Hydrographic station numbers for samples collection in Legs 2 and 3.

		Station	Niskin No.
Leg 2	RGU	1	0, 36, 35, 34, 33,
		29	0, 36, 35, 34, 33, 32
		45	0, 36, 35, 34, 33, 32
		58	0, 36, 35, 34, 33, 32
	JAMSTEC	2	35
		9	35
		15	34
		19	34
		24	5
Leg 3	RGU	71	0, 36, 35, 34, 33, 32
		88	0, 36, 35, 34, 33, 32
		114	0, 36, 35, 34, 33, 32
	JAMSTEC	59	2
		62	2
		65	33
		68	2
		77	33
		79	36
		82	36
		84	36
		90	36
		94	36
		100	36
		106	36
		112	36

(3) Objective

Chlorophyll *a* is one of the most convenient indicators of phytoplankton stock, and has been used extensively for the estimation of phytoplankton abundance in various aquatic environments. The object of this study is to investigate the vertical distribution of phytoplankton in various light intensity depth.

(4) Materials and Methods

Seawater samples were collected 250 mL at 6 depths from surface to about 200 m with Niskin bottles, except for the Surface water, which was taken by the bucket. For JAMSTEC stations, water samples were collected 500 mL bottle. The samples were gently filtrated by low vacuum pressure (<0.02 MPa) through Whatman GF/F filter (diameter 25 mm) in the dark room. Phytoplankton pigments were immediately extracted in 7 mL of N,N-dimethylformamide (DMF) after filtration and then, the samples were stored at –20°C under the dark condition to extract chlorophyll *a* for 24 hours or more. The extracted samples are measured the fluorescence by Turner fluorometer (10-AU-005, TURNER DESIGNS) which was previously calibrated against a pure chlorophyll *a* (Sigma-Aldrich Co.). We applied the fluorometric "Non-acidification method" (Welschmeyer, 1994)

(5) Results

The results of chlorophyll *a* at RGU sampling stations and relationship between chlorophyll *a* concentrations and chlorophyll *a* estimated from chlorophyll fluorometer were shown in Figures 1 and 2 respectively.

(6) Data archives

All processed Chlorophyll *a* data were submitted to Principal Investigator according to the data management policy of JAMSTEC.

Reference

Welschmeyer, N. A.: Fluorometric analysis of chlorophyll *a* in the presence of chlorophyll *b* and pheopigments. Limno. Oceanogr., 39, 1985-1992, 1994.

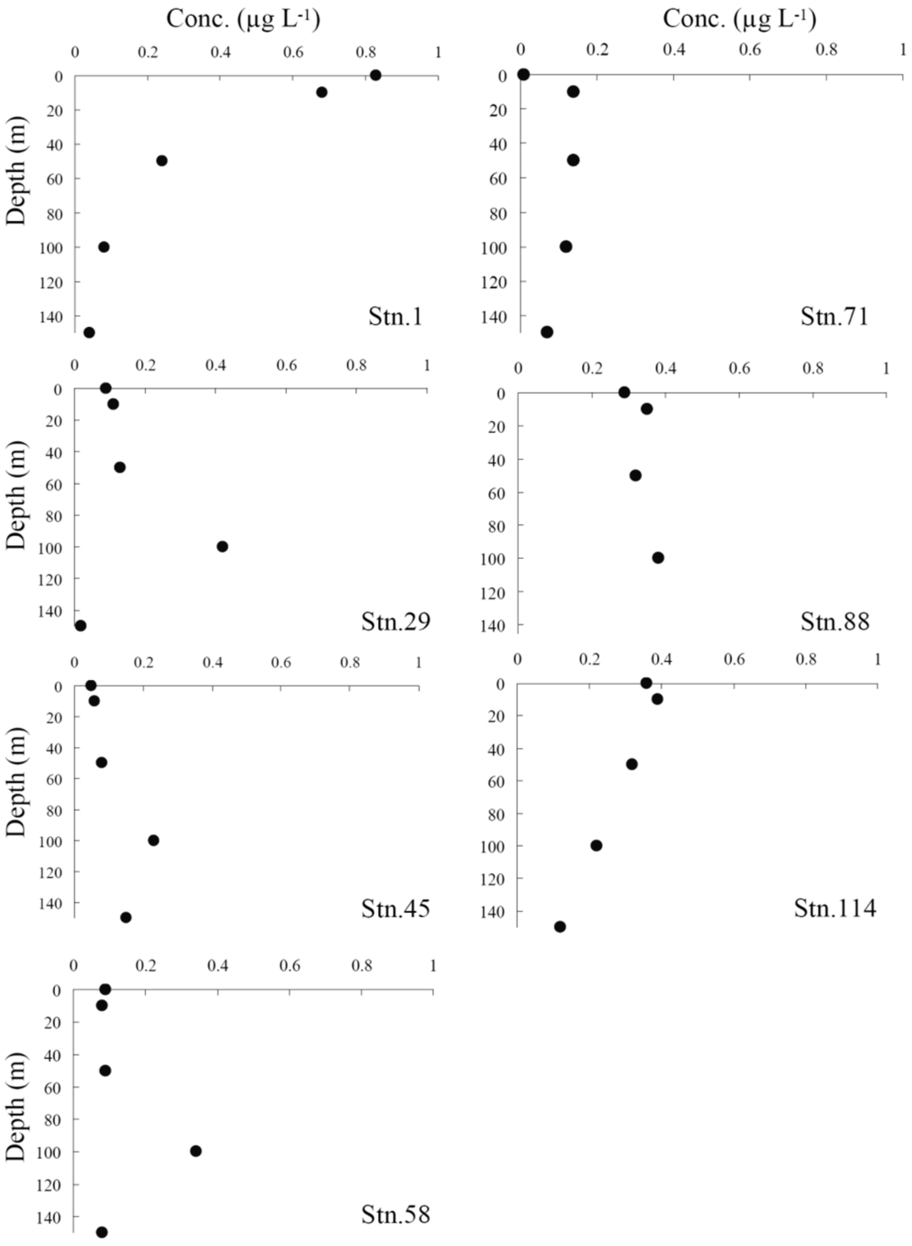

Figure 1. The vertical distributions of chlorophyll *a* at RGU stations.

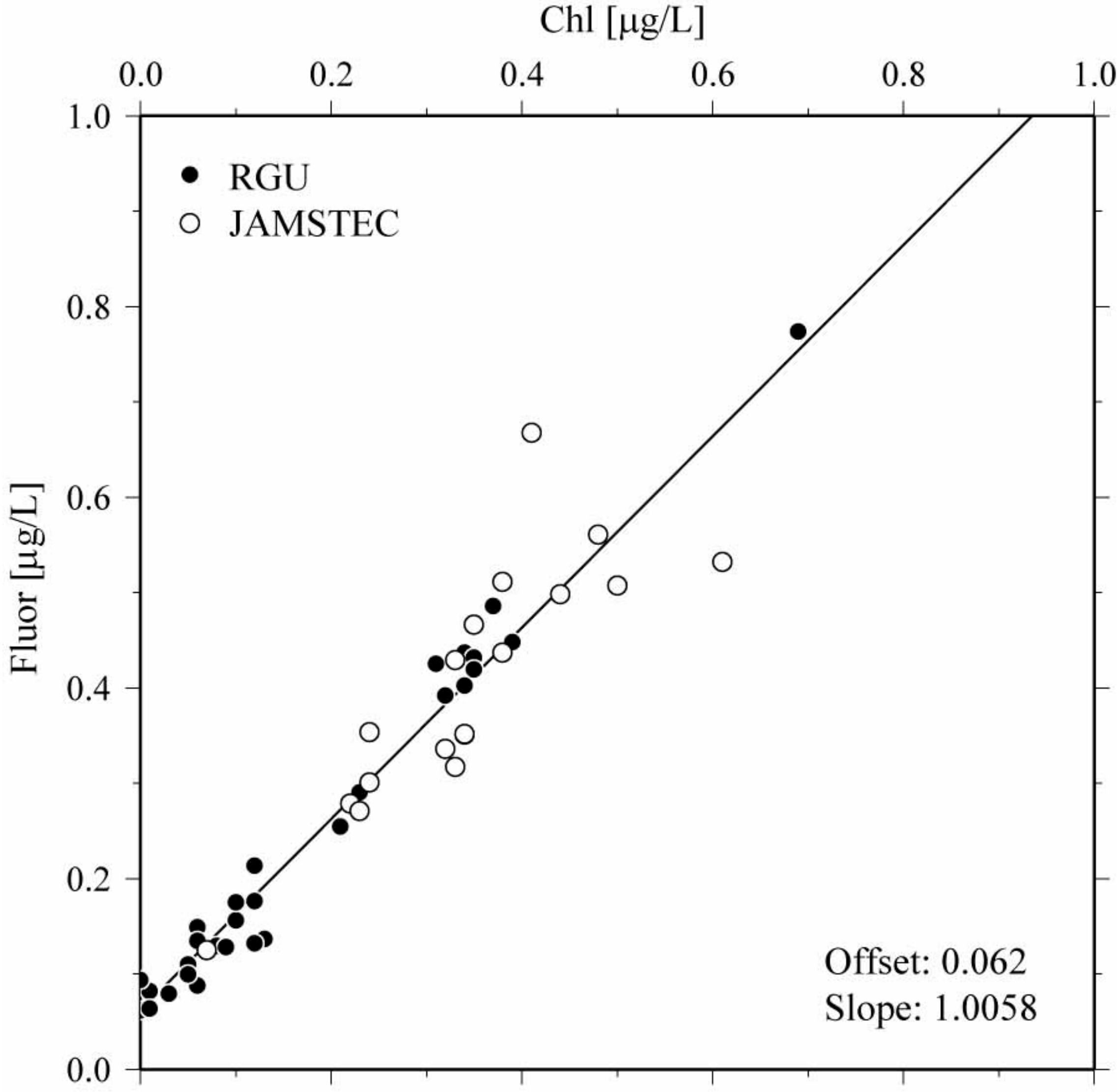

Figure 2. Relationship between fluorescent values of seawater and chlorophyll *a* concentrations at RGU (solid circles) and JAMSTEC (open circles) stations.

3.9 Carbon isotopes

March 09, 2012
Yuichiro Kumamoto
Japan Agency for Marine-Earth Science and Technology (JAMSTEC)

(1) Personnel

Yuichiro Kumamoto

Japan Agency for Marine-Earth Science and Technology

(2) Objective

In order to investigate the water circulation and carbon cycle in the Western Pacific, seawaters for measurements of carbon-14 (radiocarbon) and carbon-13 (stable carbon) of total dissolved inorganic carbon (TDIC) were collected by the hydrocasts from surface to near bottom during MR11-08 cruise.

(3) Sample collection

The sampling stations and number of samples are summarized in Table 3.9.1. All samples for carbon isotope ratios (total 627 samples) were collected at 19 stations using 12-liter Niskin-X bottles. The seawater sample was siphoned into a 250 cm^3 glass bottle with enough seawater to fill the glass bottle 2 times. Immediately after sampling, 10 cm^3 of seawater was removed from the bottle and poisoned by 0.1 cm^3 μl of saturated $HgCl_2$ solution. Then the bottle was sealed by a glass stopper with Apiezon grease M and stored in a cool and dark space on board.

(4) Sample preparation and measurements

In our laboratory, dissolved inorganic carbon in the seawater samples will be stripped cryogenically and split into three aliquots: radiocarbon measurement (about 200 μmol), carbon-13 measurement (about 100 μmol), and archive (about 200 μmol). The extracted CO_2 gas for radiocarbon will be then converted to graphite catalytically on iron powder with pure hydrogen gas. The carbon-13 of the extracted CO_2 gas will be measured using Finnigan MAT252 mass spectrometer. The carbon-14 in the graphite sample will be measured by Accelerator Mass Spectrometry (AMS).

Table 3.9.1 The sampling stations and number of samples for carbon isotope ratios.

Station	Lat. (N)	Long. (E)	Sampling Date (UTC)	Number of samples	Number of replicate samples	Max. Pressure (dbar)
P10-005	-03-18.56	145-9.14	2012/01/04	20	1	2181
P10-010	-02-00.14	145-34.13	2012/01/04	11	1	731
P10-017	-00-14.79	146-4.00	2012/01/06	31	2	4778
P10-023	01-14.90	146-30.10	2012/01/07	30	2	4527
P10-027	02-15.17	146-46.98	2012/01/01	30	2	4683

P10-034	05-00.12	147-51.22	2011/12/30	29	2	4246
P10-041	08-30.26	149-19.80	2011/12/29	28	2	3692
P10-047	11-09.42	149-19.99	2011/12/27	36	2	5911
P10-051	13-50.37	149-18.84	2011/12/26	36	2	6096
P10-056	17-09.95	149-25.88	2011/12/24	34	2	5434
P10-060	19-49.86	149-19.98	2012/01/14	28	2	3707
P10-064	22-29.80	149-19.98	2012/01/16	36	2	5810
P10-067	24-14.43	149-01.99	2012/01/17	36	2	5891
P10-074	28-29.84	149-19.68	2012/01/19	36	2	6334
P10N-081	32-09.38	149-19.03	2012/01/23	35	2	5606
P10N-090	34-47.46	148-55.05	2012/01//30	36	2	6363
P10N-098	37-24.83	147-11.33	2012/02/03	36	2	5777
P10N-106	40-06.35	145-19.97	2012/02/04	34	2	5469
P10N-110	41-29.97	144-19.30	2012/02/05	29	2	4132
			Total	591	36	

3.10 Radioactive Cesium and Tritium

March 09, 2012
Yuichiro Kumamoto
Japan Agency for Marine-Earth Science and Technology (JAMSTEC)
Tatsuo Aono
National Institute of Radiological Sciences (NIRS)

(1) Personnel

Yuichiro Kumamoto 1)„ ***Tatsuo Aono*** 2)„ ***Makoto Takada*** 3)„ ***and Hideki Yamamoto*** 3)

1) Japan Agency for Marine-Earth Science and Technology
2) National Institute of Radiological Sciences
3) Marine Works Japan Co. Ltd

(2) Objective

In order to investigate the water circulation and ventilation process in the Western Pacific, seawaters for measurements of radioactive cesium (Cs-134 and -137) and tritium (H-3), which were released from the Fukushima Daiichi nuclear power plant after its serious accident on the March 11 of 2011, were collected by the hydrocasts from surface to about 800 m depth during MR11-08 cruise.

(3) Sample collection

The sampling stations and number of samples are summarized in Table 3.10.1. Seawater samples for radioactive cesium (total 284 samples) and tritium (total 108 samples) were collected at 42 stations using 12-liter Niskin-X bottles except surface seawater, which was collected by a bucket. The seawater sample for radioactive cesium was collected into a 20-L plastic container and after two time washing. Immediately after sampling, the seawater was filtrated using membrane filter (Millipore HAWP14250, 142mm, 0.45μm) and acidified by 40-cm^3 of concentrated nitric acid (RCI Labscan Ltd., Nitric Acid 70% , AR). The seawater for tritium was siphoned into 1-L glass bottle and tightly sealed with a screwed cap after two time washing

(4) Sample preparation and measurements

In our laboratory on shore, radioactive cesium in the seawater samples will be concentrated using ammonium phosphomolybdate (AMP) that forms insoluble compound with cesium. The radioactive cesium in AMP will be measured using Ge γ-ray spectrometer. Tritium in the seawater sample will be analyzed by a He-3 ingrowth method that measures He-3 concentration generated from tritium using a mass spectrometer.

Table 3.10.1 The sampling stations and number of samples for radioactive cesium and tritium.

Station	Lat.	Long. (E)	Sampling	Number of	Number of	Max. Pressure

	(N)		Date (UTC)	samples for radioactive cesium (20-L container)	samples for tritium (1-L bottle)	(dbar)
R0	-09-12.12	100-24.00	2011/12/10	2	none	0
P10-002	-03-59.01	144-49.89	2012/01/03	10	10	790
P10-010	-02-00.14	145-34.13	2012/01/04	10	10	720
P10-017	-00-14.79	146-04.00	2012/01/06	3	1	0
P10-023	01-14.90	146-30.10	2012/01/07	10	10	830
P10-030	03-00.25	146-59.91	2011/12/31	1	1	0
P10-034	05-00.12	147-51.22	2011/12/30	10	1	800
P10-038	07-00.01	148-41.62	2011/12/29	1	1	0
P10-040	08-00.20	149-09.92	2011/12/29	6	none	2800
P10-043	09-29.30	149-10.03	2011/12/28	1	1	0
P10-046	10-29.96	149-19.99	2011/12/27	2	none	0
P10-047	11-09.20	149-19.98	2011/12/27	10	1	830
P10-050	13-10.03	149-19.96	2011/12/26	1	1	0
P10-053	15-10.08	149-29.86	2011/12/25	10	1	830
P10-056	17-09.84	149-25.87	2011/12/24	1	1	0
P10-060	19-49.86	149-19.98	2012/01/14	12	1	770
P10-063	21-49.99	149-20.02	2012/01/15	1	1	0
P10-067	24-14.43	149-01.99	2012/01/17	10	1	800
P10-071	26-29.81	149-20.11	2012/01/18	10	1	830
P10-074	28-29.84	149-19.68	2012/01/19	1	1	0
P10N-077	29-58.88	149-14.98	2012/01/21	11	1	830
P10N-079	31-10.10	149-20.10	2012/01/22	2	1	0
P10N-081	32-09.38	149-19.03	2012/01/23	13	1	770
P10N-084	33-09.47	149-20.00	2012/01/24	2	1	0
P10N-086	33-44.46	149-19.82	2012/01/25	11	1	830
P10N-088	34-14.88	149-10.23	2012/01/25	2	1	0
P10N-090	34-45.83	148-52.32	2012/01/27	13	10	770
R1	34-37.18	147-44.22	2012/01/27	1	none	0
R2	34-29.44	146-44.37	2012/01/27	1	none	0
R3	34-49.28	145-42.49	2012/01/28	1	none	0
P10N-092	35-24.95	148-27.27	2012/01/31	2	1	0
P10N-094	36-05.00	148-02.61	2012/01/31	23	1	830

P10N-096	36-44.67	147-37.63	2012/01/31	2	1	0
P10N-098	37-25.03	147-11.90	2012/02/01	22	9	800
P10N-100	38-04.80	146-45.18	2012/02/03	2	1	0
P10N-102	38-45.06	146-18.90	2012/02/03	13	1	770
P10N-104	39-24.97	145-50.73	2012/02/04	2	1	0
P10N-106	40-04.98	145-22.22	2012/02/04	13	10	830
P10N-108	40-45.35	144-52.74	2012/02/05	2	1	0
P10N-110	41-14.93	144-30.54	2012/02/05	19	10	800
P10N-112	41-45.12	144-07.67	2012/02/05	2	1	0
P10N-114	42-10.02	143-48.57	2012/02/05	13	11	720
Total				284	108	

3.11. LADCP

(1) Personnel

Shinya Kouketsu (JAMSTEC)
Hiroshi Uchida (JAMSTEC)
Katsurou Katsumata (JAMSTEC)
Toshimasa Doi (JAMSTEC)

(2) Overview of the equipment

An acoustic Doppler current profiler (ADCP) was integrated with the CTD/RMS package. The lowered ADCP (LADCP), Workhorse Monitor WHM300 (Teledyne RD Instruments, San Diego, California, USA), which has 4 downward facing transducers with 20-degree beam angles, rated to 6000 m. The LADCP makes direct current measurements at the depth of the CTD, thus providing a full profile of velocity. The LADCP was powered during the CTD casts by a 50.4 volts expendable Alkali battery pack. The LADCP unit was set for recording internally prior to each cast. After each cast the internally stored observed data was uploaded to the computer on-board. By combining the measured velocity of the sea water and bottom with respect to the instrument, and shipboard navigation data during the CTD cast, the absolute velocity profile can be obtained (e.g., Visbeck, 2002).

The instruments used in this cruise were Teledyne RD Instruments, WHM300(S/N 155500, S/N 155130, and S/N 135930).

(3) Data collection

In this cruise, data were collected with the following configuration.

Bin size: 4 m
Number of bins: 25
Pings per ensemble: 1
Ping interval: 1 sec

(4) Data collection problems

Echo intensities are sufficiently high along the section (Fig. 3), except at the stations of 96 and 98, where the echo intensities of beam 2 of SN 155130 suddenly decreased.

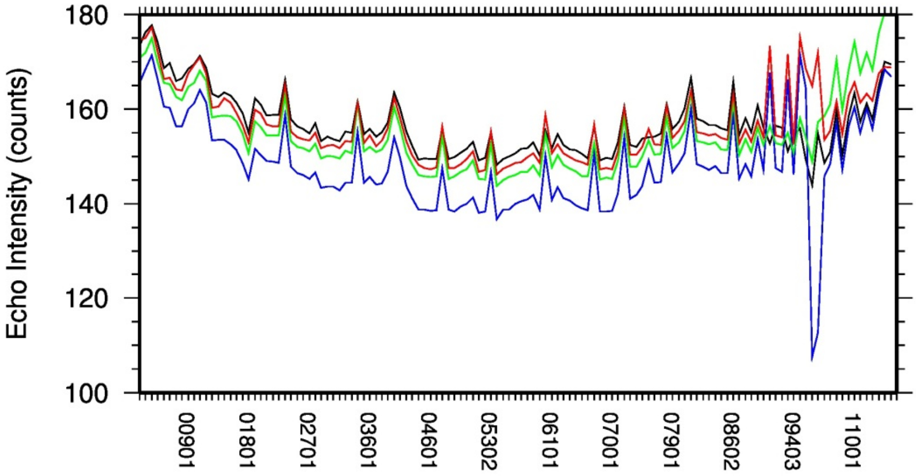

Fig. 3. Cast-averaged echo intensities at the first bin. Black, blue, green and red denote beam 1, 2, 3, and 4 respectively.

(5) Data process

Vertical profiles of velocity are obtained by the inversion method (Visbeck, 2002). Since the first bin from LADCP is influenced by the turbulence generated by CTD frame, the weight for the inversion is set to 0.1. GPS navigation data and the bottom-track data are used in the calculation of the reference velocities. Shipboard ADCP data averaged for 1 minutes are also included in the calculation. The CTD data are used for the sound speed and depth calculation. The directions of velocity are corrected using the magnetic deviation estimated with International Geomagnetic reference field data.

However, the inversion method doesn't work well due to no-good velocity data due to the instrument problems as well as weak echo intensity at deep layers. We again plan to process carefully after the cruise.

Reference

Visbeck, M. (2002): Deep velocity profiling using Lowered Acoustic Doppler Current Profilers: Bottom track and inverse solutions. *J. Atmos. Oceanic Technol.*, 19, 794-807.

3.12. Expendable Microstructure Profiler

(1) Personnel

K. Katsumata (JAMSTEC)

(2) Objectives

Turbulence mixing in the ocean has been a difficult quantity to measure directly despite its important role in the ocean energy budget and general circulation dynamics. Recent improvements on materials such as optic fibre and on sensors such as high precision shear sensors now enable the measurement using the newly developed expendable microstructure profiler (XMP)

(3) Apparatus

XMP probe and its tow frame are manufactured by Rockland Scientific International, Canada. The expendable sensor has a cylindrical shape with the length of about 152 cm and a diameter of 18 cm. Two shear sensors, one temperature sensor, a pressure sensor, and an accelerometer are mounted on the deeper tip of the cylinder. The tail is fringed with plastic drag brushes to stabilise its drop rate.

The shear sensors measure the shear at a 2.5×10^{-3} s^{-1} rms resolution. Least squares fit of the shear spectrum to the Nasmyth theoretical curve yields an estimate of the turbulent kinetic energy dissipation rate. The instrument oscillation is measured by the accelerometer and corrected during the spectrum estimation

The measured data are transmitted to the deck unit through an optic fibre. Twelve kilometre of the fibre on a spool is used and the fibre freely comes off the spool as the instrument falls underwater. The fibre spool is mounted underwater in a two frame which is towed from the stern of the vessel. It is recommended that the vessel travels no faster than 2 knots.

The turbulent kinetic energy dissipation rate ϵ is estimated by

$$\varepsilon = \frac{15}{2} \nu \overline{u_z^2} ,$$

where ν is the kinematic molecular viscosity of water and u_z is the vertical derivative of the horizontal velocity and the overbar denotes a spatial or ensemble averaging. Detailed description of the principle and sensors can also be found in Lueck *et al.*, (2002).

(4) Deployments

Four probes were deployed at two different CTD stations right after the CTD cast. Serial numbers 19 and 20 were deployed at the CTD station 67, Serial numbers 21 and 23 were at the Station 76. The time below is in UT and in the year of 2012.

Serial number	Lat	Lon	Water depth (m)	Time (UT)
20	20-29.67°N	149-19.76°E	4542	15 Jan 03:02
19	20-33.38°N	154-19.85°E	4629	15 Jan 05:57
23	29-50.32°N	149-20.14°E	6145	20 Jan 04:57
21	29-47.56°N	149-23.45°E	6144	20 Jan 07:21

(5) Calibration

It was necessary to calibrate the conversion coefficients for temperature and pressure defined in the configuration file. After noise reduction with the ODAS software the temperature offset (T_coef0) and the pressure coefficients (P_coef0 and P_coef1) were tuned to match the temperature-pressure profile to he profiles observed by the nearest CTD casts. Our calibration is only tentative.

(6) Results

Serial Number (SN) 19 and 20 survived to the sea bottom. SN 21 and 23 lost connection at about 1130 dbar and 2800 dbar, respectively. Figs 3.15.1 shows the vertical distribution of the eddy kinetic energy dissipation rate, tentatively estimated by quick_look_XMP.m in the ODAS library. The method for estimating the dissipation rate follows that of Lueck *et al.* (2002). Not all noise was removed and high dissipation rate for SN 23 can be contaminated by the noise.

References

Lueck, R.G., F. Wolk, and H. Yamazaki (2002) Oceanic Velocity Microstructure Measurements in the 20th Century. Journal of Oceanography 58, 153-174.

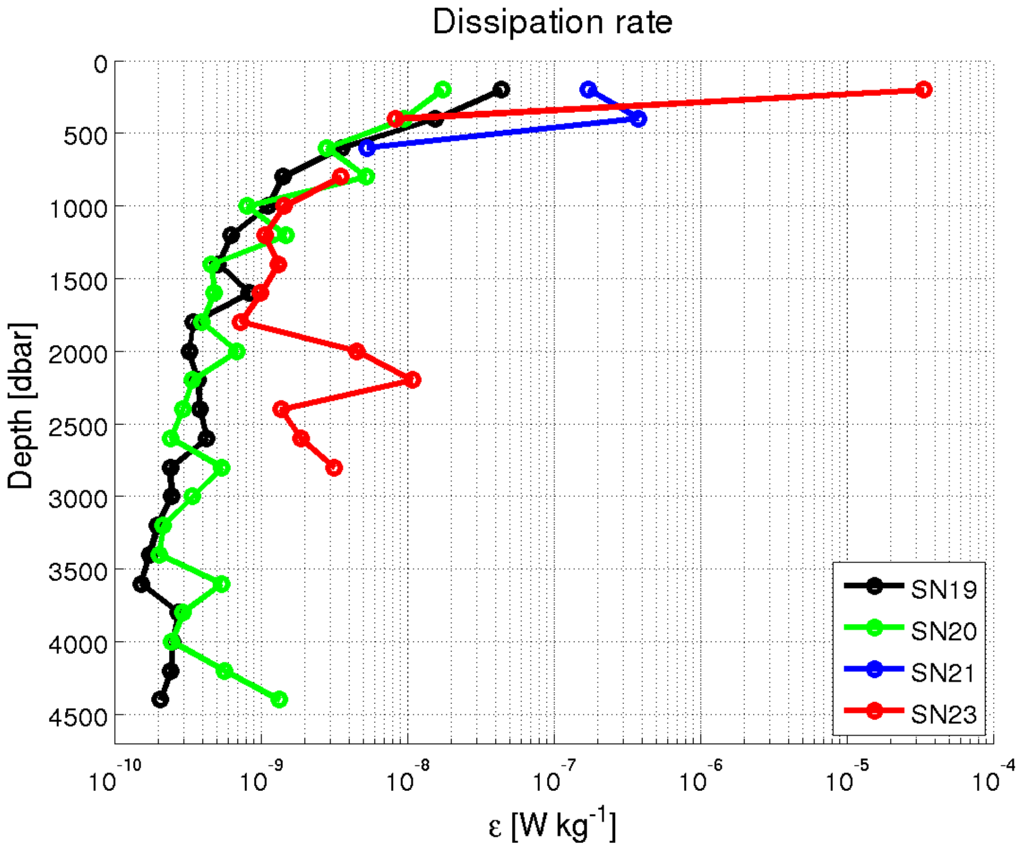

Fig. 3.12.1 Kinetic energy dissipation rate estimated at intervals of 100-300 dbar, 200-400 dbar and so forth using quick_look_XMP.m in the ODAS library.

3.13 XCTD

March 4, 2012

(1) Personnel

Hiroshi Uchida (JAMSTEC)
Katsuhisa Maeno (GODI)
Ryo Ohyama (GODI)
Asuka Doi (GODI)
Toshimitsu Goto (GODI)

(2) Objectives

In this cruise, XCTD (eXpendable Conductivity, Temperature and Depth profiler) measurements were carried out to evaluate the fall rate equation and temperature by comparing with CTD (Conductivity, Temperature and Depth profiler) measurements, and to substitute for CTD measurements.

(3) Instrument and Method

The XCTDs used were XCTD-2 (Tsurumi-Seiki Co., Ltd., Yokohama, Kanagawa, Japan) with an MK-150N deck unit (Tsurumi-Seiki Co., Ltd.). The manufacturer's specifications are listed in Table 3.13.1. In this cruise, the XCTD probes were deployed by using 8-loading automatic launcher (stations 64, 67, 89_1, 89_2, 91, 93, 95, 103 and 105) or hand launcher (Tsurumi-Seiki Co., Ltd.). For comparison with CTD, XCTD was deployed at about 10 minutes after the beginning of the down cast of the CTD (stations 64, 67, 110, 112).

Table 3.13.1. Manufacturer's specifications of XCTD-2.

Parameter	Range	Accuracy
Conductivity	0 ~ 60 mS cm^{-1}	±0.03 mS cm^{-1}
Temperature	–2 ~ 35 °C	±0.02 °C
Depth	0 ~ 2000 m (for XCTD-2)	5 m or 2%, whichever is greater *

* Depth error is shown in Kizu et al (2008).

(4) Data Processing and Quality Control

The XCTD data will be processed and quality controlled based on a method by Uchida et al. (2011).

(5) Preliminary results

The XCTD depth error was preliminary estimated by using the XCTD data obtained at stations 64 and 67 (Figure

3.12.1). Similar depth error was seen in the comparison conducted in the MR09-01 cruise (Uchida et al., 2011).

Reference

Kizu, S., H. Onishi, T. Suga, K. Hanawa, T. Watanabe, and H. Iwamiya (2008): Evaluation of the fall rates of the present and developmental XCTDs. *Deep-Sea Res I*, **55**, 571–586.

Uchida, H., K. Shimada, and T. Kawano (2011): A method for data processing to obtain high-quality XCTD data. *J. Atmos. Oceanic Technol.*, **28**, 816–826.

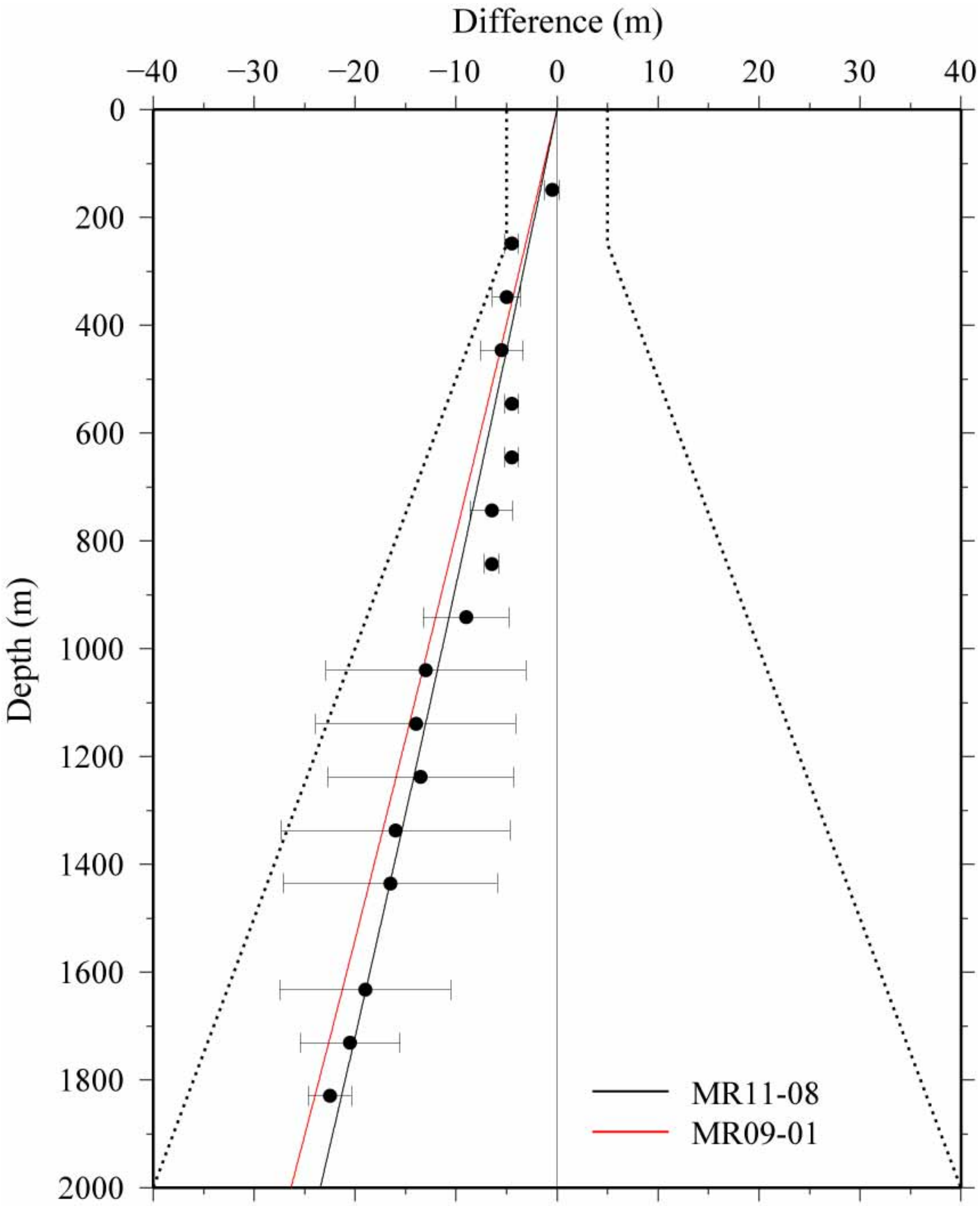

Figure 3.13.1. Differences between XCTD and CTD depths for stations 64 and 67. Differences were estimated with the same method as Uchida et al. (2011). Standard deviation of the estimates (horizontal bars) and the manufacturer's specification for XCTD depth error (dotted lines) are shown. The regression for the XCTD-2 data obtained in this cruise (black line) and for the XCTD-2 data obtained in the MR09-01 cruise (red line) are shown.

3.14 Ocean-origin-gases

Methane (CH_4), Nitrous oxide (N_2O), Carbonyl sulfide (COS), and related substances

February 29, 2012

(1) Personnel

Osamu Yoshida[1,2,3], Yuki Okazaki[3], Shinichi Oikawa[2], Hikari Shimizu[2], Chisato Yoshikawa[4,5], and Naohiro Yoshida[4]*

[1] *College of Agriculture, Food and Environment Sciences, Rakuno Gakuen University*
[2] *Faculty of Environment Systems, Rakuno Gakuen University*
[3] *Graduate School of Dairy Science, Rakuno Gakuen University*
[4] *Interdisciplinary Graduate School of Science and Engineering, Tokyo Institute of Technology*
[5] ***Japan Society for the Promotion of Science***
* *Principal Investigator*

(2) Sampling elements

All sampling elements of Rakuno Gakuen University group at hydrographic stations are listed below.

Table 1. Parameters and hydrographic station numbers for samples collection in Legs 2 and 3.

Parameters	Hydrographic station Numbers (WHP-P10)
1. Dissolved CH_4 (concentration)	1,8,18,29,34,39,45,49,54,58,62,66,71,74,79,88,98,106,114
2. Dissolved CH_4 (carbon isotope ratio)	1,29,45,58,71,88,114
3. Dissolved N_2O (concentration)	1,8,18,29,34,39,45,49,54,58,62,66,71,74,79,88,98,106,114
4-5. Dissolved N_2O (nitrogen and oxygen isotopomers)	1,29,45,58,71,88,114
6. CH_4 isotopomer (hydrogen isotope ratio)	1,29,45,58,71,88,114
7. NO_3^- (nitrogen isotope ratios)	1,29,45,58,71,88,114
A. Air samples for air-sea flux of CH_4 and N_2O	1,29,45,58,71,88,114
B. Air samples for concentration and sulfur isotope ratio of COS	1,29,45,58,71,88,114

(3) Methane

Methane concentration and stable isotopic distribution as indicators of biogenic methane dynamics in the Pacific Ocean

i. Dissolved CH_4

i-a Introduction

Atmospheric methane (CH_4) is a trace gas playing an important role in the global carbon cycle as a greenhouse gas. Its concentration has increased by about 1050 ppbv from 700 ppbv since the pre-industrial era (IPCC, 2007). In order to understand the current global methane cycle, it is necessary to quantify its sources and sinks. At present, there remain large uncertainties in the estimated methane fluxes from sources to sinks. The ocean's source strength for atmospheric methane should be examined in more detail, even though it might be a relatively minor source, previously reported to be 0.005 to 3% of the total input to the atmosphere (Cicerone and Oremland, 1988; Bange et al., 1994; Lelieveld et al., 1998).

To estimate an accurate amount of the methane exchange from the ocean to the atmosphere, it is necessary to explore widely and vertically. Distribution of dissolved methane in surface waters from diverse locations in the world ocean is often reported as a characteristic subsurface maximum representing a supersaturation of several folds (Yoshida et al., 2004). Although the origin of the subsurface methane maximum is not clear, some suggestions include advection and/or diffusion from local anoxic environment nearby sources in shelf sediments, and *in situ* production by methanogenic bacteria, presumably in association with suspended particulate materials (Karl and Tilbrook, 1994; Katz et al., 1999). These bacteria are thought to probable live in the anaerobic microenvironments supplied by organic particles or guts of zooplankton (Alldredge and Cohen, 1987).

So, this study investigates in detail profile of methane concentration and stable isotopic distribution in the water column in the Pacific Ocean to clarify methane dynamics and estimate the flux of methane to the atmosphere.

i-b Materials and methods

Seawater samples are taken by CTD-CAROUSEL system attached Niskin samplers of 12 L at 24 layers and surface layer taken by plastic bucket at 19 hydrographic stations as shown in Table 1. Each sample was carefully subsampled into 30, 125, 600 mL glass vials to avoid air contamination for analysis of methane concentration, carbon isotope ratio, and hydrogen isotope ratio respectively. The seawater samples were poisoned by 20 μL (30 and 125 mL vials) or 100 μL (600 mL vial) of mercuric chloride solution (Tilbrook and Karl, 1995; Watanabe et al., 1995), and were closed with rubber and aluminum caps. These were stored in a dark and cool place until we got to land, where we conducted gas chromatographic analysis of methane concentration and mass spectrometric analysis of carbon and hydrogen isotopic composition at the laboratory.

The analytical method briefly described here: The system consists of a purge and trap unit, a desiccant unit, rotary valves, a gas chromatograph equipped with a flame ionization detector for concentration of methane, GC/C/IRMS for carbon isotope ratio of methane, GC/TC/IRMS for hydrogen isotope ratio of methane, and data acquisition units. The entire volume of seawater in each glass vial was processed all at once to avoid contamination and loss of methane.

Precision obtained from replicate determinations of methane concentration was estimated to be better than 5% for the usual concentration of methane in seawater.

i-c Expected results

Subsurface maximum concentrations of methane (>3 nmol kg^{-1}) were expected to be observed in the Pacific Ocean. A commonly-encountered distribution in the upper ocean with a methane peak within the pycnocline (e.g., Ward et al., 1987; Owens et al., 1991; Watanabe et al., 1995). Karl and Tilbrook (1994) suggested the suboxic conditions would further aid the development of microenvironments within particles in which methane could be produced. The organic particles are accumulated in the pycnocline, and methane is produced in the micro reducing environment by methanogenic bacteria. Moreover, *in situ* microbial methane production in the guts of zooplankton can be expected (e.g., Owens et al., 1991; de Angelis and Lee, 1994; Oudot et al., 2002; Sasakawa et al., 2008). Watanabe et al. (1995) pointed out that the diffusive flux of methane from subsurface maxima to air-sea interface is sufficient to account for its emission flux to the atmosphere. In the mixed layer above its boundary, the methane is formed and discharged to the atmosphere in part, in the below its boundary, methane diffused to the bottom vertically. By using concentration and isotopic composition of methane and hydrographic parameters for vertical water samples, it is possible to clarify its dynamics such as production and/or consumption in the water column.

ii. References

Alldredge, A. A., Y. Cohen: Can microscale chemical patches persist in the sea? Microelectrode study of marine snow, fecal pellets, Science, 235, 689-691, 1987.

Bange, H. W., U. H. Bartell, S. Rapsomanikis, and M. O. Andreae: Methane in the Baltic and the North seas and a reassessment of the marine emissions of methane, Global Biogeochem. Cycles, 8, 465–480, 1994.

Cicerone, R. J., and R. S. Oremland: Biogeochemical aspects of atmospheric methane, Global Biogeochem. Cycles, 2, 299–327, 1988.

de Angelis, M. A., and C. Lee: Methane production during zooplankton grazing on marine phytoplankton, Limnol. Oceanogr., 39, 1298-1308, 1994.

Intergovernmental Panel on Climate Change (2007), Couplings Between Change in the Climate System and Biogeochemistry, in Climate Change 2007: The Physical Science Basis: Contribution of Working Group I to the Fourth Assessment Report of the Intergovernment Panel on Climate Change, edited by S. Solomon, et al., pp. 501-568, Cambridge University Press, Cambridge, United Kingdom and New York, NY, USA.

Karl, D. M., and B. D. Tilbrook: Production and transport of methane in oceanic particulate organic matter, Nature, 368, 732–734, 1994.

Katz, M. E., D. K. Pak, G. R. Dickkens, and K. G. Miller (1999), The source and fate of massive carbon input during the latest Paleocene thermal maximum, Scince, 286, 1531–1533.

Lelieveld, J., P. J. Crutzen, and F. J. Dentener (1998), Changing concentration, lifetime and climate forcing of atmospheric methane, Tellus Ser. B, 50, 128–150.

Oudot, C., P. Jean-Baptiste, E. Fourre, C. Mormiche, M. Guevel, J-F. Ternon, and P. L. Corre: Transatlantic equatorial distribution of nitrous oxide and methane, Deep-Sea Res., Part I, 49, 1175–1193, 2002.

Owens, N. J. P., C. S. Law, R. F. C. Mantoura, P. H. Burkill, and C. A. Llewellyn: Methane flux to the atmosphere from the Arabian Sea, Nature, 354, 293–296, 1991.

Sasakawa, M., U. Tsunogai, S. Kameyama, F. Nakagawa, Y. Nojiri, and A. Tsuda (2008), Carbon isotopic characterization for the origin of excess methane in subsurface seawater, J. Geophys. Res., 113, C03012, doi: 10.1029/2007JC004217.

Tilbrook, B. D., and D. M. Karl: Methane sources, distributions and sinks from California coastal waters to the oligotrophic North Pacific gyre, Mar. Chem., 49, 51–64, 1995.

Ward, B. B., K. A. Kilpatrick, P. C. Novelli, and M. I. Scranton: Methane oxidation and methane fluxes in the ocean surface layer and deep anoxic waters, Nature, 327, 226–229, 1987.

Watanabe, S., N. Higashitani, N. Tsurushima, and S. Tsunogai: Methane in the western North Pacific, J. Oceanogr., 51, 39–60, 1995.

Yoshida, O., H. Y. Inoue , S. Watanabe, S. Noriki, M. Wakatsuchi: Methane in the western part of the Sea of Okhotsk in 1998-2000, J. Geophys. Res., 109, C09S12, doi:10.1029/2003JC001910, 2004.

(4) Nitrous oxide and related substances

Nitrous oxide Production, consumptions and air-sea flux in the Pacific Ocean

i. Introduction

Recently considerable attention has been focused on emission of biogenic trace gases from ecosystems, since the gases contain a significant amount of greenhouse gases. Isotopic signatures of these gases are well recognized to provide constraints for relative source strength and information on reaction dynamics concerning their formation and biological pathways. Nitrous oxide (N_2O) is a very effective heat-trapping gas in the atmosphere because it absorbs outgoing radiant heat in infrared wavelengths that are not captured by the other major greenhouse gases, such as water vapor and CO_2. The annual input of N_2O into the atmosphere is estimated to be about 16 Tg N_2O-N yr^{-1}, and the oceans are believed to contribute more than 20% of the total annual input (IPCC, 2007).

N_2O is produced by the biological processes of nitrification and denitrification (Dore et al., 1998; Knowles et al., 1981; Rysgaard et al., 1993; Svensson, 1998; Ueda et al., 1993). Depending on the redox conditions, N_2O is produced from inorganic nitrogenous compounds (NH_4 or NO_3^-), with subsequently different isotopic fractionation factors. The isotopic signatures of N_2O confer constraints on the relative source strength, and the reaction dynamics of N_2O biological production pathways are currently under investigation. Furthermore, isotopomers of N_2O contain more easily interpretable biogeochemical information as to their sources than obtained from conventional bulk ^{15}N and ^{18}O measurements (Yoshida and Toyoda, 2000).

The Pacific Ocean is the largest of the world's five oceans (followed by the Atlantic Ocean, Indian Ocean, Southern Ocean, and Arctic Ocean) (CIA, www) and expected to be important for the biogeochemical and biological cycles. Thus, the study of N_2O production and nutrients dynamics are very important to examine the origins of N_2O in seawater and to estimate the inventory of N_2O from this region with respect to the troposphere.

ii. Materials and methods

The purpose of the expedition was to study on the heat and material transports and their variability of the general ocean circulation and a study on chemical environment and its changes in the ocean. In order to investigate the production and consumption of dissolved N_2O in the Pacific, seawater samples for dissolved N_2O concentration/isotopomer ratio analysis and those for nitrate isotope ratio analysis were collected at total 19 and 7 stations, respectively (Table 1). Air samples were also collected into pre-evacuated stainless-steel canisters (total 7 stations, Table 1).

ii-a Air-sea flux measurement

Concentration of N_2O at the surface water and ambient air will be measured using GC/ECD at Rakuno Gakuen University and/or GC/IRMS at Tokyo Institute of Technology.

ii-b N_2O concentration and isotope analyses

Seawater samples collected by CTD-CAROUSEL system was subsampled into three glass vials: one 30 mL vial for concentration analysis and two 125 or 225 mL glass vials for isotopomer ratio analysis. The subsamples were then sterilized with saturated $HgCl_2$ solution (about 20 µL per 100 mL seawater). The vials were sealed with butyl-rubber septa and aluminum caps, taking care to avoid bubble formation, and then brought back to the laboratory and stored at 4˚C until analysis. Dissolved N_2O concentrations and its isotopic compositions will be measured by GC/ECD and/or GC/IRMS.

ii-c Isotope ratios of NO_3^-

Water sample was collected into a 50 mL syringe equipped with a DISMIC® filter (pore size: 0.45 m). The sample was then filtrated and divided into five polypropylene tubes. One of the tubes was stored at -40ºC until analysis. The rest of the tubes were stored at room temperature after adding 0.5 mL of 1 mol L^{-1} NaOH. Isotope ratios of NO_3^- will be measured by denitrifer method (Sigman et al., 2001) in which N_2O converted from nitrate is measured by using GC/IRMS.

iii. Expected results

In the surface layer, N_2O concentration of water affects the sea-air flux directly (Dore et al., 1998). However the pathway of N_2O production in surface layer is still unresolved. In the surface layer, N_2O is predominantly produced by nitrification, but also by denitrification if oxygen concentration is low (Maribeb and Laura, 2004). Moreover, it was reported that N_2O production by nitrification is photo-inhibited (Olson, 1981). Therefore, concentration and isotopomer ratios of N_2O/nitrate together with N_2O production rate from ammonium/nitrate obtained by this study will reveal the pathway of N_2O production and N_2O production rate in the surface layer (especially euphotic zone).

In deeper layer, N_2O could be produced through *in situ* biological processes of settling particles or fecal pellets derived from phytoplankton or zooplankton, and N_2O maximum was indeed observed at 600-800 m depth in the North Pacific (Popp et al., 2002; Toyoda et al., 2002). However, following problems have not been resolved: (i) what the major pathway for the N_2O maximum is and (ii) whether the N_2O is produced *in situ* or transported from other area. Although there is a report on distribution of concentration and isotopomer ratio of N_2O in the central and eastern South Pacific (Charpentier et al., 2007), this study will be the first one which reveals the distribution and production pathway of N_2O in the Pacific.

iv. References

Charpentier, J., L. Farias, N. Yoshida, N. Boontanon, and P. Raimbault: Nitrous oxide distribution and its origin in the central and eastern South Pacific Subtropical Gyre, Biogeosciences, 4 (5), 729-741, 2007.

Dore, J.E., Popp, B.N., Karl, D.M. and Sansone, F.J.: A large source of atmospheric nitrous oxide from subtropical North Pacific surface water, Nature, 396, 63-66, 1998.

IPCC, Climate Change 2007: The Physical Science Basis. Contribution of Working Group I to the Fourth Assessment Report of the Intergovernmental Panel on Climate Change, edited by S. Solomon et al., pp. 996, Cambridge

University Press, Cambridge, United Kingdom and New York, NY, USA, 2007.

Knowles, R., Lean, D.R.S. and Chan, Y.K.: Nitrous oxide concentrations in lakes: variations with depth and time, Limnology and Oceanography, 26, 855-866, 1981.

Maribeb, C.-G. and Laura, F.: N_2O cycling at the core of the oxygen minimum zone off northern Chile, Marine Ecology Progress Series, 280, 1-11, 2004.

Olson, R.J.: Differential photoinhibition of marine nitrifying bacteria: a possible mechanism for the formation of the primary nitrite maximum, Journal of Marine Research, 39, 227-238, 1981.

Popp, B. N., et al.: Nitrogen and oxygen isotopomeric constraints on the origins and sea-to-air flux of N_2O in the oligotrophic subtropical North Pacific gyre, Global Biogeochem. Cycles, 16(4), 1064, 2002. doi: 10.1029/2001GB001806.

Rysgaard, S., Risgaard-Petersen, N., Nielsen, L.P. and Revsbech, N.P.: Nitrification and denitrification in lake and estuarine sediments measured by the ^{15}N dilution technique and isotope pairing, Applied and Environmental Microbiology, 59, 2093-2098, 1993.

Sigman, D. M., K. L. Casciotti, M. Andreani, C. Barford, M. Galanter, and J. K. Boehlke: A bacterial method for the nitrogen isotopic analysis of nitrate in seawater and freshwater, Anal. Chem., 73, 4145-4153, 2001.

Svensson, J.M.: Emission of N_2O, nitrification and denitrification in a eutrophic lake sediment bioturbated by Chironomus plumosus, Aquatic Microbial Ecology, 14, 289-299, 1998.

Toyoda, S., N. Yoshida, T. Miwa, Y. Matsui, H. Yamagishi, U. Tsunogai, Y. Nojiri, and N. Tsurushima: Production mechanism and global budget of N_2O inferred from its isotopomers in the western North Pacific, Geophys. Res. Lett., 29 (3), 7-1-7-4, 2002.

Ueda, S., Ogura, N. and Yoshinari, T.: Accumulation of nitrous oxide in aerobic ground water, Water Research, 27, 1787-1792, 1993

www.cia.gov/cia/publications/factbook/geos/zn.html

Yoshida, N. and Toyoda, S.: Constraining the atmospheric N_2O budget from intramolecular site preference in N_2O isotopomers, Nature, 405, 330-334, 2000.

(5) Carbonyl sulfide

i. Introduction

Carbonyl sulfide (COS) is the most abundant (about 500 pptv) and most stable (life time is about 16 years) gaseous sulfur species in the background (remote) atmosphere. It is oxidized in the stratosphere to form sulfate aerosols which may influence the radiation budget at the Earth's surface and the stratospheric ozone cycle (Crutzen, 1976). It is emitted from natural sources such as microbial metabolism of sulfur in the ocean and terrestrial environment and anthropogenic sources such as sulfur industry and combustion of fossil fuel and biomass (Chin and Davis, 1993; Watts, 2000; Kettle et al., 2002). Its major sinks are considered to be soil and plant uptake, reaction with OH and OD radials, and photolysis in the stratosphere. However, estimated fluxes of the sources have large uncertainty because they are based on limited observations of COS concentration, and COS budget has not been closed yet. Therefore, isotopic study of COS may provide constraints for relative source strength as well as information on reaction pathways in its formation and destruction processes. Sulfur isotope ratio of COS in the atmosphere or source gasses has not been reported so far, although there is a study on sulfur isotope fractionation in the stratospheric COS which suffers from low analytical precision by balloon-born infrared spectroscopy (Leung et al., 2002).

In this study, we are developing a high-sensitive, high-precision, and rapid analytical system for concentration and sulfur isotope ratios of COS that is applicable to trace COS in environment. Our purpose of this cruise is to collect maritime air samples which contain background COS or COS emitted from nearby oceanic sources for the isotopic analysis.

ii. Materials and methods

Air samples were collected at 7 stations listed in Table 1. At each station, ambient air near the bridge (about 10 m above sea level) was pressurized into two stainless-steel canisters (6L) at 5 atm (absolute pressure) using a sampling device which consists of a diaphragm pump, a back-pressure regulating valve, a desiccant tube packed with $Mg(ClO_4)_2$, and stainless tubes and connectors. Inner surface of the SS canisters are deactivated to prevent COS adsorption or decomposition during sample storage.

iii. Expected results

First, concentration analysis will be performed to determine the sample size and detail procedure for isotopic measurement. Then, stability of COS in the glass bottle and canister will be checked by periodic analysis of concentration using an aliquot of the same sample. Finally, sulfur isotope ratio will be measured by the newly developed analytical system. If succeeded, sulfur isotope ratio of atmospheric COS will be revealed for the first time.

iv. References

Crutzen, P. J.: The possible importance of OCS for the sulfate layer of the stratosphere, Geophys. Res. Lett., 3, 73-76, 1976.

Chin, M., and D. D. Davis: Global sources and sinks of OCS and CS2 and their distributions, Global Biogeochem. Cycles, 7 (2), 321-337, 1993.

Kettle, A. J., U. Kuhn, M. von Hobe, J. Kesselmeier, and M. O. Andreae: Global budget of atmospheric carbonyl sulfide: Temporal and spatial variations of the dominant sources and sinks, J. Geophys. Res., 107 (D22), 4658, 2002.

Leung, F.-Y., A. J. Colussi, and M. R. Hoffmann: Isotopic fractionation of carbonyl sulfide in the atmosphere: Implications for the sources of background stratospheric sulfate aerosol, Geophys. Res. Lett., 29 (10), 1474, 2002.

Watts, S. F.: The mass budgets of carbonyl sulfide, dimethyl sulfide, carbon disulfide and hydrogen sulfide, Atmos. Environ., 34, 761-779, 2000.

3.15. PFCs

(1) Personnel

Nobuyoshi Yamashita and Sachi Taniyasu

National Institute of Advanced Industrial Science and Technology (AIST)

(2) Objectives

Environmentally persistent perfluorinated acids (PFAs, shown in figure 1) have appeared as a new class of global pollutants for the last ten years. These compounds in general, and perfluorooctane sulfonate (PFOS) in particular, have recently emerged as a priority environmental pollutant due to its widespread finding in biota including both Arctic and Antarctic species and its persistent and bioaccumulative nature. The physicochemical properties of PFAs are unique in that they have high water solubility despite the low reactivity of carbon-fluorine bond, which also imparts high stability in the environment. However, little is known on the distribution of PFAs in the oceans around the world, so far. We have conducted several international joint cruises, including South China Sea and Sulu Seas (KH-02-4), the central to Eastern Pacific Ocean (KH03-1), North and middle Atlantic Ocean, Southern Pacific and Antarctic Ocean (KH04-5), Labrador Sea and coastal seawater from Asian countries (Japan, China, Hong Kong, Korea) (1, 2, 3). Vertical profiles of PFAs in the marine water column were associated with the global ocean circulation theory. We found that vertical profiles of PFAs in water columns from the Labrador Sea reflected the influx of the North Atlantic Current in surface waters, the Labrador Current in subsurface waters, and the Denmark Strait Overflow Water in deep layers below 2000 m. Striking differences in the vertical and spatial distribution of PFAs, depending on the oceans, suggest that these persistent organic acids can serve as useful chemical tracers to allow us to study oceanic transportation by major water currents. The results provide evidence that PFA concentrations and profiles in the oceans adhere to a pattern consistent with the global ‘‘Broecker’s Conveyor Belt’’ theory of open ocean water circulation.

In MR11-08, we tried to confirm the vertical profiles of PFCs found in water columns from above cruises and the Pacific Ocean (KH03-1) and obtained open ocean samples for further analysis..

(3) *Samples:*

Seawater samples were taken by Conductivity temperature depth profiler-Carousel multiple sampling system (CTD-CMS) attached X-Niskin samplers of 12 L, together with surface seawater samples taken by bucket at all the water sampling stations. At two sampling site, atmospheric materials taken with a moisture sampler (prototype, AIST/SIBATA Co.). The air sampler was operated with a flow rate of 3– 10 L/min. Samples were collected during underway to avoid contamination from exhaust gas from ship. Water, air samples were stored at below -20°C until chemical analysis in AIST laboratory.

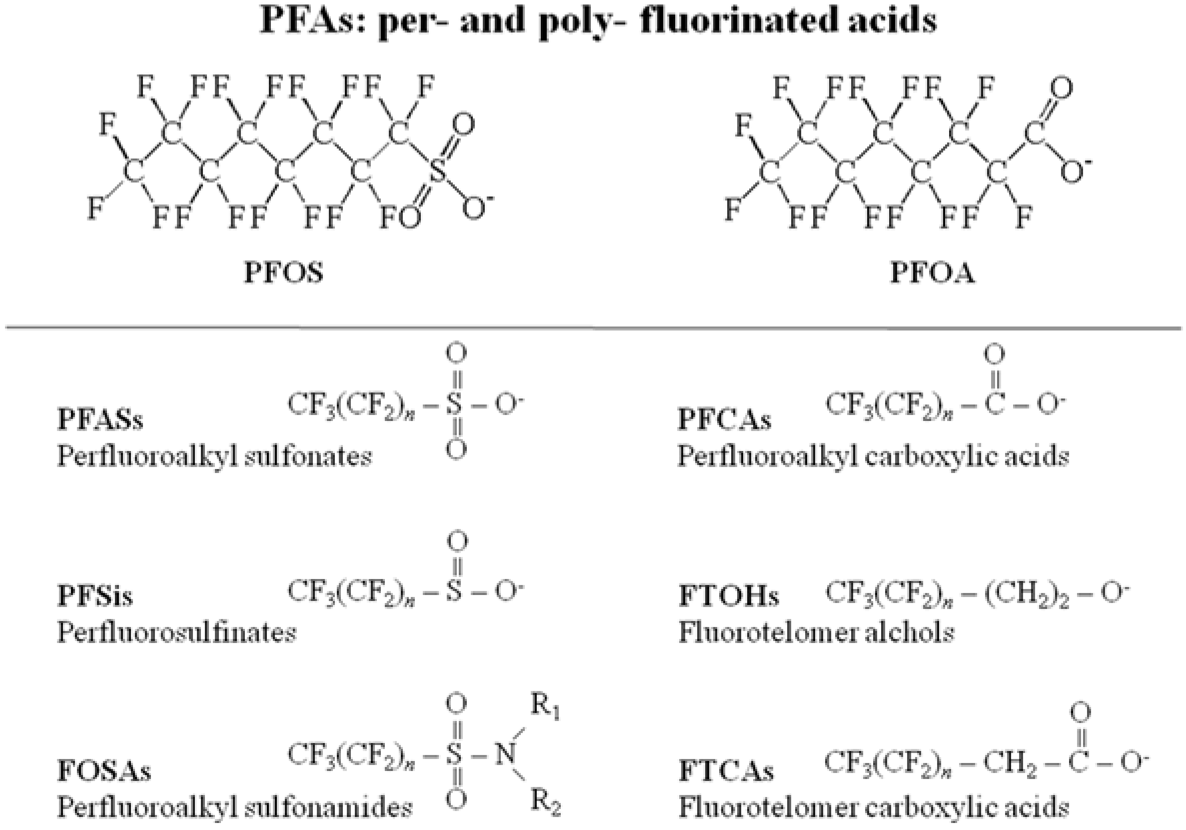

Figure 1. PFOS and related chemicals

(4) *Chemical analysis*:

Water samples were stored in clean 1 L polypropylene bottles and were kept frozen until analysis. Samples were thawed at room temperature, and a solid phase extraction method using WAX® cartridge (Waters Co.) was used for the determination of PFAs by HPLC tandem mass spectrometry (HPLC-MS/MS) as described elsewhere (4,5). Briefly, after preconditioning with 4 mL ammonium hydroxide in methanol, 4 mL methanol, and then 4 mL Millipore water, the cartridges were loaded with 900-1000 mL samples at approximately 1 drop sec-1. The cartridges were then washed with 4mL of 25 mM ammonium acetate buffer (pH 4) in Millipore water and dried by centrifugation at 3000rpmfor 2 min. The elution was then divided into two fractions. The first fraction was carried out with 4 mL methanol and the second with 4 mL 0.1%ammoniumhydroxide in methanol. Both fractions were reduced to 0.5 mL under a nitrogen stream and analyzed separately. HPLC-MS/MS, composed of a HP1100 liquid chromatograph (Agilent Technologies, Palo Alto, CA) interfaced with a Micromass® (Beverly, MA) Quattro Ultima Pt mass spectrometer was operated in the electrospray negative ionization mode.A 5 or 10-µL aliquot of the sample extract was injected into a Betasil C18 column (2.1 mm i.d.×50 mm length, 5µm; Thermo Hypersil-Keystone, Bellefonte, PA). The capillary is held at 1.2 kV. Cone-gas and desolvation-gas flows are kept at 60 and 650 L/h, respectively. Source and desolvation temperatures were kept at 120 and 420°C respectively. MS/MS parameters are optimized so as to transmit the [M-K]- or [M-H]- ions.

(5) *Quality assurance and quality control according to ISO25101*:

More than two hundreds of PFOS related chemicals were discussed for international regulation of use, namely Stockholm convention agreement (POPs; persistent organic pollutants) in 2008 because of potential risk to the environment and human being. Finally, PFOS and PFOSF were added to a list of international regulation in May 2009. Because of serious worldwide concern about PFOS, strong necessity to establish reliable standard operation procedure (SOP) were indicated. Hence, analytical method developed by AIST was validated by International Organization of Standard (ISO) and proved its reliability. This was successfully published as ISO25101 in 2009 (6). National standard, namely Japanese Industrial Standard (JIS) is also to be established after ISO25101. In the inter-laboratory calibration study oriented for JIS, thirty laboratories were registered for participation and 23 of the laboratories provided the final results. Twenty commercial laboratories, nine municipal corporations and one institute were participated. Test standard solutions, calibration curve standards and labeled surrogate standards were provided from Wellington Laboratories / Kanto Chemical. PFOS and PFOA were analyzed in two kinds of waste water, river water, spiked Milli-Q water and standard solution in methanol. Participating laboratories were requested to determine the levels of PFOS and PFOA in the water samples. Other PFCs, C4 to C14, C16, C18 PFCAs, C4, C6, C7, C10 PFASs were also reported, if possible. All determinations were required to be done in triplicate. Laboratories were requested to follow a unified analytical method, as described in draft document of Japanese Industrial Standard (JIS) modified from ISO25101. Standard operation procedure was provided as a guide and this document included step by step details of analytical methods. Because of requirement as JIS, two waste water samples were tested in this trial. Although ISO25101 is a method for unfiltrated water samples, applicable filtration method using glass fiver or nylon filter was used to remove particles to enable smooth extraction by SPE. The brief procedure is as follows.

1. Filtration of waste water/river water using glass fiver or nylon filter.
2. Extraction by SPE using Oasis®WAX.
3. HPLC-MS/MS quantification by following parameters; HPLC column, Betasil® C18 (Thermo Hypersil-Keystone), Ace®3 C18 (Advanced Chromatography Technologies) or comparable HPLC column. No HPLC-MS (single mass) was allowed to use because of unreliable potency to resolve interferences.
4. Quantification by ISTD method using ^{13}C-labeled surrogates. Participants were allowed to report both external standard and internal standard based results.
5. Instruction to resolve interference of branched isomer of PFOS and PFOA from linier isomer (test target) was provided.
6. Standard chemicals and instrumental parameter to measure C4 to C14, C16, C18 PFCAs, C4, C6, C7, C10 PFASs were provided.

Only summary of PFOS and PFOA were described here. Only those laboratories which provided internal standard recoveries were selected for this report, and the results that reported less than 70% and more than 125% for internal standard recoveries were rejected from data analysis. Accuracy of the current values as represented by Coefficient of Variation (23% for PFOS, 27% for PFOA) in ISO25101 were smaller than that reported during another calibration study (95%% for PFOS, 118% for PFOA) conducted in 2005 2. This improvement is considerable, particularly when considering the fact that the concentration of target chemicals in the test sample in our exercise was 10 times lower than the earlier study. Although the aims of inter-laboratory trial with and without SOP are different, it can be mentioned that determination of PFOS and PFOA in water samples, when provided with a standard protocol documenting appropriate QA/QC protocol, improved the accuracy and prevision. CV from JIL-PFOS-2008 and JIL-PFOS-2009 were comparable to ISO25101 only exception of trace level tap water sample (PFOS) and waste water with high concentration. This can be explained as insufficient use of calibration curve on instrument. Linearity and reliability of calibration curve on HPLC-MSMS supposed to be limited at the end of curve (lowest point and highest point) for qualification of PFOS and PFOA. Some laboratories couldn’t use accurate procedure of Oasis®WAX because of insufficient in-house method using formic acid. This cartridge has good performance for trace analysis of shorter chain PFCs but necessary to use accurate procedure using buffer solution. Future development of much more capable SPE will enable easy to use and high throughput analysis of PFCs. Another limitation of the method is maximum amount of water samples applicable to SPE. No commercially available SPE can be used for larger than 1000 ml at this stage without QAQC information. We have tested the point using large volume water samples by in-situ SPE method.

MR11-08 is the third international research cruise that conducted measurement of POPs in Open ocean waters using ISO method (ISO25101). Because of recent scene of analytical chemistry, uncertainty and reliability of measurement supported by suitable quality assurance and quality control (QAQC) becoming to the essential issue. Our experimental result with ISO25101 supported by the international QAQC (ISO17025 with Guide45) and Japanese Industrial Standard (JIS) will provide the most reliable information of environmental chemistry in Open ocean research for now.

(6) Results

In figure 2, concentrations of PFOS and PFOA in two water-column samples collected from Japan Sea in KT-05-11. (10–3250 m, N40 430, E136 340, 10–3440 m, N44 120, E138 540) were presented (modified from original figure by Yamashita, Chemosphere 2008). Vertical water samples collected in MR11-08 will provide current situation of PFAs in comparison to water column after six years. This can be useful to estimate the source function of PFAs closely related to use of industrial chemicals in Asia.

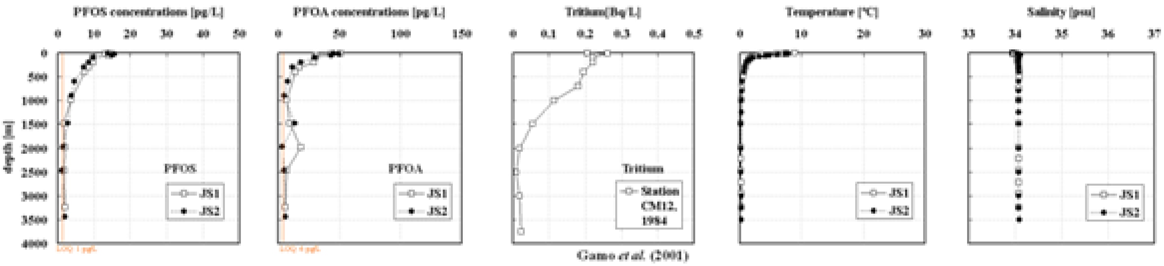

Figure 2. Concentrations of PFOS and PFOA in two water-column samples collected from Japan Sea in KT-05-11. (10–3250 m, N40 430, E136 340, 10–3440 m, N44 120, E138 540) (modified from original figure by Yamashita, Chemosphere 2008).

We have collected several water column samples, two ocean airs, more than five rain events and during the cruise. Precipitation may wash down the PFCs deposited in the air, dust or other matrices present in the atmospheric environment. The measurement of concentrations of PFCs in precipitation samples can provide deeper understanding on fluxes and depositions of PFCs in the atmosphere. Loewen et al. had reported concentrations of fluorinated acids and PFOS in Canadian precipitation samples using HPLC/MSMS. Only one rainfall event (*n*=3) was captured and analyzed, 8:2 FTCA concentrations (1.00 ± 0.08 ng/L) was found to be highest, while the concentrations of PFOS (0.59 ± 0.04 ng/L) was higher than those of 10:2 FTCA (0.30 ± 0.04 ng/L), 8:2 FTUCA (0.12 ng/L ± 0.02 ng/L) and 10:2 FTUCA (0.12 ng/L ± 0.01 ng/L).

Using chemical derivatization by GC/MS, Scott et al. had reported concentrations of C_2-C_{12} PFCAs and fluorinated acids in North American precipitation samples. Among the 9 sites with urban and rural area, the concentrations of TFA was highest compared to those of other PFCAs. Apart from TFA, higher concentrations were detected in short-chain compounds (C_3-C_7) than PFOA and PFNA. FTCA and FTUCA concentrations were considerably lower than those of PFCAs. Also, higher concentrations of PFCs were detected in the urban area than the rural area. As for Albany, New York, USA precipitation samples, Kim and Kannan had measured concentrations of C_7-C_{12} PFCAs, C_6, C_8, C_{10} PFASs and FtS by HPLC/MSMS. PFHpA with a median concentration of 0.56 ng/L was detected in almost all samples. Highest concentrations were detected for PFOA and PFNA, and PFOS was the only detectable PFASs. The concentration range of PFOA measured in that study was comparable to the concentrations found in Scott and his co-worker' study. Interestingly, PFOS concentrations were found to be highest in Dailin, China precipitation samples.

Kwok investigated concentrations of twenty PFCs, including C_3-C_5 short chain PFCs, were quantified using LC/MS/MS in precipitation samples from Japan (*n*=31), USA (*n*=12), China (*n*=5), India (*n*=2) and France (*n*=2). A total of 52 precipitation samples in the period of June 2006 to September 2008 from seven cities were analyzed. Overview of individual PFC concentrations in precipitation samples were shown in figure 3. PFCs, dominated by C_3-C_{12} PFCAs, were measured in all of the precipitation samples. The highest concentration of PFCAs for most of the precipitation samples was found to be PFPrA. PFPrA was firstly detected in precipitation samples using LC/MSMS in this study. One of the possible sources of PFPrA may due to the use of perfluoroketone.

Perfluoroketone can be served as a clean fire suppression agent, which was a replacement of Halon 1301 and Halon 1211. PFPrA is considered to be the final product of the reaction between perfluoroketone and water present in the atmosphere, which can then be exposed to the atmospheric environment during fire protection.

No clear seasonal trends were found for both locations in Japan, which is similar to that reported earlier in three northeastern US locations showing a lack of seasonal trend for PFOA and PFNA fluxes. Elevated total PFC and PFCA concentrations were found in samples collected in August in Tsukuba and Kawaguchi; however, no such trend was observed for PFASs. The composition profiles of PFCs varied depending on the month of sampling. These observations were probably related to the seasonal differences in the usage pattern of PFC chemicals. No temperature-related seasonal trend was observed for all PFCs at both locations. Generalization could not be made between wind direction and concentrations of PFCs at each of the rain events. The fluctuating concentrations of PFCs and differences in composition profiles of PFCs at different precipitation events may be governed by meteorological conditions and

PFC concentrations in precipitation are affected by the dilution process as evidenced by lower concentrations when amount of precipitation was high. Differences in the composition of PFCs in precipitation at various location suggested that precipitation reflects only the local sources of contamination.

Snow is another kind of wet precipitation and might also be a very efficient scavenger of organic vapors due to its high specific surface area. In order to further investigate the scavenging potential of PFCs in the atmosphere by precipitation, a preliminary comparison was made between rain and snow samples collected in Tsukuba, Japan. In general, PFC concentrations were similar between rain and snow samples, however rain water could scavenge a higher percentage of most of the PFCs (PFBA, PFOA, PFNA, PFDA, PFUnDA, PFDoDA, PFOS, 8:2 FTUCA, PFOSA and *N*-EtFOSAA) than snow. As rain and snow are in different physical state, rain droplets can dissolve PFCs more efficiently also in addition to sorption to the droplet surface.

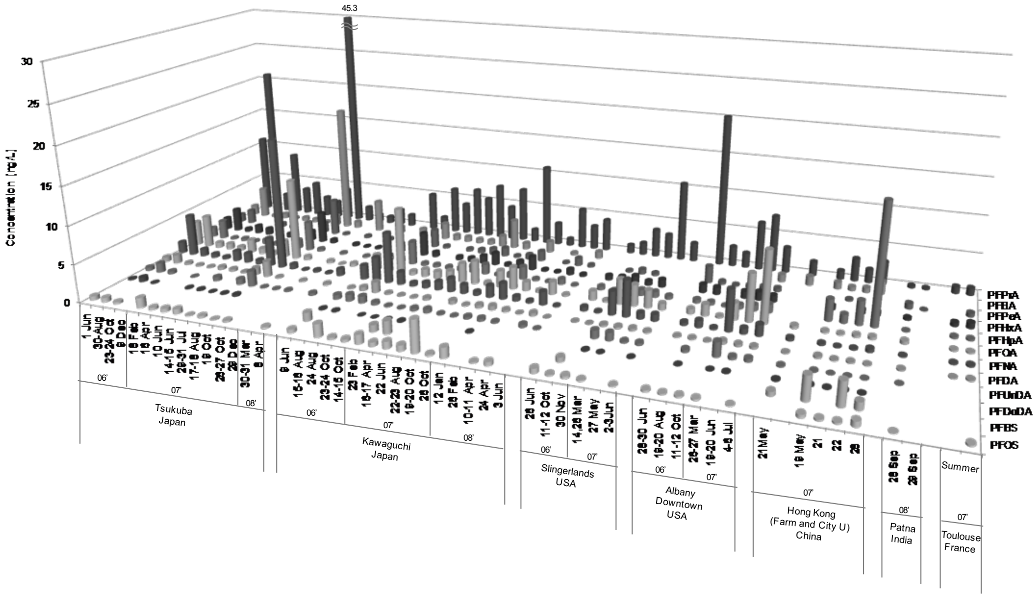

Figure 3. PFC concentrations in each precipitation samples from seven locations from five countries. No bar:

Sample < corresponding LOQ, i.e., 0.05 – 0.25 ng/L.
(modified from original figure by Kwok K, EST 2010).

The global circulation of ocean water and deep seawater might play a major role in scavenging of several POPs and therefore their role in the global fate of PFOS related chemicals must be examined to estimate the environmental destiny of persistent hazardous chemicals on our planet.

References

(1) Yamashita N, Kannan K, Taniyasu S, Horii Y, Petrick G, Gamo T, A global survey of perfluorinated acids in oceans, Marine Pollution Bulletin 51 (2005) 658–668

(2) Wei S, Chen LQ, Taniyasu S, So MK, Murphy MB, Yamashita N, Yeung LWY, Lam PKS, Distribution of perfluorinated compounds in surface seawaters between Asia and Antarctica, Marine Pollution Bulletin 54 (2007) 1813–1838

(3) Yamashita N, Taniyasu S, Petrick G, Wei S, Gamo T, Lam PKL, Kannan K, Perfluorinated acids as novel chemical tracers of global circulation of ocean waters, *Chemosphere* 70 (2008) 1247–1255

(4) Yamashita N, Kannan K, Taniyasu S, Horii Y, Okazawa T, Petrick G, Gamo T, Analysis of Perfluorinated Acids at Parts-Per-Quadrillion Levels in Seawater Using Liquid Chromatography-Tandem Mass Spectrometry, Environ. Sci. Technol. (2004) 38, 5522-5528

(5) Taniyasu S, Kannan K, So MK, Gulkowskad A, Sinclair E, Okazawa T, Yamashita N, Analysis of fluorotelomer alcohols, fluorotelomer acids, and short- and long-chain perfluorinated acids in water and biota, *Journal of Chromatography A*, 1093 (2005) 89–97

(6) ISO 25101 (2009 March 1st) Water quality — Determination of perfluorooctanesulfonate (PFOS) and perfluorooctanoate (PFOA) — Method for unfiltered samples using solid phase extraction and liquid chromatography/mass spectrometry

(7) Kwok K, Taniyasu S, Yeong L, Murphy M, Lam P, Horii Y, Kannan K, Petrick G, Sinha R and Yamashita N, Flux of Perfluorinated Chemicals through Wet Deposition in Japan, the United States, And Several other countries, Environ. Sci. Technol. (2010) 44, 7043-7049

3.16 Iodine-129

(1) Personnel

Shigeyoshi Otosaka
Japan Atomic Energy Agency

(2) Objective

In order to investigate the water circulation and ventilation process in the Western Pacific, seawaters for measurements of radioactive cesium (cesium-134 and -137) and tritium (H-3), which were released from the Fukushima Daiichi nuclear power plant after its serious accident on the March 11 of 2011, were collected by the hydrocasts from surface to about 2000 m depth during MR11-08 cruise.

(3) Sample collection

The sampling stations and number of samples are summarized in Table 3.16.1. Seawater samples for iodine-129 (total 59 samples) were collected at 3 stations using 12-liter Niskin-X bottles except surface seawater, which was collected by a bucket. The seawater sample for iodine-129 was collected into a 1-L plastic bottle after two time washing.

(4) Sample preparation and measurements

In our laboratory on shore, radioactive cesium in the seawater samples will be concentrated using ammonium phosphomolybdate (AMP) that forms insoluble compound with cesium. The radioactive cesium in AMP will be measured using Ge γ-ray spectrometer. Tritium in the seawater sample will be analyzed by a He-3 ingrowth method that measures He-3 concentration generated from tritium using a mass spectrometer.

Table 3.16.1 The sampling stations and number of samples for iodine-129.

Station	Lat. (N)	Long. (E)	Sampling Date (UTC)	Number of samples	Max. Pressure (dbar)
P10-090	34-47.46	148-55.05	2012/01/30	20	1932
P10-098	37-24.83	147-11.33	2012/02/03	20	2000
P10-106	40-12.40	145-05.09	2012/02/04	19	2070
Total				59	

3.17. Plankton net sampling

(1) Personnel

Minoru Kitamura (JAMSTEC)

Eric Cruz (NOAA)

(2) Objectives

On 11 March 2011, a great earthquake occurred off Tohoku, Japan. This earthquake and the ensuing tsunami inflicted heavy damage on the Fukushima Daiichi nuclear power plant. The fuel rods were exposed and a meltdown occurred in the power plant. By venting, hydrogen explosions and water, contaminated with radionuclides, leaking into the ocean, large amounts of anthropogenic radioactive materials were emitted. These emitted radioactive materials may have an effect on the marine environment, marine resources and consequently human health. To assess its impact, it is important to describe how far the radioactive materials were spread from the Fukushima nuclear power plant and to quantify their concentrations are. Because concentrations of cesium in seawater, sediments and marine biota were previously well documented among the radioactive materials, it is useful to compare the concentrations between before and after the Fukushima power plant accident. In this cruise, we will quantify concentrations of radioactive cesium (^{137}Cs and ^{134}Cs) in zooplankton communities. On the other hand, cesium concentrations in seawater will be also observed in this cruise (see chapter 3.10 Radioactive Cesium and Tritium).

(3) Methods

Zooplankton was collected from the surface layer (from 0 to ca. 200 m) at ten stations during the night (Table 3.18.1). The ORI net (1.6 m in diameter, 8 m long, and 0.33 mm in mesh) was obliquely towed at an average ship speed of 2 knots. Filtering volume of water and maximum sampling depth of each trawl were estimated and recorded using a flow meter and pressure-temperature sensor (SBE39, SeaBird Co. Ltd) mounted in the net mouth, respectively. Collected zooplankton sample was divided onboard using a sample splitter. 1/16 or 1/32 subsamples were fixed and preserved in 5% buffered formalin seawater to analyze community structure. In the four stations (Stns. 77, 82, 88 and 112), 1/32 subsamples were provided to Dr. Yamashita who will quantify concentrations of PFAs in zooplankton community. Micronektonic fish and fish larvae were sorted out from the remained subsamples, and they were fixed and preserved in 10% buffered formalin seawater to understand fauna of them. Finally, the remaining zooplankton samples was filtered using two to eight pre-weighed 0.1 mm meshes, and was frozen in -20 degree C to estimate bulk biomass of zooplankton communities and quantify concentrations of ^{134}Cs and ^{137}Cs. All formalin fixed or frozen subsamples except ones provided to Dr. Yamashita are stored under Kitamura until analyzing.

Table 3.18.1. Zooplankton samplings for RI analysis

Sampling gear: ORI net (2-m^2 net with a 0.33-mm mesh). Flow meter ID: 3120. Sampling layer was recorded using SBE39 (SN0389).

Stn.	Date & Time				Position		Sampling layer	F-meter read	Filtering vol.	Subsamples	Filter No.	Remarks
	LST	net in out	UTC	net in out	Lat. (N)	Long. (E)	(db)		(m^3)			
59	2012.1.14	20:33 22:20	2012.1.14	11:33 13:33	19°10.11' 19°13.79'	149°19.31' 149°21.11'	1~198	68,435	11,627.1	1/16: Formalin fix. 15/16: Frozen	RI-a17 ~ RI-a19	
62	2012.1.15 2012.1.16	23:53 1:50	2012.1.15	14:53 16:50	21°10.84' 21°13.51'	149°20.42' 149°21.33'	1~218	69,288	11,772.0	1/16: Formalin fix. 15/16: Frozen	RI-a20 ~ RI-a22	
68	2012.1.17	20:07 21:50	2012.1.17	11:07 12:50	24°29.95' 24°28.39'	149°20.68' 149°17.43'	1~211	67,520	11,471.6	1/16: Formalin fix. 15/16: Frozen	RI-a23, RI-a24	
71	2012.1.18 2012.1.19	22:15 0:15	2012.1.18	13:15 15:15	26°29.98' 26°33.26'	149°20.14' 149°23.34'	1~209	78,598	13,353.8	1/16: Formalin fix. 15/16: Frozen	RI-a25 ~ RI-a27	net mouth was broken due to rough sea
77	2012.1.20	19:40 21:35	2012.1.20	10:40 12:35	29°59.22' 29°55.86'	149°16.00' 149°19.52'	1~223	74,190	12,604.9	1/32: Formalin fix. 1/32: for Dr. Yamashita 15/16: Frozen	RI-a28 ~ RI-a31	net mouth was broken due to rough sea
82	2012.1.24	0:25 2:10	2012.1.23	15:25 17:10	32°29.79' 32°25.82'	149°20.07' 149°20.73'	1~194	64,576	10,971.5	1/32: Formalin fix. 1/32: for Dr. Yamashita 15/16: Frozen	RI-a32 ~ RI-a34	
88	2012.1.25	21:23 23:20	2012.1.25	12:23 14:23	34°15.10' 34°18.67'	149°10.19' 149°07.41'	1~222	76,310	12,965.1	1/32: Formalin fix. 1/32: for Dr. Yamashita 1/16: Formalin fix. 7/8: Frozen	RI-a35 ~ RI-a37	
98	2012.2.1	19:30 21:30	2012.2.1	10:30 12:30	37°25.11' 37°25.02'	147°12.09' 147°09.02'	1~234	70,310	11,945.7	1/16: Formalin fix. 15/16: Frozen	RI-a38 ~ RI-a42	
106	2012.2.4	21:55 22:55	2012.2.4	12:55 13:55	40°05.09' 40°06.35'	145°22.31' 145°19.97'	1~191	35,590	6,046.7	1/16: Formalin fix. 15/16: Frozen	RI-a43 ~ RI-a45	1 hour trawl
112	2012.2.5 2012.2.6	22:40 0:40	2012.2.5	13:40 15:40	41°44.81' 41°42.53'	144°07.45' 144°01.14'	1~173	79,862	13,568.6	1/32: Formalin fix. 1/32: for Dr. Yamashita 15/16: Frozen	RI-a46 ~ RI-a53	

(4) Results and future analysis

Horizontal distribution of zooplankton biomass (mg wet weight m^{-3}) is illustrated in Fig. 3.18.1. Concentrations of 137- and 134-Cs will be determined by gamma-spectrometry after sample preparation. Community structure of zooplankton in each sampling station will be also analyzed.

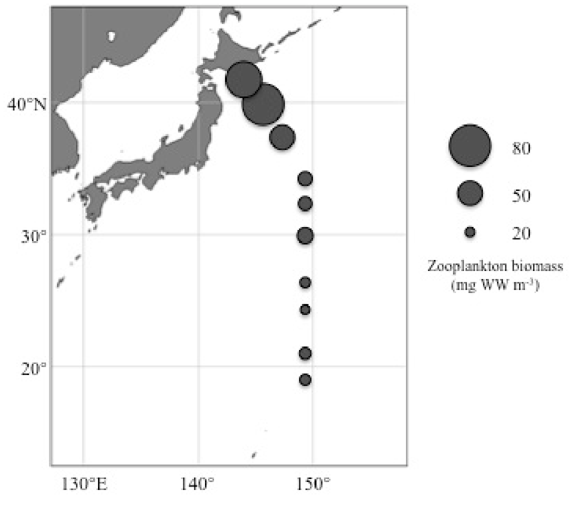

Fig. 3.17.1. Horizontal distribution of zooplankton biomass (mg WW m^{-3}) along the P10 line.

4. Floats, Drifters and Moorings

4.1 Argo floats

(1) Personnel

Toshio Suga	*(JAMSTEC/RIGC): Principal Investigator (not on board)*
Shigeki Hosoda	*(JAMSTEC/RIGC): not on board*
Kanako Sato	*(JAMSTEC/RIGC): not on board*
Mizue Hirano	*(JAMSTEC/RIGC): not on board*
Naoko Miyamoto	*(MWJ): Technical Staff (Operation Leader)*

(2) Objectives

The objective of deployment is to clarify the structure and temporal/spatial variability of water masses in the North Pacific such as North Pacific Subtropical Mode Water and North Pacific Intermediate Water and their formation mechanism. To achieve the objective, profiling floats are launched to measure vertical profiles of temperature and salinity automatically every ten days. As the vertical resolution of the profiles is very fine, the structure and variability of the water mass can be displayed well. Therefore, the profile data from the floats will enable us to understand the variability and the formation mechanism of the water mass.

(3) Parameters

・water temperature, salinity, and pressure

(4) Methods

i. Profiling float deployment

We launched two Provor floats manufactured by nke Instrumentation. Each float equips SBE41 CTD sensor manufactured by Sea-Bird Electronics Inc.

The floats usually drift at a depth of 1000 dbar (called the parking depth), diving to a depth of 2000 dbar and rising up to the sea surface by decreasing and increasing their volume and thus changing the buoyancy in ten-day cycles. During the ascent, they measure temperature, salinity, and pressure. They stay at the sea surface for approximately nine hours, transmitting the CTD data to the land via the ARGOS system, and then return to the parking depth by decreasing volume. The status of floats and their launches are shown in Table 4.1.1.

Table 4.1.1 Status of floats and their launches

Float(2000dbar)

Float Type	Provor floats manufactured by nke Instrumentation
CTD sensor	SBE41cp manufactured by Sea-Bird Electronics Inc.
Cycle	10 days (approximately 11 hours at the sea surface)
ARGOS transmit interval	30 sec
Target Parking Pressure	1000 dbar
Sampling layers	115(2000, 1950, 1900, 1850, 1800, 1750, 1700, 1650, 1600, 1650,

	1500, 1450, 1400, 1350, 1300, 1250, 1200, 1150, 1100, 1050, 1000, 980, 960, 940, 920, 900, 880, 860, 840, 820, 800, 780, 760, 740, 720, 700, 680, 660, 640, 620, 600, 580, 560, 540, 520, 500, 490, 480, 470, 460, 450, 440, 430, 420, 410, 400, 390, 380, 370, 360, 350, 340, 330, 320, 310, 300, 290, 280, 270, 260, 250, 240, 230, 220,210, 200, 195, 190, 185, 180, 175, 170, 165, 160, 155, 150, 145, 140, 135, 130, 125, 120, 115, 110, 105, 100, 95, 90, 85, 80, 75, 70, 65, 60, 55, 50, 45, 40, 35, 30, 25, 20, 15, 10, 4 or surface dbar)

Launches

Float S/N	ARGOS ID	Date and Time of Reset (UTC)	Date and Time of Launch(UTC)	Location of Launch	CTD St. No.
10039	**97950**	**2012/01/19 04 : 05**	**2012/01/19 05 : 34**	**27-49.90 [N] 149-19.73[E]**	**P10-73**
10041	**97952**	**2012/01/23 01 : 18**	**2012/01/23 02 : 56**	**31-49.60 [N] 149-19.75[E]**	**P10N-80**

(5) Data archive

The real-time data are provided to meteorological organizations, research institutes, and universities via Global Data Assembly Center (GDAC: http://www.usgodae.org/argo/argo.html, http://www.coriolis.eu.org/) and Global Telecommunication System (GTS), and utilized for analysis and forecasts of sea conditions and climates.

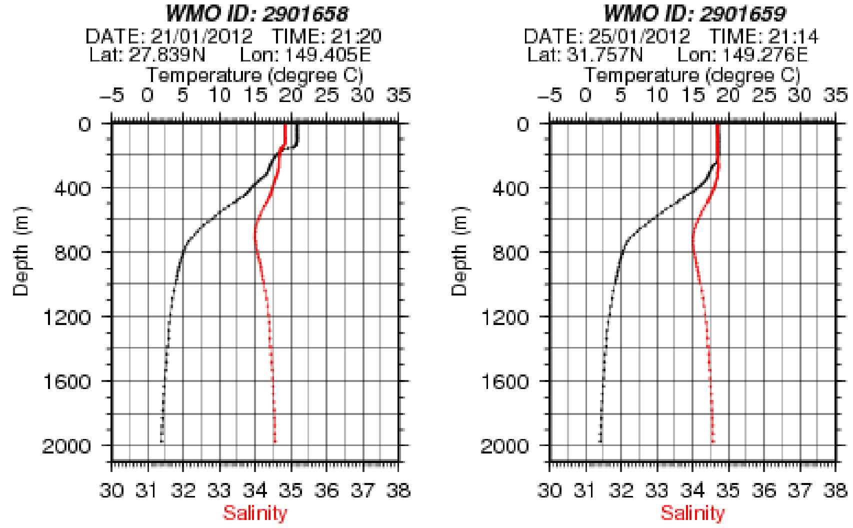

Fig. 4.1.1. The profile of each float launched during MR11-08.

III. Notice on Using

This cruise report is a preliminary documentation as of the end of the cruise. It may not be corrected even if changes on content (i.e. taxonomic classifications) are found after publication. It may also be changed without notice. Data on the cruise report may be raw or not processed. Please ask the Chief Scientist for the latest information before using.

Users of data or results of this cruise are requested to submit their results to Data Management Group (DMG), JAMSTEC.